Hygro-mechanical characterisation of hypercompacted earth for building construction

Agostino Walter Bruno

Hygro-mechanical characterisation of hypercompacted earth for building construction

By

Agostino Walter Bruno

A thesis submitted in fulfilment of the requirements for the degree of Doctor of Philosophy in Civil Engineering

Université de Pau et des Pays de l'Adour
École Doctorale des Sciences Exactes et de leur applications

Public defence on 28th October 2016

Members of the Thesis Jury:

Pr. Jean-Emmanuel AUBERT	President
Pr. Jean-Claude MOREL	Reviewer
Pr. Charles AUGARDE	Reviewer
Pr. Monika WOLOSZYN	Invited member
Pr. Antonin FABBRI	Invited member
Dr. Christophe CANTAU	Invited member
Pr. Domenico GALLIPOLI	Supervisor
MCF Céline PERLOT	Supervisor

The string has not been cut

I am not far

You see, everything is fine

Wipe your tears and cry no more

If you love me: your smile is my peace

St. Augustine

TABLE OF CONTENTS

LIST OF FIGURES

LIST OF TABLES

ACKNOWLEDGEMENTS

I acknowledge the “Conseil regional d’Aquitaine” and the “Agglomération Côte Basque Adour” for supporting this project which was carried out in the laboratory SIAME at the Université de Pau et des Pays de l’Adour.

I would like to express my gratitude to Pr. Domenico Gallipoli, MCF Céline Perlot-Bascoulès and Dr. Joao Mendes for supervising this project and offering me their passionate and enthusiastic support. Their high standard supervision has been precious for my scientific and personal enrichment.

I would like to thank all the members of SIAME and ISA-BTP, specially Pr. Christian La Borderie for the useful discussions about my research.

I would also like to thank Nicolas Salmon, Christophe Cantau and Laurène Felix (Nobatek – INEF4) for the periodic meetings and exchanges throughout this project.

My sincere thanks go to my friends and colleagues with whom I shared the past three years.

Very special thanks to my family. I am deeply grateful to my father Agatino and my two sisters Valeria and Elena for all the sacrifices they have made for me. Finally, I could not have completed this work without the emotional support of Federica, who unreservedly encouraged me mainly in the most difficult times.

ABSTRACT

The present work explores the hygro-mechanical behaviour of a raw earth material and investigates different stabilisation techniques to improve the durability of the material against water erosion. An extensive campaign of laboratory tests was performed on both unstabilised and stabilised materials at two different scales: small cylindrical samples and large bricks.

An innovative manufacturing method based on the application of very high compaction pressures (hypercompaction) was proposed. Also, the compaction load was maintained constant for a sufficient period of time to allow soil consolidation. The main objective was to increase material density, thus improving mechanical performance. Samples compacted with the proposed method exhibited a dry density of about 2320 kg/m^3, which is the highest value registered in the literature for an unstabilised earthen material.

The effect of the compaction pressure on the material fabric was assessed by means of mercury intrusion porosimetry and nitrogen adsorption tests. Results showed that the increase of compaction pressure reduced material porosity with major effects on large inter-aggregate pores. On the contrary, small intra-aggregate pores were not affected by the mechanical compaction.

Mechanical tests were then performed to measure stiffness and strength of both unstabilised and stabilised samples. These tests demonstrated that hypercompaction can largely improve the mechanical response of the material over conventional manufacturing methods. Hypercompacted bricks showed a compressive strength comparable with that of traditional building materials, such as stabilised compressed earth and fired bricks.

The hygroscopic behaviour of both unstabilised and stabilised samples was investigated. The capacity of the samples to absorb/release water vapour was assessed by measuring their moisture buffering value (MBV). Results showed that unstabilised earth has an excellent capacity to buffer ambient humidity. This capacity was significantly reduced by the different stabilisation techniques tested in the present work.

Finally, the durability against water erosion of both unstabilised and stabilised bricks was assessed by performing different tests prescribed by the norm DIN 18945 (2013). Stabilised bricks exhibited a higher resistance against water erosion compared to unstabilised bricks. Still, these materials cannot be adopted for structural applications exposed to natural weathering as indicated by the norm DIN 18945 (2013). Therefore, further investigation is required to identify novel stabilisation methods that can balance the needs of sustainability, durability, moisture buffering and mechanical performance.

KEYWORDS: Raw earth construction, hypercompaction method, compressed earth bricks, stiffness, compressive strength, moisture buffering capacity, stabilisation techniques, durability.

RESUMÉ

Cette étude vise à contribuer au développement d'un produit de construction à faible impact environnemental utilisant la terre crue. Pour cela, le comportement hygro-mécanique de la terre crue compressée à haute pression par une technique novatrice mise au point dans ce projet a été caractérisé. De plus, plusieurs méthodes de stabilisation ont été évaluées afin d'améliorer la durabilité de ce matériau, notamment vis-à-vis de l'érosion induite par l'eau. Une vaste campagne d'essais expérimentaux a été menée sur ces matériaux stabilisés ou non, à deux échelles différentes : les caractérisations des échantillons cylindriques (petite échelle) ont tout d'abord permis de sélectionner la formulation optimale. Par la suite, les tests menés à grande échelle sur les briques de terre compressée ont contribué à développer un produit pour la construction.

Une nouvelle technique de fabrication basée sur l'application d'une contrainte de compactage très élevée (hyper-compactage) a été mise au point. Son objectif principal est d'augmenter la densité du matériau afin d'améliorer ses performances mécaniques. Les échantillons compactés par la méthode proposée présentent une densité sèche d'environ 2320 kg/m^3, ce qui représente la valeur la plus élevée jamais enregistrée dans la littérature pour une terre non stabilisée.

Les effets de la contrainte de compactage sur la microstructure du matériau ont été analysés par intrusion au mercure et adsorption d'azote liquide. Les résultats montrent que l'augmentation de la contrainte de compactage réduit la porosité du matériau, majoritairement les grands pores inter-agrégats. Cependant, le compactage mécanique influence peu les petits pores intra-agrégats. L'approfondissement de la caractérisation des propriétés microstructurales des échantillons stabilisés constitue un développement intéressant de ce travail.

La résistance et la rigidité des échantillons non stabilisés et stabilisés ont été mesurées. Ces essais mécaniques confirment que la méthode d'hyper-compactage permet d'améliorer grandement la réponse mécanique du matériau par rapport aux techniques de fabrication existantes. Ainsi, les briques réalisées présentent une résistance en compression comparable à celle-là des matériaux traditionnels de construction (e.g. terre

stabilisée et briques en terre cuite). Pour compléter cette étude, des essais mécaniques à l'échelle paroi sont à mener.

Le comportement hygroscopique des échantillons stabilisés et non stabilisés a été analysé par la mesure du paramètre MBV (i.e. Moisture Buffering Value), qui traduit la capacité d'échange avec la vapeur d'eau. Il s'avère que la terre non stabilisée possède une excellente capacité à absorber et relarguer l'humidité ambiante. Cette capacité est, par contre, réduite pour les échantillons stabilisés testés dans le cadre de cette étude. La caractérisation du comportement thermique de la terre compressée à haute pression ainsi que l'analyse expérimentale des transferts thermo-hygroscopiques à l'échelle paroi représentent deux compléments d'étude afin de préciser le comportement hygroscopique d'un mur à base de terre crue.

Enfin, la durabilité par rapport à l'érosion induite par l'eau des briques stabilisées et non stabilisées a été estimée à travers les essais d'immersion, de succion et de contact qui sont prévus par la norme DIN 18945 (2013). Les briques stabilisées montrent une meilleure résistance à l'eau par rapport aux briques non stabilisées. Toutefois, des études supplémentaires sont nécessaires pour améliorer les méthodes de stabilisation garantissant la durabilité dans le cas d'applications structurelles exposées aux intempéries, tout en maintenant de bonnes performances hygro-mécaniques et un faible impact environnemental.

MOTS-CLÉS : Construction en terre crue, méthode d'hyper-compactage, briques de terre compressée, microstructure, rigidité, résistance en compression, comportement hygroscopique, MBV, stabilisation, durabilité.

1

Introduction

1.1 Raw earth materials

Raw earth ("terre crue" in French) is a construction material consisting of a mix of soil and water that has been used since ancient times in a variety of forms. Unlike "cooked earth" (e.g. conventional masonry bricks), raw earth is unfired and is subjected to the least possible transformation before being put in place. Chemical binders, such as cement and lime, can be added to the soil for increasing inter-granular bonds and enhancing macroscopic strength. However, if cement and lime are added, the material is referred to as "stabilised earth" in order to mark a difference with respect to "unstabilised earth", which contains no binders and whose strength originates entirely from the inter-granular capillary "pull" exerted by pore water tension.

Environmental impacts associated to the construction and operation of buildings are among the highest across all areas of human activity. The development of sustainable construction practices is therefore essential to comply with current targets for reducing carbon emissions and energy consumption worldwide. In this respect, the use of sustainable and energy-efficient construction materials, which can replace conventional energy-intensive options, is being explored and the use of raw earth material is one of the most promising possibilities.

In fact, raw earth materials can be locally sourced (Morel et al., 2001) and, when used without addition of chemical stabilisers, it is an entirely renewable material that generates limited demolition waste. Moreover, the hygroscopic properties of earthen materials allow buildings to "breathe" by absorbing or releasing ambient moisture depending on room humidity. In addition, condensation or evaporation of water inside earthen walls generates exchanges of latent heat, which helps regulating temperature of interiors. Earthen buildings therefore require little energy for air conditioning of the indoor space (Allinson and Hall, 2010) and offer a very high quality ambience for occupants without involving additional energy costs (Pacheco-Torgal and Jalali, 2012).

Despite these benefits, the relatively poor strength and stiffness of earthen materials and erosion owed to liquid water infiltration have impeded the diffusion of this construction technique beyond a very niche market. One possible solution that has been tried over past years is to "stabilise" earthen materials by adding chemical binders to improve both mechanical and durability properties (Walker, 2000; Jayasinghe and Kamaladasa, 2007). This, however, lessens the "green" attributes of earthen materials as it increases levels of embodied energy and reduces the possibility of recycling demolition waste. These drawbacks must be overcome in order to promote the adoption of earthen materials in mainstream construction.

1.2 Historical overview

Historical earth structures, from rural habitats to impressive military citadels, can be found all over the world, e.g. in France, Spain, Portugal, the Maghreb region (Morocco, Algeria), Central and South America (Mexico, Peru, Brazil) and China.

Archaeological remains indicate that, between 1500 and 300 BC, the Phoenician civilisation had developed a building technique based on the use of raw earth in the cities of Tyr, Ugarit and Sidon. This technique was subsequently exported by the Carthaginians to the entire Mediterranean region.

Other ancient examples of earth construction include the Great Wall of China, part of which was erected using rammed earth over 2,000 years ago, and the Alhambra Palace in Spain, which was built in the 10^{th} century (Figure 1.1). Similar construction techniques were also developed by pre-Columbian civilisations.

In more recent times, raw earth construction has been practised in France and Germany. In the Rhône-Alpes region, a large number of residential buildings dating back between one or two hundred years ago, are still in use and exhibit excellent performance in terms of structural stability, durability and environmental comfort. In Germany, the seven storeys "Haus Rath", built in 1828 by the industrial Jacob Wimpfin in Weilburg an der Lahn, is still one of the tallest earthen buildings to date (Figure 1.2).

Figure 1.1. Example of historical rammed earth building: the Alhambra Palace in Granada, Spain, built in the 10th century

Figure 1.2. Example of modern rammed earth building: the Haus Rath in Weilburg an der Lahn, Germany, built in 1828

During the late eighteenth century and throughout the nineteenth century, earthen construction experienced a strong revival due to the initiative of the Lyonnais architect and professor of rural architecture François Cointeraux (1740-1830), who was an ardent propagator of this construction technique and whose writings contributed to dissemination of earthen buildings throughout Europe (e.g. in France, Germany, Italy,

Switzerland and Denmark) and even in the United States and Australia. One of the most cited definition of rammed earth ("pisé de terre" in French) is indeed due to Cointeraux and appears in his publication "Ecole d'Architecture Rurale" (1790-1791):

«the "pisé" is a process by which houses are built from earth without the support of wood and without mixing straw or other filling. It consists in compacting, layer by layer, between two wooden planks, separated by the width of an ordinary wall, a given amount of earth prepared for this purpose. Compacted in this way, the earth binds, takes consistency and forms a homogeneous mixture that can be erected to heights suitable for dwellings» (Translated from French).

In France, the revival of earthen construction lasted until the beginning of the past century affecting a varied typology of buildings such as farms, barns, mansions, castles, churches, factories, mills, housing estates, town halls and schools.

Between 1920 and 1950, thousands of raw earth dwellings were also built in Germany under the instigation of the political authorities of the time. The regions of Prussia and Saxony, in particular, launched an effective programme of promotion of earthen construction between 1920 and 1921, which resulted in the realisation of nearly 20,000 dwellings made of raw earth.

However, after the Second World War, the post-bellic reconstruction effort demanded fast building techniques with little concern about environmental impact. Materials such as concrete and steel rapidly became the preferred choice of architects and engineers while raw earth became increasingly obsolete and, towards the end of the 1950s, was virtually abandoned in the developed world. In spite of this decline, it is estimated that about 50% of the current world population still lives in earth dwellings that are either legacy structures or new buildings especially in the poorest countries.

Earthen construction has always been regarded as an "art" transmitted from generation to generation. This art was practiced by craftsmen with good empirical knowledge of the hydro-thermo-mechanical properties of earthen materials and a sound experience of the construction process. The loss of these skills is one of the main obstacles to the utilisation of raw earth as a mainstream construction material in modern practice.

1.3 Raw earth construction techniques

1.3.1 Ancient raw earth construction

The following ancient techniques of earthen construction, although developed centuries ago, are still presently employed, often with little changes compared to the past.

(1) **Adobe.** This technique uses a wet mixture of soil, water and natural fibres as the base construction material. The mixture, which has the consistency of a thick mud, is poured into parallelepiped moulds with dimensions of conventional bricks and dried to the sun for several days. After this, the blocks are extruded from the moulds and used to build masonry structures likewise ordinary fired bricks.

(2) **Ancient rammed earth** ("Pisé" in French). Ancient rammed earth structures are built by manual compaction of moist earth in consecutive layers inside a formwork of parallel flat shutters. The shutters, which have typical lengths of 700-1000 mm and heights of 600-900 mm, are held at a distance equal to the wall width by props and rope ties. A layer of moist loose earth, between 10 cm and 25 cm deep, is poured inside the formwork and compacted by about 50%. Earth is manually tamped by using a long ramming pole, layer after layer, until the top of the formwork. At this point, the shutters are dismantled and moved either horizontally, to build the next section of the current lift, or vertically, to start a new lift.

(3) **Cob.** This technique consists in the construction of massive load bearing walls made of soil, water and natural fibres (e.g. straw, reed or heath). The soil/fibre mixture is manufactured in a very wet state into clods that are 50 cm to 120 cm large. The dimension of the clods depends on the plasticity and particle sizes of the soil, but also on the experience of the builder. Clods are stacked in consecutive lifts without formworks and trimmed to provide a smooth surface. Walls are usually 50-60 cm thick for single-floor buildings and 70-80 cm tick for two-floor buildings. Because of the high water content and plasticity of the clods at the time of emplacement, each lift must dry for about four weeks before the subsequent one is placed on top. Cob building is therefore time-consuming but it offers the flexibility of producing walls of variable shapes (e.g. non-rectilinear walls).

(4) **Wattle and daub** ("Torchis" in French). This is a very old technique for the construction of non–load bearing walls, either partition walls or external walls, with

widths between 8 cm and 20 cm. The technique consists in filling a lattice of inter-woven wooden strips with a wet mixture of soil and vegetal fibres, such as straw or hemp. A heavyweight and lightweight version of wattle and daub can be distinguished. In the heavyweight version, the soil mix includes only a small amount of vegetal fibres. This increases thermal capacity, which in turn makes the material best suited for internal walls. In the lightweight version, a significant portion of the soil is replaced by vegetal fibres, which improves thermal insulation and makes the material best suited for external walls.

Figure 1.3 illustrates the application of the four raw earth construction techniques revised in this section.

Figure 1.3. Ancient raw earth construction

1.3.2 Modern raw earth construction

The main difference between modern and ancient earth construction techniques relate to the building process. For example, earth is nowadays compacted with the help of heavy

machinery rather than manual tamping, which reduces time and costs compared to past. Among the most popular techniques of modern earth construction, are:

(1) **Casted earth** ("Terre coulée" in French). This is a novel construction technique developed for non-load bearing walls by the laboratory CRATerre-ENSAG in France. The technique consists in the manufacture of an "earth concrete" that uses a clay binder instead of cement. To achieve good mechanical properties, it is essential to use standard proportions of gravel, sand and clay. Similar to concrete, the earth mix is blended with the right amount of water for optimising the mechanical properties of the final product but also the consistency of the fluid mix at the time of pouring in order to reduce lateral thrust on formworks. Casted earth is considerably quicker to build than rammed earth because pouring a fluid earth mix takes considerably less time than tamping consecutive layers of moist soil.

(2) **Compressed earth bricks.** Compressed earth blocks are often manufactured on site by compacting moist soil to a relatively high density inside a parallelepiped mould with the dimensions of a standard brick. Compaction is achieved by means of hydraulic or mechanical presses that apply loads between 2 MPa and 15 MPa. Electrical or diesel engines are most frequently used, though lever-action manual presses also exist. Blocks are subsequently assembled as masonry structures without mortar but with a thin joint of mud slurry to compensate surface roughness and enhance airtightness. The present work focuses on this construction technique and aims to improve the current practices by defining an innovative hypercompaction procedure.

(3) **Modern rammed earth.** Modern rammed earth construction follows the same basic principles as in ancient times but benefits from greater process efficiency. Manual tamping by poles is replaced by vibro-compaction via pneumatic hammers or plate compactors. This shortens construction times and allows a higher densification of the soil together with better quality control of the final product. The small movable wooden shutters of ancient times are replaced by larger metallic formworks (similar to those for casting concrete), placed on rollers or slides to facilitate displacement and speed up construction. These formworks are lighter and stronger than in the past, which facilitates assembly and dismantling as well as increasing resistance to vibrations during heavy ramming.

(4) **Prefabricated rammed earth panels.** Modern rammed earth construction involves continuous assembly and dismantling of formworks. When this is not possible due to

logistic constraints, prefabricated panels can be used instead. Prefabricated panels are produced either on-site or off-site by compaction of a wet soil mix into formworks of variable shapes and sizes. Typical panels are up to 2.5 m high and long, with a width up to 500 mm and a weigh up to 7000 kg. After stripping the formworks, panels are left to dry to the atmosphere and subsequently put in place on a bed of lime with the help of cranes. Because panels are manufactured in advance, there is no need for the soil to dry between subsequent lifts as it is instead the case in rammed earth construction. Prefabricated panels retain the architectural flexibility of rammed earth construction while reducing time and labour costs with a better control of material quality.

Figure 1.4 shows some examples of modern raw earth construction.

Casted earth

Compressed earth bricks

Modern rammed earth

Prefabricated rammed earth panels

Figure 1.4. Modern raw earth construction

1.4 Advantages and limitations of raw earth materials

1.4.1 Reasons behind current renaissance of earthen construction

The adjective “sustainable” describes a product or a technology that “fulfils the needs of the present without compromising the ability of future generations to meet their own

needs" (WCED, 1987). The pursuit of sustainable development, or sustainability, has become a key priority in economic activities and continues to attract interest from media and policy makers across the world. A first reason for this is the scarcity of natural resources, which has become particularly evident in today globalised society. Current world population stands at around 7 billion, a number that has continuously increased since the end of the Great Famine and Black Death in 1350, when it stood at 370 million. At this rate, unless actions are taken at global level, it is not difficult to envisage a time when humanity will run out of resources for its subsistence.

In addition, sustainable policies aim to mitigate the climatic impact of greenhouse gases such as carbon dioxide. These gases are produced by the combustion of fossil fuels, which are the basis of modern economy.

Construction is the largest industry in Europe with 10-11% of GDP (Eurostat, 2011) and, as such, must embrace sustainable practices if the environmental targets set by political authorities are to be met. The cement industry alone accounts for 5% of global carbon emissions and production of each ton of cement generates more than one ton of carbon dioxide. Cement is a primary ingredient of concrete and its consumption is expected to grow from 2.5 billion tons in 2006 to 4.4 billion tons by 2050. Figure 1.5 shows the energy consumption of the building, transport and industry sectors in Europe, the US and Japan as estimated in a report by the OECD (2003). In Figure 1.5, only the energy necessary for operation of dwellings is attributed to the building sector. The energy used for transportation of construction materials to site is instead included under the transport heading while the energy required for building and demolition is given under the industry heading. This means that the total energy consumed by all activities associated to construction, operation and demolition of buildings is even greater than that attributed to the building sector in Figure 1.5. In a more recent publication, Szalay (2007) arrived to similar conclusions estimating that operation of residential buildings is responsible for about 40% of all energy consumed in Europe.

The building sector is also the largest consumer of raw minerals and produces about 33% of all waste generated every year in the European Union (EEA, 2010). Construction waste is usually not recyclable and is disposed in landfills, resulting in loss of land, pollution and social alienation.

Very similar data are provided by the French agency of environment and energy management, which stated that in France the building sector is responsible for 22% of

greenhouse gas emissions, 44% of primary energy consumption and 31% of generated waste (ADEME, 2013).

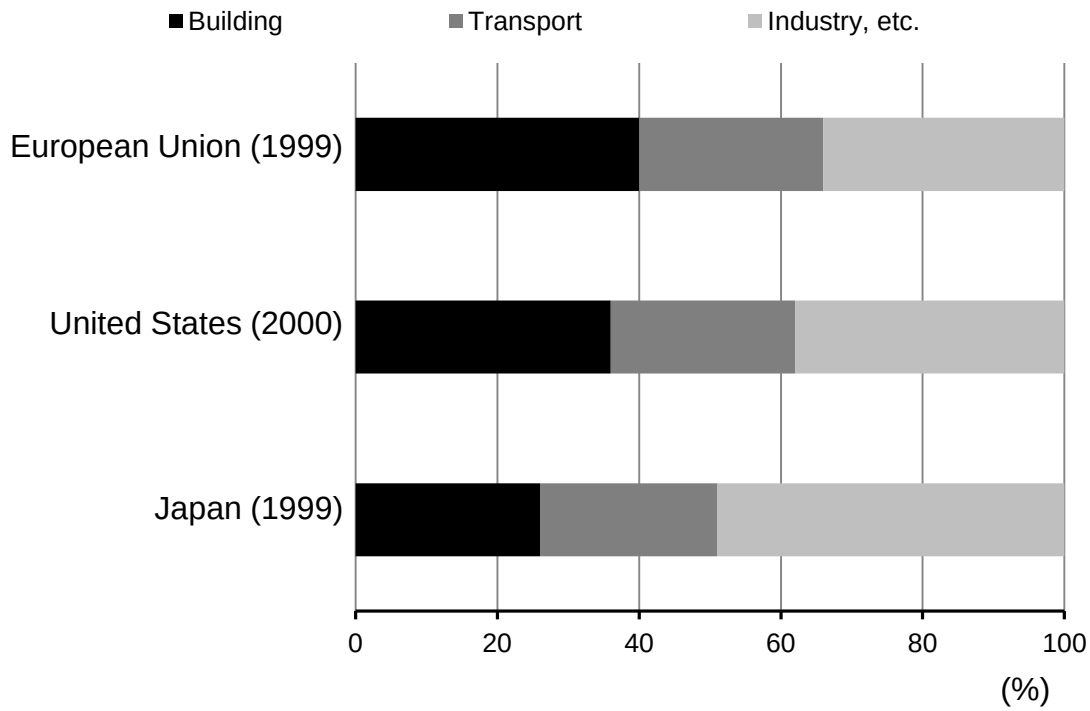

Figure 1.5. Energy consumption by sectors. Source: European commission, US Department of Energy, Japanese Resource and Energy Agency (OECD, 2003)

Since the 1970s, a number of studies have quantified the environmental costs of construction, which has in turn triggered new interest in alternative building materials with environmentally friendly characteristics. Among these, earth is one of the most attractive options because it is harmless to humans and can be locally sourced and easily transported to site. Earth is also recyclable, inexhaustible and, when properly manufactured, offers high strength, excellent hygro-thermal properties and low embodied energy at very low costs. Because of these attributes, earthen materials can dramatically reduce exploitation of natural resources not only during construction, but also during service life, by cutting down on heating/air conditioning needs, and at the end of life, by limiting demolition waste.

The advantages of earth as a building material have been known for years but have only started to be quantified in the last few decades. The most important of these advantages are summarised below:

(1) **Reduction of embodied energy.** Extraction, transportation and manufacture of earthen materials require only 1% of the energy needed for the production of cement-based materials (Deboucha and Hashim, 2011). Similarly, the manufacture of earth blocks requires, at most, one third of the energy required to fabricate conventional fired bricks of similar dimensions, namely 440 kWh/m^3 compared to 1300 kWh/m^3 (Morton and Little, 2001).

(2) **Reduction of operational energy (hygro-regulator effect).** Due to their extended network of very fine pores (of the order of nanometers), earthen materials can absorb vapour from humid environments and release it into dry ones, with typical changes in weight of about 3-4%. An earth wall can therefore help to regulate hygroscopic conditions inside a building by absorbing, storing and releasing moisture as necessary. This is a very advantageous property which can contribute to ensuring healthy levels of ambient humidity inside dwellings while reducing air conditioning needs.

(3) **Reduction of operational energy (thermal-regulator effect).** The thermal conductivity of earthen materials is relatively high (of the order of 10^{-1} W/mK) compared to that of standard insulating materials (of the order of 10^{-2} W/mK). Moreover, as pointed out by Houben and Guillaud (2006), the heat capacity of earthen materials is of similar magnitude to that of ordinary concrete (of the order of 10^3 kJ/m^3K). These values might erroneously suggest that raw earth does not offer any particular advantage over conventional construction materials in terms of thermal performance. This conclusion is however incorrect because it does not take into account the strong thermal-regulator effect of capillary condensation and evaporation of water inside the earth nanopores (as described in point 2 above). Evaporation is an endothermic process, which subtracts latent heat from the environment during the hottest hours of the day, while condensation is an exothermic process which releases latent heat during the coolest hours. Moreover, due to the relatively large width of structural earthen envelopes, the thermal capacity per unit area of wall can be very high. This confers to earthen structures the ability to store significant amounts of heat during the day and to return it during night with a phase shift of 10-12 hours (Houben and Guillad, 2006).

(4) **Acoustic insulation.** Raw earth presents excellent acoustic characteristics and provides good sound insulation due to its high dry density (usually in excess of 2000 kg/m^3) and width (often larger than 0.25 m). According to the British Standard 8233

(1999), the sound reduction index R (in dB) of an ordinary masonry wall depends on its dry density, ρ (in kg/m^3) and width, t (in m) according to the following empirical equation:

$$R = 21.65 \log(\rho t) - 2.3 \quad (1.1)$$

Equation (1.1) predicts that an earthen wall with a width of 0.30 m and a dry density of 2100 kg/m^3 has a sound reduction index of 58.3 dB, which is well above the requirement of most building regulations. As an example, the UK Building Regulations by HM Government (2010) specify that "laboratory values of the sound reduction index for new internal walls and floors within dwelling-houses, flats and rooms for residential purposes, whether purpose built or formed by material change of use" should be at least 40 dB.

(5) **Recycling or safe disposal of demolition waste.** According to Bossink and Brouwers (1996), the waste generated by construction and demolition activities accounts for between 13% and 30% of all landfill waste worldwide. Of this amount, demolition waste represents the largest share, with an estimated ratio to construction waste of about 2:1 (Bossink et al., 1996). In this respect, unstabilised earth presents considerable advantages over conventional construction materials because demolition waste consists mainly of ordinary soil that can be easily recycled or safely released into the environment. Of course, this is no longer true if earth is stabilised by cement or lime because the addition of such chemical binders compromises the ecologic credentials of the material and hence complicates disposal of demolition waste.

1.4.2 Some limitations of raw earth construction

Despite the environmental credentials and relatively low cost of raw earth, this building material is still confined to a niche market. This is mainly because of the following limitations, which have hindered its adoption within mainstream practice:

(1) **Inadequacy of local soil.** Earthen construction employs soil mixes with variable proportions of gravel, sand, silt and clay. The exact influence of soil grading on material strength and durability remains unclear (Keable, 1996) but most studies agree that an optimum mix should include 30% clay/silt and 70% sand/gravel. The clay fraction, despite being relatively small (around 10%), plays a very important role as it is responsible for capillary bonding of coarse grains, which is the main source of strength

in unstabilised earth (Jaquin et al., 2009). In addition, the clay fraction interacts with the atmosphere by absorbing, storing and releasing moisture depending on ambient humidity, thus contributing to the hygro-thermal regulation of indoor space. Therefore, if an earthen material with the recommended proportions of clay, silt, sand and gravel is not available locally, suitable constituents must be quarried further away and transported to site with consequent increases in energy consumption and financial costs. Local but poorer soils can still be used, though they must be stabilised by chemical binders (e.g. cement) to compensate for the substandard properties of the earth base. Regardless of whether unstabilised good quality soils are imported from elsewhere or local, but poorer, soils are stabilised by chemical binders, the overall carbon footprint of construction will inevitably increase.

(2) **Poor quality control.** Two different levels of quality control can be identified with reference to earthen construction, a "precautionary" level and a "confirmatory" level. The precautionary level of control consists in monitoring the selection, mixing and storage of soil constituents prior to compaction. The confirmatory level of control consists instead in ensuring that the final density, strength and durability of the built product are compliant with design requirements. The former level of control can be performed on site with relative ease, while the latter one is more difficult to accomplish as material characteristics remain highly dependent on workmanship (Crowley, 1997).

(3) **Long construction times.** This limitation mainly applies to rammed earth construction, which is slower than other earthen building techniques. Soil ramming can be more or less fast depending on whether it is performed manually or with the help of electrical/diesel-powered machinery. However, a large amount of time is taken by continuous setting-up, aligning and stripping of formwork, which can account for up to 60% of the total duration of site operations. Building time can increase considerably for projects requiring significant dismantling and reassembly of formworks, with escalating costs that make realisations no longer viable (Maniatidis and Walker, 2003).

(4) **Empiricism of design methods.** Several countries (e.g. Australia, New Zealand, USA, Zimbabwe, Germany and Spain) have published national standards for earthen construction. These documents are, however, based on empiricism and practical know-how rather than engineering science. In particular, the role of pore water capillarity in bonding grains together, and hence generating material strength, is still poorly understood. For instance, some of the above standards mention that unstabilised earth

must “cure” for weeks before full strength is attained, which is in clear contradiction with the fact that unstabilised earth does not contain any cement to be cured. The contradiction originates from the poor understanding of capillarity effects in earthen materials as the “curing” time advocated by national standards is nothing else than the time necessary for soil suction to attain thermodynamic equilibrium with ambient humidity and therefore exert a satisfactory level of capillary bonding (Jaquin et al., 2009). The chemo-physical origin of capillary bonding is currently ignored by national design codes and its contribution to material strength is therefore not explicitly quantified. Disregarding this innate and inexpensive source of strength is equivalent to wasting a gift of nature that might otherwise reduce safety margins and, consequently, cut costs and environmental impact.

(5) **Sensitivity to moisture ingress.** The wicking action of capillary pores causes the rapid absorption of any free water that comes into contact with earthen materials. Experiments have shown that, during the initial phase of exposure of a stabilised raw earth sample to free water, the moisture content increases linearly with the square root of time, a phenomenon often referred to as the “wick effect” (Lucas, 1918; Washburn, 1921). This moisture ingress reduces material strength and, depending on soil mineralogy, may also cause swelling of the clay component, which in turn produces structural damage. Nevertheless, moisture ingress can be limited by controlling pore volume, pore size and degree of saturation of the material as shown by Hall and Djerbib (2004).

(6) **Uncertainties about durability.** In dry climates raw earth is very durable, as demonstrated by the large number of well-preserved earthen structures dating back hundreds, or even thousands, of years ago. In wet climates, however, rainfall causes surface erosion, especially in unstabilised earth structures. Bui et al. (2009) measured between 5 mm and 10 mm of erosion from the surface of a 400 mm thick unstabilised earth wall exposed to a wet continental climate during a period of twenty years. Similarly, an unstabilised earth wall built on the campus of the Massachusetts Institute of Technology in 2005 has shown a surface erosion of about 5-7 mm during nine years of exposition to the temperate climate of the North-eastern coast of United States (Dahmen, 2015). The chronological extrapolation of these results indicates that a surface erosion between 25 mm and 80 mm can be expected over a period of 100 years, which is clearly not acceptable for most structures. Freeze-thaw cycles can also induce spalling, especially if these cycles occur soon after construction when the material is

still relatively wet and hence particularly vulnerable to sub-zero temperatures. Tests by Guettala et al. (2006) have observed a loss of 2% of earth mass after 12 freeze-thaw cycles between 21 °C and – 23 °C. Durability becomes an even greater concern if raw earth is reinforced with natural (i.e. biodegradable) fibres, which may decompose and therefore lose strength over time.

(7) **Use of chemical stabilisers.** Chemical stabilisers are often used in earthen construction. The most common stabilisers are cement, lime and bitumen, which are added to the soil in proportions between 5% and 15% by weight. Stabilisers increase strength, improve durability, reduce shrinkage/swelling and provide waterproofing. However, besides these benefits, they bring at least three significant disadvantages. Firstly, they increase costs, e.g. stabilisers can account for more than half of the overall material costs. Secondly, they considerably increase the carbon footprint of construction, e.g. production of every tonne of cement results in the emission of 1.25 tonnes of carbon dioxide. Thirdly, they complicate recycling of demolition waste because stabilised earth is no longer a natural material but rather a "weak concrete" made of aggregates linked by a binding matrix (Chilkoti, 2012).

(8) **Uncertainties about energy efficiency.** Past studies have demonstrated the low embodied energy of earthen structures compared to, for example, concrete or steel (Lawson and Rudder, 1996). The operational energy of earthen buildings is also lower than other conventional structures because of the larger hygro-thermal inertia of earthen walls, which helps to regulate temperature and humidity inside buildings by averaging day/night extremes, as discussed by Soudani et al. (2016). Despite the importance of these properties, the hygro-thermal buffering characteristics of earthen materials are yet to be fully understood and the consequent savings of operational energy are yet to be fully quantified. In addition, no research to date has quantified the end-of-life energy consumption and carbon emission resulting from demolition and disposal of earthen structures. These knowledge gaps have so far impeded a full appreciation of the potential of earthen construction for minimising energy consumption and carbon emissions at all stages of structural life. In particular, a full Life Cycle Assessment should be undertaken for assessing the environmental performance of this construction technique compared to other standard ones.

1.5 Research objectives

The objective of this work has been to study the mechanical, hygroscopic and durability properties of hypercompacted earth (i.e. earth compressed at very high pressures) as a construction material by means of a vast campaign of laboratory tests. The main objectives of the project can be summarised as follows:

- To manufacture an earthen material for construction by proposing an innovative hypercompaction procedure which relies on the application of very high pressures up to 100 MPa. This has required design and fabrication of all laboratory equipment for applying high compaction loads at the scale of both small cylindrical samples and larger bricks;
- To investigate the effect of the above hypercompaction procedure on the microstructural properties of the material by performing different types of porosimetry analyses;
- To investigate the dependency of stiffness and strength on material density at the scale of small cylindrical samples;
- To investigate the dependency of stiffness and strength on ambient humidity at the scale of small cylindrical samples;
- To investigate the dependency of compressive strength on aspect ratio at the scale of large bricks:
- To investigate the dependency of compressive strength on Teflon capping at the scale of large bricks;
- To investigate the effect of a cement mortar joint on the compressive strength of dry-sawn half bricks;
- To investigate the effect of compaction-induced anisotropy on the compressive strength of dry-sawn cubic specimens;
- To investigate the moisture buffering capacity of the material (i.e. the capacity of the material to adsorb/release water vapour from/into indoor environments) at the scale of both small cylindrical samples and larger bricks;
- To investigate the durability of the material against water erosion at the scale of both small cylindrical samples and larger bricks;
- To propose alternative stabilisation techniques to improve durability of the material while preserving adequate mechanical properties, good moisture buffering capacity and low environmental impact;

1.6 Thesis layout

Chapter 1 retraces the history of raw earth construction and analyses the advantages and limitations of using raw earth as a construction material. The main objectives of the present project are also outlined.

Chapter 2 discusses the main engineering properties of raw earth for construction applications such as grain size distribution and plasticity. The effect of these properties on the macroscopic hydro-mechanical behaviour of the material is analysed. The chapter also reviews past studies on mechanical behaviour, moisture buffering capacity and durability of earthen materials.

Chapter 3 describes the main geotechnical properties of the material tested in this work as well as the compaction procedures followed to manufacture both small cylindrical samples and compressed earth bricks. This chapter concludes by presenting the different stabilisation methods adopted to improve material durability.

Chapter 4 presents the results from both mercury intrusion porosimetry and nitrogen adsorption tests. The main objective of these tests is to assess the effect of the hypercompaction procedure on the microstructural properties of earthen samples.

Chapter 5 reports results from mechanical tests conducted to measure the stiffness and strength of unstabilised and stabilised earth at the scale of small cylindrical samples and larger bricks. This chapter also describes the effect of material density and ambient humidity on the mechanical behaviour of the material.

Chapter 6 investigates the hygroscopic behaviour of unstabilised and stabilised earth samples under cyclic variations of relative humidity in the surrounding environment.

Chapter 7 presents the results from durability tests on unstabilised and stabilised compressed earth bricks. A classification of the tested bricks is also proposed in agreement with the German norm DIN 18945.

Finally, Chapter 8 presents the conclusions drawn from the present project and gives recommendations for future work.

2

Raw earth: review of main engineering properties

The present chapter discusses the main engineering properties of raw earth such as grain size distribution and plasticity. The chapter also reviews past studies on mechanical behaviour, moisture buffering capacity and durability of raw earth materials.

2.1 Physical properties of raw earth materials

In this section, the main physical properties of raw earth materials such as grain size distribution, plasticity and fabric are discussed. Also, the relationship between these properties and the macroscopic hydro-mechanical behaviour is highlighted.

2.1.1 Grain size distribution

The grain size distribution is the first property to consider when assessing the suitability of an earthen material for construction. The most common techniques to determine the grain size distribution are wet or dry sieving and sedimentation. Other simplified methods (e.g. visual examination, touch, shine test, jar test, hand washing, etc.) can provide a preliminary estimation of soil granularity. Ideally, a suitable earth material should contain a "high sand content, silt and enough clay to act as a binder" (Maniatidis and Walker, 2003).

Delgado and Guerrero (2007) reviewed more than 20 technical documents (including national standards and general reviews) about the grain size distribution of earthen materials. From these documents, they concluded that particle size prescriptions are most restrictive for rammed earth than adobe construction. Figure 2.1 shows the lower and upper limits of the grain size distribution for compressed earth bricks as recommended by AFNOR (2001), CRATerre - EAG (1998) and MOPT (1992). The French norm XP P13-901 (AFNOR, 2001) coincides with the guidelines by CRATerre and the School of Architecture of Grenoble (CRATerre - EAG, 1998).

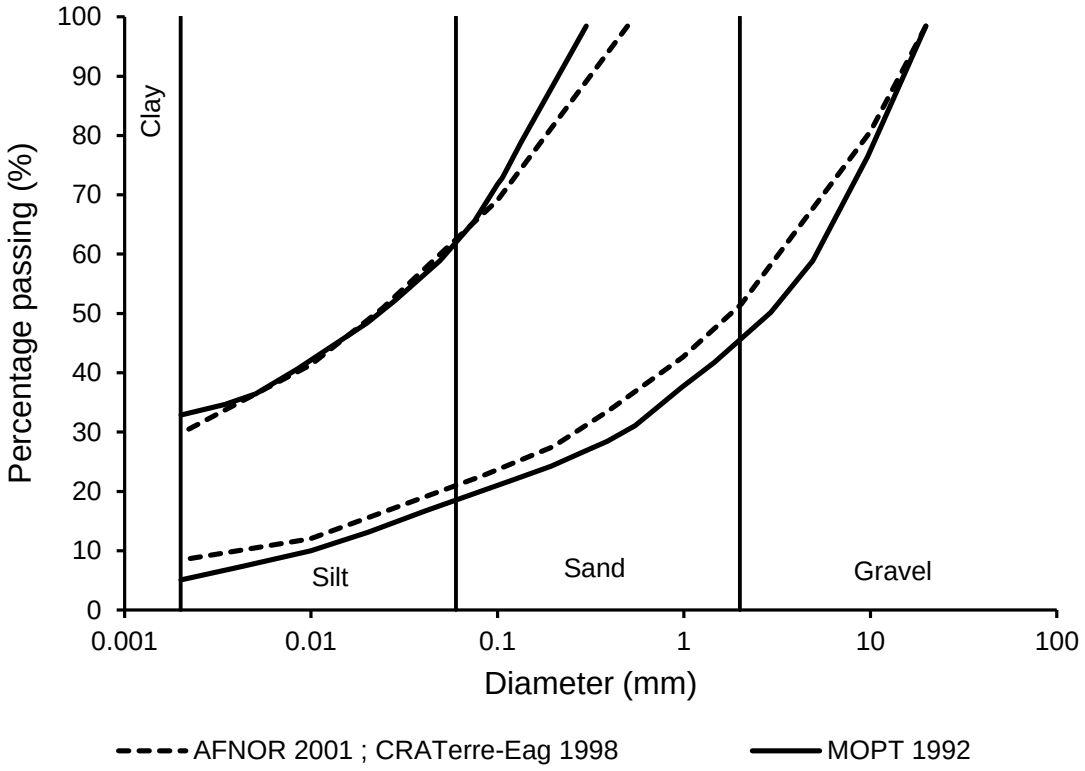

Figure 2.1. Grain size distribution: upper and lower limits for compressed earth blocks according to AFNOR (2001), CRATerre- EAG (1998) and MOPT (1992)

Figure 2.2 shows the recommended lower and upper limits of the different fractions in raw earth materials according to various authors. All authors tend to agree with Maniatidis and Walker (2003) on the fact that a suitable soil should contain a high sand content of about 70% and a fine fraction of about 30%.

The influence of particle grading on the strength and stiffness can be significant as shown, for example, by Wu et al. (2013). These authors analysed four earthen materials with a coarse sandy fraction ranging from 60% to 45% and a fine clayey-silty fraction from 40% to 55%. The four different earthen materials were obtained by mixing a natural soil (clay-silt 88.6% and sand 11.4%) with a coarser fraction (sand 74.7% and gravel 25.3%) in different proportions of 1:0.6, 1:0.8, 1:1 and 1:1.2 by weight. The four mixes were lightly compacted at a water content of 19.5% into parallelepiped wood moulds with dimensions of 200 x 90 x 50 mm^3. After drying, the bricks were subjected to unconfined compression for measuring stiffness and strength. Wu et al. (2013) did not measure the respective percentages of clay and silt, thus the impact of the fine fraction on mechanical response could not be precisely assessed. Inspection of Figure 2.3 shows that both compressive strength and stiffness increase when the clay-silt

content increases from 40% to 49%, but they start to decrease when the clay-silt content increases further from 49% to 55%.

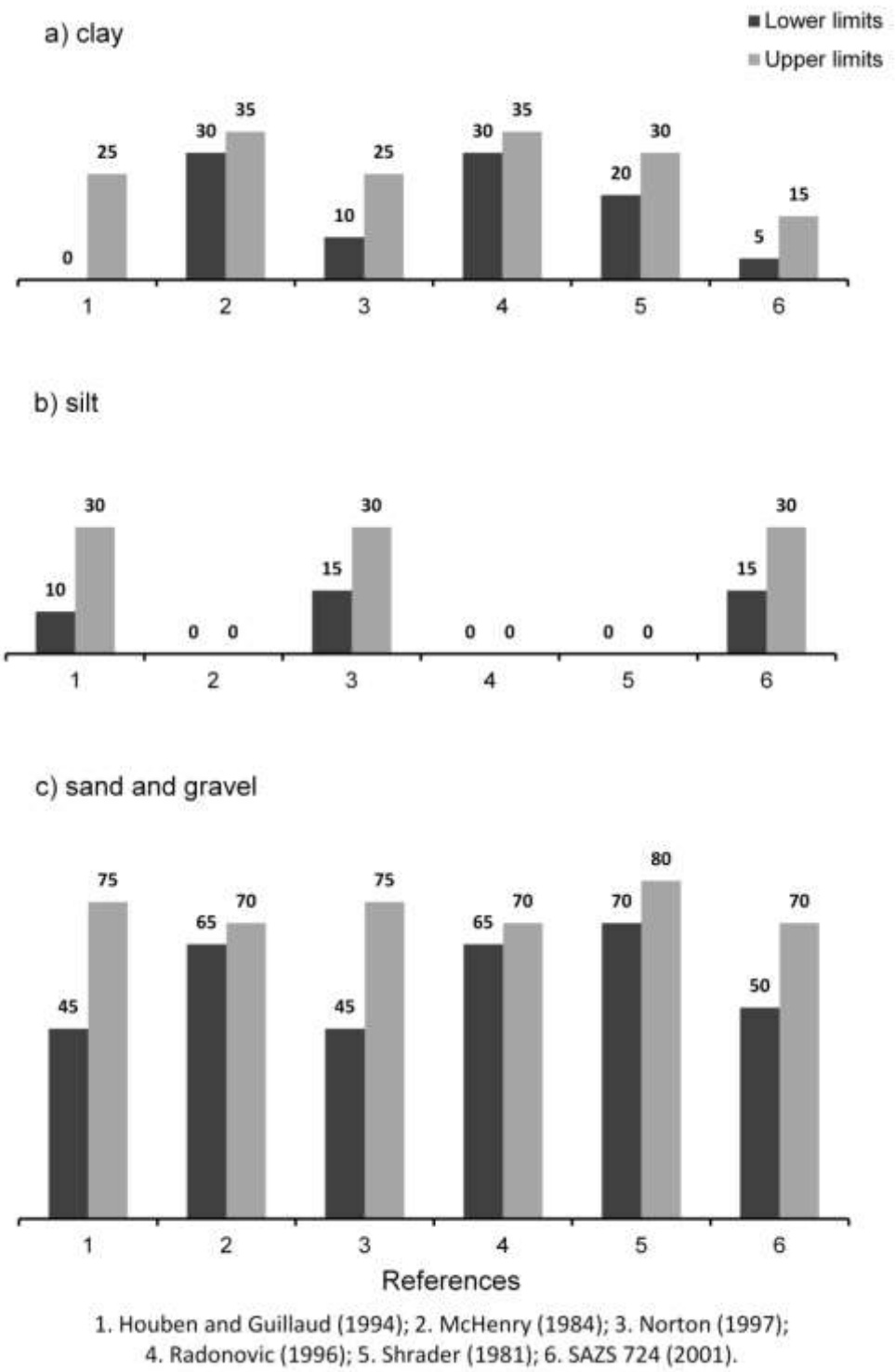

Figure 2.2. Recommended lower and upper proportions of a) clay, b) silt and c) sand and gravel in earthen materials according to various authors

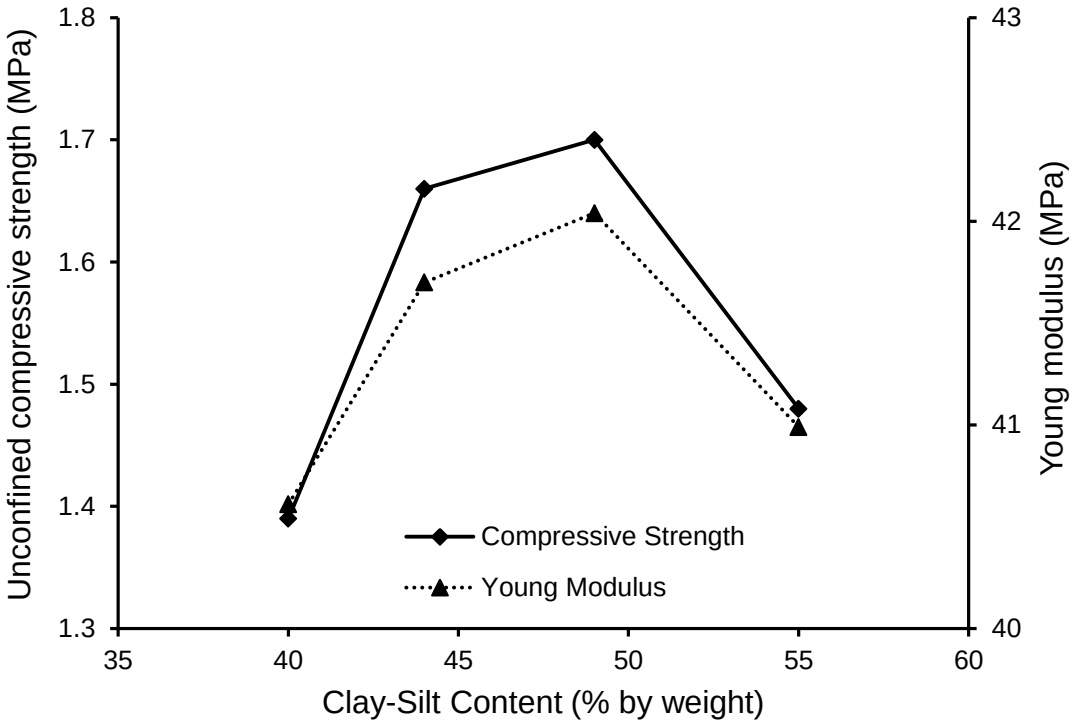

Figure 2.3. Stiffness and strength of earth mixes with different clay-silt fractions (after Wu et al. 2013)

The grain size distribution also affects hydraulic behaviour. Jaquin et al. (2008) investigated the water retention properties of rammed earth by means of filter paper tests. The tests were performed on two different materials, i.e. mix A and mix B, obtained by modification of a base soil consisting of sand 74%, silt 16% and clay 10%. The two materials were obtained by adding an extra 10% of sand (mix A) or an extra 10% of clay/silt (mix B) to the base soil. The mixes were statically compacted in layers at a water content of 10% to attain a dry density of about 2050 kg/m^3.

Figure 2.4 shows the drying curves for mixes A and B, which include measurements of both matric and total suction. Inspection of Figure 2.4 indicates that the coarser mix A exhibits lower water contents at the same suction compared to the finer mix B, thus emphasising the importance of the clay fraction for the hygroscopic behaviour of the material. Figure 2.4 also indicates that total and matric suction data follow a unique curve suggesting that the osmotic component of suction can be neglected for both mixes.

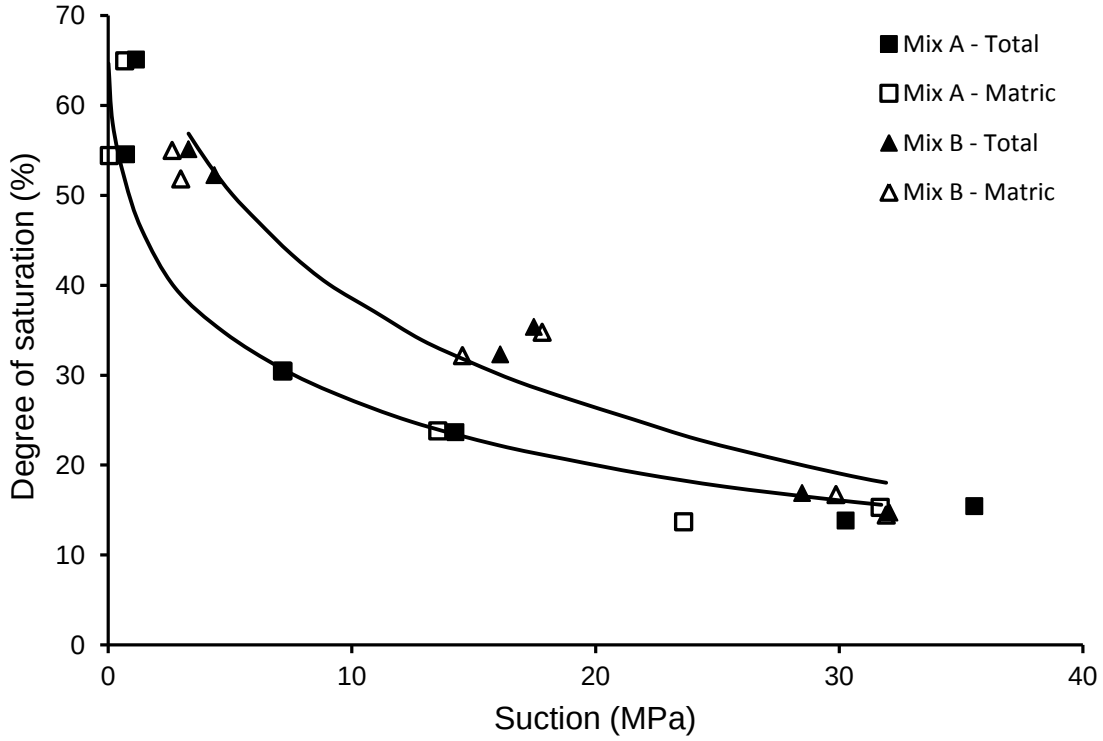

Figure 2.4. Drying curves for coarse earth Mix A and fine earth Mix B (after Jaquin et al. 2008)

A similar study was performed by Beckett and Augarde (2012) who tested two soil mixes consisting of 50% sand, 10% gravel and 40% clay (mix 5:1:4) and 70% sand, 10% gravel and 20% clay (mix 7:1:2). These two mixes contained the maximum and minimum amounts of clay as recommended by Houben and Guillaud (1996). The gravel content was, in both cases, the minimum recommended by Houben and Guillaud (1996). Samples were statically compacted in layers, at a water content of 12%, to a dry density between 1918 kg/m^3 and 1947 kg/m^3. The water content of 12% corresponds to the light Proctor optimum, which was approximately the same for both mixes. Inspection of Figure 2.5 indicates that the coarser 7:1:2 mix exhibits lower values of water content at the same suction compared to the finer 5:1:4 mix, a result consistent with that obtained by Jaquin et al. (2008).

In summary, both studies by Jaquin et al. (2008) and Beckett and Augarde (2012) indicate that fine earthen materials retain more water than coarser ones at the same suction. Note that, in both studies, the fine and coarse earth samples had approximately the same dry density and, hence, the same total pore volume. This implies that the difference in retention behaviour is only due to variations in the pore size distribution. The fine earth samples include a larger share of pores of small size and a lesser share of

pores of large size compared to the coarse earth samples for which the opposite is true. This explains why more water is retained by the fine earth samples compared to the coarse ones at any given suction. These results are directly linked to the moisture buffering properties of the two materials and have therefore important repercussions on their hygroscopic behaviour.

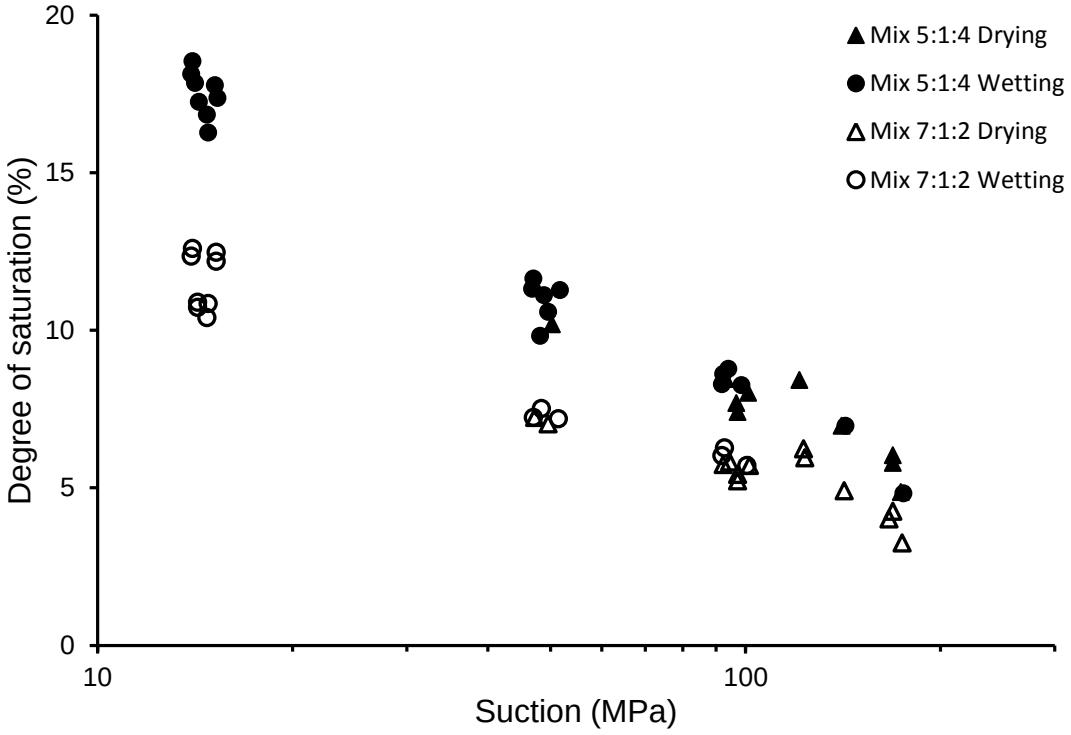

Figure 2.5. Drying curves for coarse earth Mix 7:1:2 and fine earth Mix 5:1:4 (after Beckett and Augarde. 2012)

2.1.2 Clay mineralogy

The hydro-mechanical behaviour of raw earth is significantly influenced by the nature of the clay fraction. Clays with different structures and chemical properties induce different responses to mechanical or environmental actions. "Two-layer" clays, such as kaolinite, are characterised by a relatively low specific surface (10 m^2/g). They therefore exhibit limited swelling/shrinkage upon wetting/drying but are also weak binders of the coarse fraction. Conversely, "three-layer" clays are characterised by a large specific surface (1000 m^2/g) and are therefore strong binders of the coarse fraction. The higher bonding capacity of three-layer clays compared to two-layer clay is due to their ability of generating higher suctions at the same moisture content. Three-layer clays are also

divided into two categories, i.e. swelling clays (Smectite) and non-swelling clays (Micas and Illite).

Although the type of clay employed during construction is often dictated by local availability, it is still important to have a good knowledge of clays properties in order to optimise application. For example, a two-layer clay fraction is best suited for surface coatings because of the reduced risk of cracking due to the limited occurrence of swelling/shrinkage upon wetting/drying. Conversely, for structural applications such as load-bearing walls, three-layer non-swelling clays are most appropriate because of their powerful binding properties. If locally available clays are unsuitable for the proposed application, natural fibres (commonly straw, flax, hemp and cellulose) can also be added to enhance inter-granular bonding and/or to reduce swelling/shrinkage while limiting environmental impact (Röhlen and Ziegert, 2013).

2.1.3 Plasticity

The consistency of an earthen material can vary from plastic to liquid depending on water content. The Atterberg limits are commonly employed to analyse the plasticity of a soil:

- The plastic limit w_p is the water content at which the behaviour of a soil changes from solid to plastic. This is determined by rolling threads of moist soil that break apart at a diameter of 3 mm according to the norm NF P94-051 (AFNOR, 1993).
- The liquid limit w_l is the water content at which the behaviour of a soil changes from plastic to liquid. The Casagrande cup and the fall cone test are the two standard techniques to measure the liquid limit w_l.
- The plasticity index I_p is defined as the difference between liquid limit and plastic limit and it represents the range of water content over which a soil exhibits plastic behaviour.

Delgado and Guerrero (2007) observed that most technical documents about earthen construction offer limited indications about soil plasticity. In general, the soils used for manufacturing rammed earth and compressed earth bricks tend to be low plasticity inorganic clays and inorganic silts of low and medium compressibility, while adobe construction requires more plastic soils with higher liquid limit and plastic index. In general, inorganic clays of medium plasticity are the most common. Figure 2.6 shows

the region of suitable plasticity values, together with the Casagrande plasticity chart, for compressed earth bricks according to Houben and Guillaud (1994) and the French norm XP P13-901 (AFNOR, 2001; CRATerre - EAG, 1998).

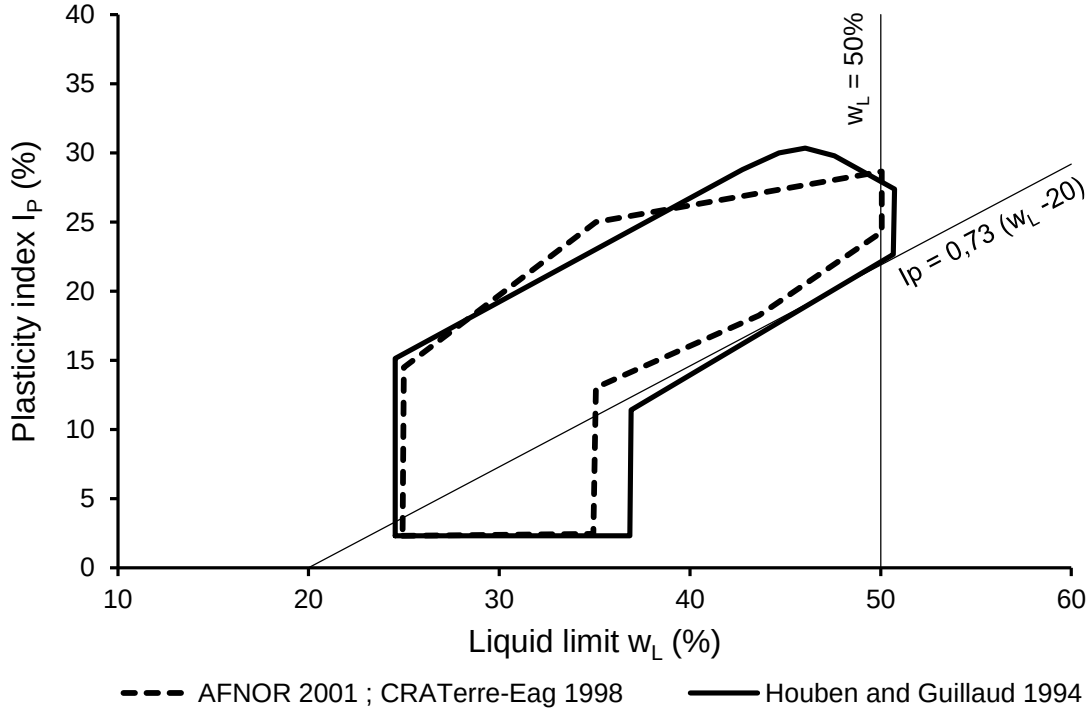

Figure 2.6. Plasticity chart: indications for CEB given by AFNOR (2001), CRATerre- EAG (1998) and Houben and Guillaud (1994)

2.1.4 Microstructural properties

Mercury intrusion porosimetry (MIP) is a powerful laboratory technique to investigate the microstructural properties of porous media. A wide range of properties, such as pore size distribution, porosity, dry and bulk density and specific surface area can be determined by means of MIP tests. These properties affect strongly the hydro-mechanical behaviour of earthen materials. Many authors (Haynes and Sneck, 1972; Maage, 1984; Robinson, 1984; Crooks et al., 1986; Winslow et al., 1988; Winslow, 1991) also observed that the durability of clay bricks depends on porosity and pore size distribution.

MIP is based on the principle that a non-wetting fluid, such as mercury, can be intruded in a porous media only if sufficient pressure is applied. After preliminary evacuation to remove moisture and air from the pore network, the pressure of mercury is increased

over the low range from 10 kPa to 200 kPa to intrude larger pores from 10^5 nm to 10^4 nm (low-pressure stage). After this, the pressure is increased up to 200 MPa to detect the smallest pores from 10^4 nm to 10^1 nm (high-pressure stage). At the end of the test, extrusion of mercury is performed by reducing the applied pressure.

Results from MIP tests can be used to determine both inter- and intra-aggregate pore volume by comparing the intruded and extruded volumes of mercury as shown in Figure 2.7. It is also possible to determine the pore entrance diameter that delimits the region of the inter-aggregate porosity from the region of intra-aggregate porosity (Tarantino and De Col, 2008). Variations of inter-aggregate porosity affect mainly material density and hence mechanical behaviour while intra-aggregate porosity controls hygroscopic behaviour of the material.

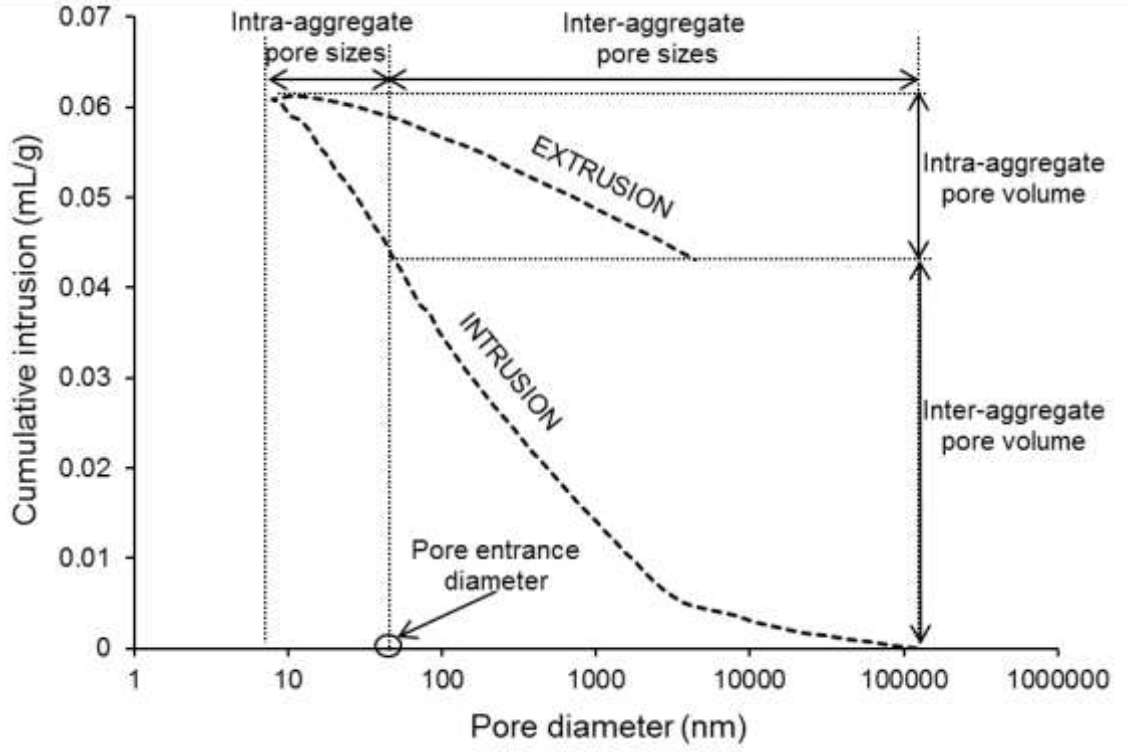

Figure 2.7. Inter- and intra- aggregate pore volume determined by MIP intrusion and extrusion (test taken from experimental campaign presented in Chapter 4)

M.J. de la Torre Lopez et al. (1996) analysed the microstructural properties of the materials constituting the walls of the Alhambra Palace. They performed MIP tests on three different materials: 1) the gray concrete, stabilised with lime and almost lacking in clay, 2) the so called "calicostrado" rammed earth wall, with high lime content in the outer part and a more clayey center, 3) the clay-packed earth, with low lime content in

both inner and outer parts of the wall. They found that materials with high lime content (i.e. gray concrete and outer part of the "calicostrado") have relatively low porosity (15-22%) and a maximum pore radius of around 0.1 μm. The materials with high clay content (i.e. inner part of "calicostrado" and clay-packed earth) showed a more heterogeneous porous system, a higher porosity of about 30% and also higher maximum pore sizes (1 – 0.1 μm).

MIP tests were also performed by Cuisinier et al. (2011) to study the effects of lime stabilisation on the microstructure of a silty soil. They stabilised the base earthen material by adding 2% and 3% of quicklime (QL) and 2.65% of hydrated lime (HL). Samples were compacted at both the optimum water content (OMC) and a wet moisture content (WMC = 1.2 x OMC) by two compaction procedures: Proctor standard (P) and Kneading compaction (K). Lime treated samples exhibited a higher optimum water content and a lower maximum dry density compared to untreated samples. From MIP tests, Cuisinier et al. (2011) observed that lime stabilisation induces formation of a new class of pores with a diameter lower than 3 x 10^3 Å (Figure 2.8). These pores are responsible for the difference in dry density between untreated samples and lime stabilised samples.

Other studies have focused on the effect of compaction on the porosity and fabric of fine-grained soils, such as silty clays (Garcia-Bengochea et al., 1979) or swelling clays (Nowamooz and Masrouri, 2010). These studies are most relevant to geotechnical applications but no extensive investigations exist about the compaction of coarser soils typically used for raw earth dwellings.

As previously mentioned, intra-aggregate pores control the hygroscopic behaviour of earthen materials . These nanometric pores cannot be investigated by MIP, which can only detect pore sizes between 10^1 nm and 10^5 nm. Smaller pores down to 2 nm can however be investigated by liquid nitrogen adsorption. This technique consists in measuring the pore volume from the amount of nitrogen adsorbed at a given pressure under a constant temperature of -196 °C. The relationship between the adsorbed/desorbed volume of nitrogen and the corresponding pressure is defined as the adsorption/desorption isotherm. The most common method to determine the pore size distribution and the specific surface area from adsorption/desorption isotherms is the Barret-Joyner-Halenda (BJH) method (Barret et al., 1951). Specific surface area can equivalently be determined by the Brunauer- Emmett- Teller (BET) method (Brunauer et al., 1938).

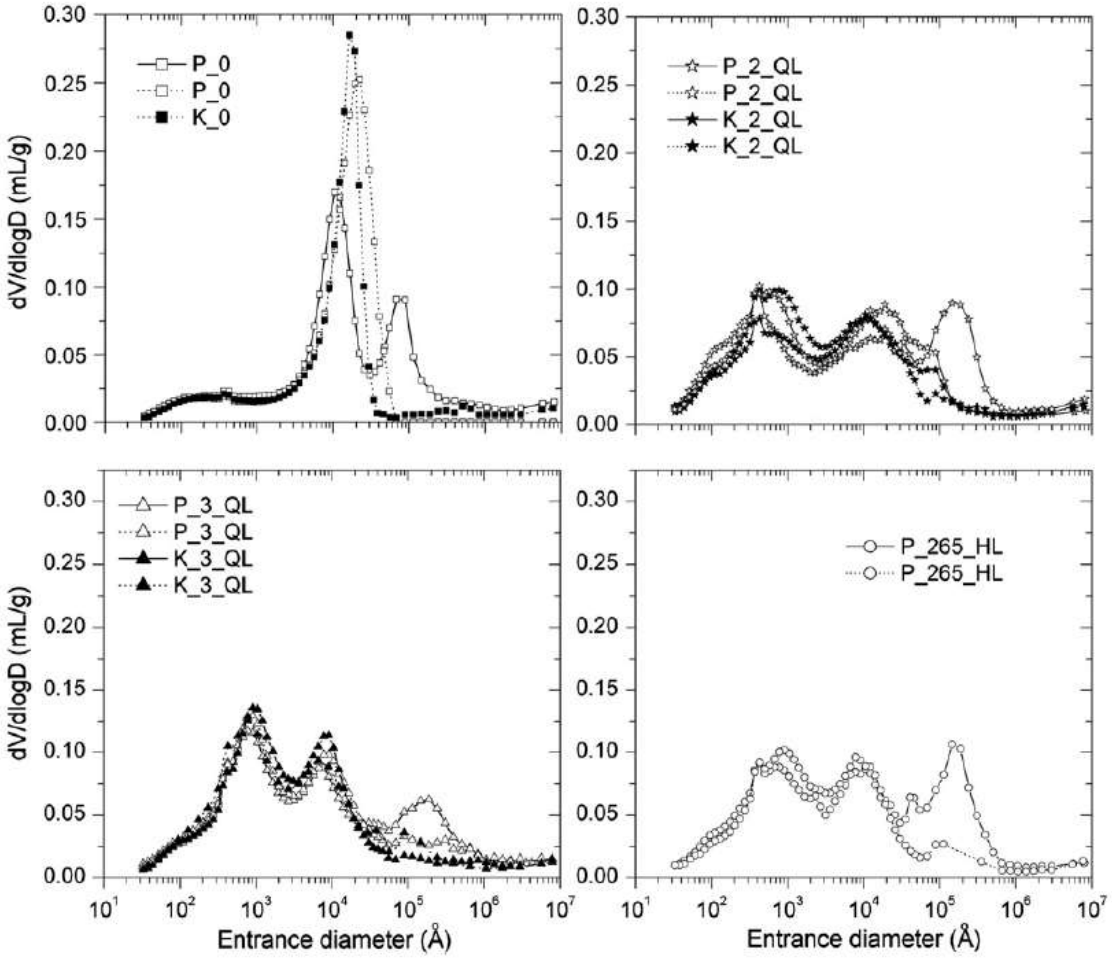

Figure 2.8. Pore size distribution of untreated and lime treated silty soil (dashed lines: WMC, solid lines: OMC) (Cuisinier et al., 2011)

In the present wok, both MIP and nitrogen adsorption tests are used to investigate the material fabric of samples manufactured according to a new hypercompaction procedure. Results from these tests have also aided interpretation of the macroscopic mechanical behaviour and moisture buffering capacity of the material as measured during the present experimental campaign.

2.2 Mechanical behaviour

This section reviews past studies about the mechanical behaviour of earthen materials. In particular, the mechanical properties are presented by subdividing them in serviceability state properties and ultimate state properties.

2.2.1 Serviceability state: Young modulus and Poisson ratio

During its lifetime, a building material is subjected to loads that will produce deformation even far from failure. The study of the stress-strain relationship at relatively low loads allows the determination of the properties relevant to serviceability states.

Kouakou and Morel (2009) investigated the mechanical behaviour of both traditional adobe blocks and pressed adobe blocks (BAP- "Bloques d'Adobe pressés") fabricated from an earth mix of 44.5% sand, 30.0% silt and 25.5% clay with a liquid limit of 38% and a plasticity index of 18%. Traditional adobe blocks were manufactured by pouring the earth mix at high water content inside wooden moulds with dimensions of 310 x 150 x 73 mm^3 and subsequently drying the demoulded blocks to the sun. Pressed adobe blocks were instead manufactured at much lower water contents and compressed to 2 MPa for increasing density.

They performed three loading- unloading cycles on both traditional adobe blocks and pressed adobe blocks to measure deformation. Results indicated that material behaviour is not elastic, but residual strains accumulate over subsequent cycles (Figure 2.9). Kouakou and Morel (2009) also subdivided the stress-strain curves into two parts: an initial adjustment phase in which the press plates and the sample enter into contact (point A in Figure 2.9) and a subsequent phase until failure. Two different stiffness moduli are also defined by these authors: the initial tangent modulus E_t and the equivalent modulus E_{eq}. The former is determined from the very first loading path while the latter is obtained from subsequent cycles.

Kouakou and Morel (2009) observed that both moduli do not vary significantly with the dry density of the BAP (Figure 2.10). The authors also remarked that this result is against expectation because an increase of dry density should intuitively produce an increase of stiffness. Moreover, the fact that equivalent modulus E_{eq} is about two times higher than the initial tangent modulus E_t confirms the elasto-plastic nature of material behaviour. In particular, the plastic strains during loading-unloading cycles produce an increase of the measured stiffness.

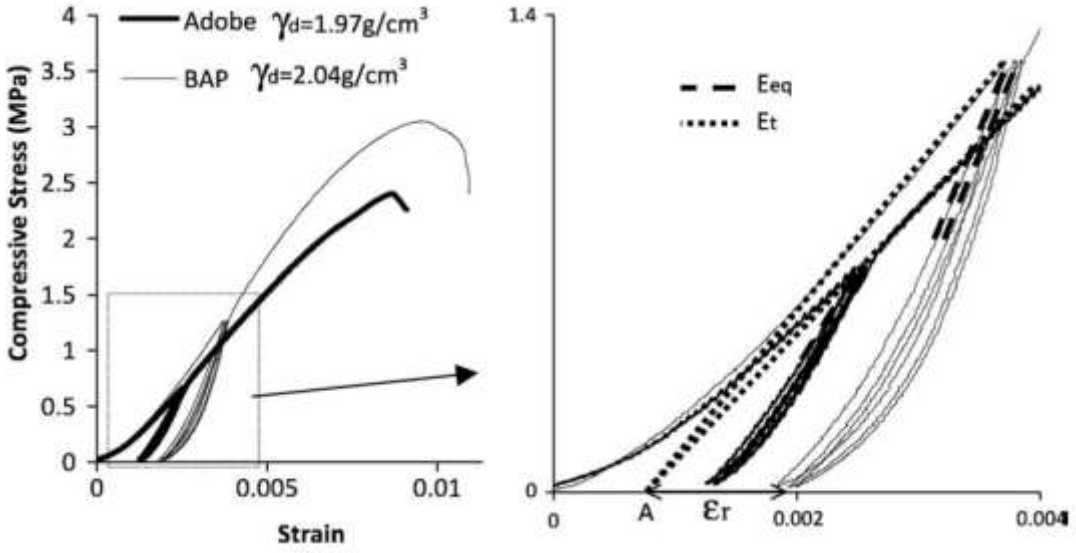

Figure 2.9. Stress-strain curve for Adobe and BAP (Kouakou and Morel, 2009)

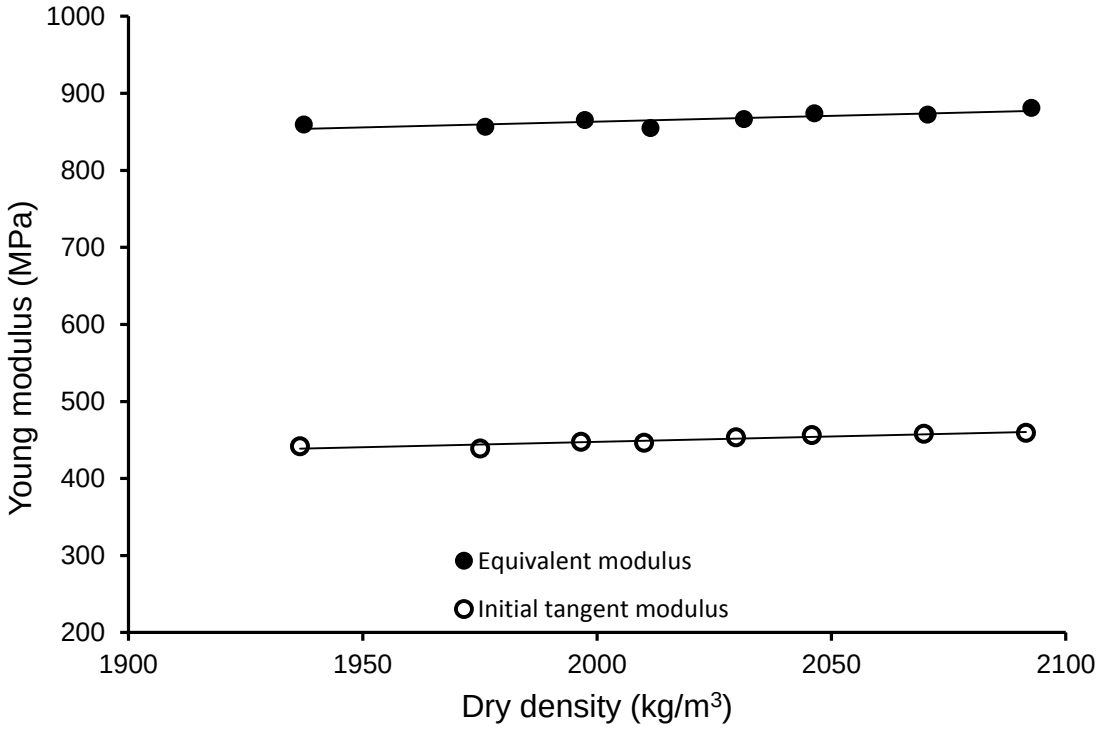

Figure 2.10. Initial tangent modulus and equivalent modulus of BAP (after Kouakou and Morel, 2009)

Another study by Bui et al. (2014) investigated the effects of moisture content on the mechanical properties of three different rammed earth mixes. Table 2.1 summarises the grain size distribution of the three materials: material A and C are both unstabilised earths while material B is a stabilised earth with 2% in weight of natural hydraulic lime (NHL).

Bui et al. (2014) compacted earthen samples according to the standard Proctor method at a water content ranging between 11% (to simulate the wet state immediately after manufacturing) and 2% (to simulate the dry state in equilibrium with atmospheric conditions). They showed that the material behaviour is approximately linear elastic only at very low stresses (below 15% of the compressive strength). Beyond this limit, plastic strains occur and hence the secant Young modulus reduces as the stress increases. Bui et al. (2014) calculated the secant Young modulus for stress levels between 0% and 20% of the compressive strength. They found that the material stiffness drops when moisture content increases above 5% for earth A (sandy soil) and earth B (stabilised soil). Instead, for earth C (clayey soil), stiffness starts to reduce as soon as water content is increased (Figure 2.11).

Bui et al. (2014) also determined the Poisson ratio of the three materials by using a transducer to measure lateral strains of the sample under axial compression. Poisson ratio increases on average from 0.2 to 0.37 as moisture content increases from 2% to 11% for all materials, as shown in Figure 2.12. This means that for a given axial displacement, earthen materials exhibit larger lateral expansions at higher water contents.

Table 2.1. Grain size distribution of tested materials (after Bui et al., 2014)

	Clay	Silt	Sand	Gravel
Earth A	5 %	30 %	49 %	16 %
Earth B + 2% NHL	4 %	35 %	59 %	2 %
Earth C	9 %	38 %	50 %	3 %

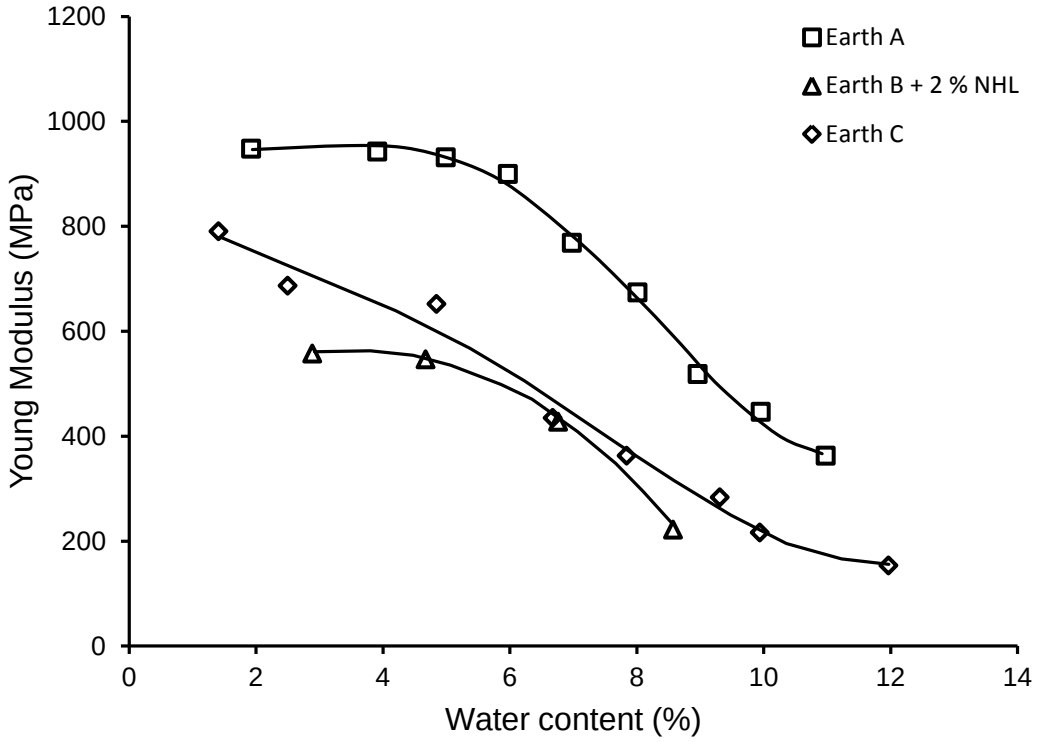

Figure 2.11. Variation of Young modulus with water content (after Bui et al., 2014)

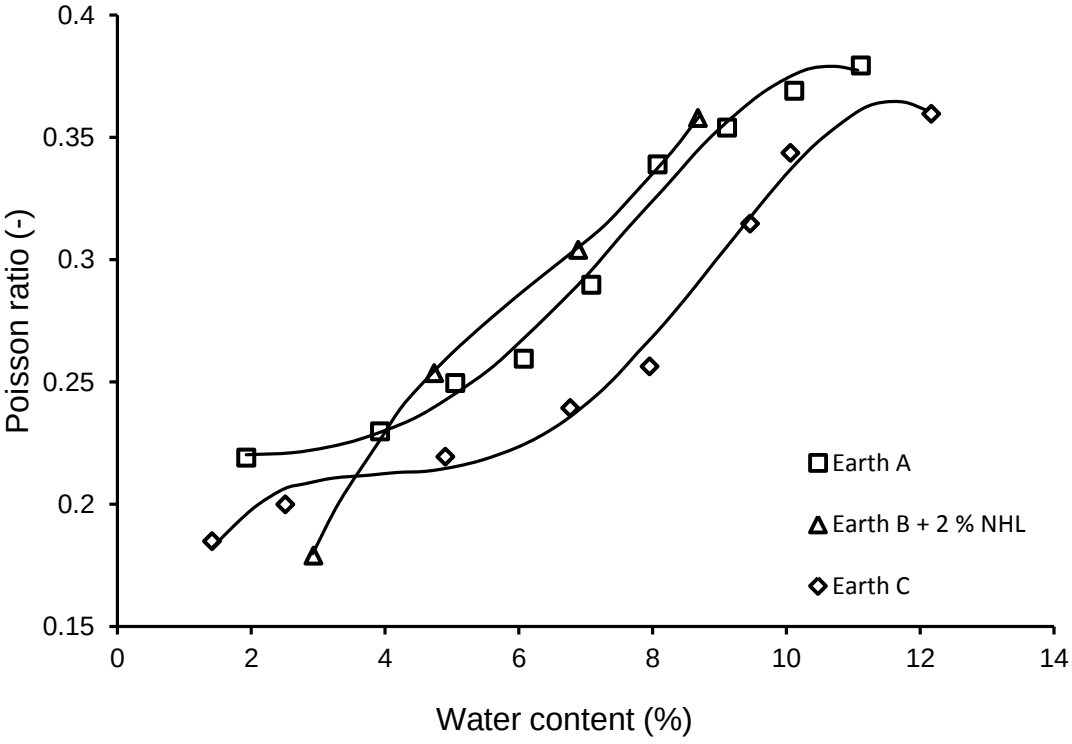

Figure 2.12. Variation of Poisson ratio with water content (after Bui et al., 2014)

For isotropic linear elastic materials, the Young modulus, E and the Poisson ratio, ν are combined to calculate the shear modulus, G by means of the following relationship:

$$G = \frac{E}{2(1+\nu)} \tag{2.1}$$

Application of Equation 2.1 to earthen materials is however not immediate due to their heterogeneity and anisotropy induced by the manufacturing process (i.e. compaction, extrusion, etc.).

A study by Bui and Morel (2009) assessed the anisotropy of rammed earth materials. They manufactured earth blocks (20 x 20 x 40 cm^3 with aspect ratio of 2) in three layers to simulate rammed earth construction. These blocks were tested under uniaxial compression in two perpendicular directions, which showed that both stiffness and strength are independent of load direction until the formation of the first crack between adjacent layers. Only after cracking, mechanical behaviour starts to depend on the load direction. Thus, Bui and Morel (2009) concluded that rammed earth can be considered as an isotropic material as long as the constituting layers remain intact.

2.2.2 Ultimate state: compressive strength

The unconfined compressive strength of compacted earth is a key property whose measurement can be affected by many factors such as test procedure, sample geometry (e.g. aspect ratio) and, of course, material properties (e.g. dry density, moisture content, stabiliser content).

According to Morel et al. (2007), three tests are commonly employed to measure the strength of compressed earth blocks, namely the direct unit strength test, the RILEM test and indirect tests.

The direct unit strength test consists in loading one brick between press plates. Bricks are tested in the direction in which they are compacted and subsequently loaded. Since brick surfaces are generally flat and parallel, only a thin plywood sheet is needed for capping the sample. A minimum number of five tests is required.

The RILEM Technical Committee 164 (1994) proposed to double slenderness by halving the brick and stacking the two halves with an earth mortar joint. The RILEM test replicates masonry construction but tends to underestimate the compressive strength of the individual brick. This is because the mortar joint, even if made of the same

material as the brick, is weaker and, under compression, expands more than the brick itself. This means that the brick is no longer subjected to uniform compression, which reduces strength. Also, results depend highly on the quality of workmanship in assembling the brick halves and the mortar joint.

Compressive strength can also be determined by means of indirect tests developed to facilitate in-situ quality control. The most common indirect test is the three-point bending test. A compressed earth brick is simply supported at the two extremities and subjected to a single point loading at the centre until failure. The correlation between compressive strength and three-point bending strength is not perfect but it is generally possible to obtain a lower bound of compressive strength from the flexural strength (Morel et al., 2007).

The friction between press plates and sample faces affects measurements of compressive strength. This friction can be reduced by capping the sample with a thin layer of plaster or by interposing a plywood sheet between the sample and the press plates (Ciancio and Gibbings, 2012). Also, Teflon spray can be smeared on the press plates before testing in order to limit friction.

Geometry can also affect the measured values of compressive strength. Test results depend mainly on the aspect ratio between height and width of the block. This is because the friction between press plates and sample faces creates stronger confinement for samples with a lower aspect ratio, thus generating an apparent increase of strength. Measured values of compressive strength are either directly accepted regardless of geometrical effects or corrected by a factor dependent on aspect ratio. Correction factors for fired clay bricks are often extended to compressed raw earth bricks (Krefeld, 1938). Specific correction factors for compressed earth bricks have been proposed in other works (Heathcote and Jankulovski, 1992). Both of these sets of correction factors are presented in Table 2.2.

Table 2.2. Aspect ratio correction factors

Aspect ratio	0	0.4	0.7	1.0	3.0	≥5.0
Krefeld (1938)	0	0.50	0.60	0.70	0.85	1.00
Heathcote and Jankulovski (1992)	0	0.25	0.40	0.58	0.90	1.00

Another study by Aubert et al. (2016) measured the compressive strength of extruded earth bricks by varying specimen size, orientation and use of Teflon plates. They also

tested dry-sawn specimens, half-bricks and entire bricks. The main purpose of this study was to propose a simple method to measure the compressive strength of earth bricks. Results indicated that:

- Measurements of compressive strength on dry-sawn samples are not reliable. Preparation of samples is complicated and poses health and safety problems. Vibrations generated by dry-sawing damage the specimens.
- Compressive strength is dependent on loading direction: samples showed higher resistance when loaded in the direction perpendicular to the extrusion plane. This is due to the orientation of clay platelets in the direction of extrusion.
- The use of cement mortar can affect the mechanical behaviour of the brick because of the sensitivity of earthen materials to water. Also, results are highly dependent on workmanship. Tests on half-bricks without mortar are easier and more reliable but require flat and parallel surfaces.
- Test on entire bricks can provide consistent results but only if the load is applied on the smaller side face of the brick. In fact, if the load is applied on the laying surface, the strong confinement leads to abnormal increases of the measured compressive strength (Aubert et al., 2013).

Aubert et al. (2016) concluded that the best way to measure compressive strength is to test entire bricks on surfaces other than the laying surface. This conclusion is drawn from tests on extruded earth bricks and further experiments are needed to extend this conclusion to bricks manufactured using different methods (i.e. moulded or compressed).

The study by Aubert et al. (2016) has been extended, in the present thesis, to the case of hypercompacted earth bricks. Compressive strength tests have been performed by varying parameters such as brick orientation or sample capping. Tests have also been performed on half-bricks, with or without a cement mortar joint, as well as on cubic specimens to investigate the effects of anisotropy. These results are presented and discussed in Chapter 5.

2.2.3 Effect of dry density on compressive strength

A number of studies have investigated the relationship between earth density and compaction effort. It is well known that, for a given compaction effort, there exist an optimum value of moisture content at which dry density is maximum. Geotechnical

structures, such as dams or embankments, are built at the optimum water content corresponding to standard Proctor compaction, which is considered representative of the compaction effort applied during construction of these structures. Similar to geotechnical structures, the mechanical performance of raw earth greatly improves as dry density increases. Many studies analysed the influence of the compaction energy on the mechanical properties of earthen materials (Olivier and Mesbah, 1986; Venkatarama Reddy and Jagadish, 1993; Attom, 1997; Mesbah et al., 1999; Kouakou and Morel, 2009). They all agree that stronger compaction increases dry density, and hence strength.

Olivier and Mesbah (1986) studied the effect of compaction pressure on the mechanical properties of the "Isle d'Abeau" earth (50% sand, 33% silt and 17% kaolinitic clay). Cylindrical samples with a diameter of 11 cm and a unitary aspect ratio were produced by static double compaction at different pressure levels from 1.2 MPa to 10 MPa. For each compaction pressure, Olivier and Mesbah (1986) tested different water contents to determine the optimum water content and the corresponding maximum dry density. They observed that compaction curves shift towards lower values of water content as the compaction stress increases (Figure 2.13). After compaction, samples were stored at constant temperature (27 °C) and relative humidity (60%) and then tested under unconfined compression until failure. Results confirmed that compressive strength increases as dry density increases (Figure 2.13).

Another study by Morel et al. (2007) investigated the mechanical characteristics of compressed earth blocks and showed that strength strongly increases with increasing dry density (Figure 2.14) for both unstabilised and stabilised earth. This is true regardless of whether non-swelling "two-layer" clays (e.g. kaolin) or swelling "three-layer" clays (e.g. bentonite) are prevalent in the fine fraction of the earthen material.

Also, Kouakou and Morel (2009) investigated the compressive strength of both traditional adobe blocks and pressed adobe blocks (BAP), whose properties have already been described in Section 2.2.1. They found that unconfined compressive strength increases more than linearly with increasing dry density (Figure 2.15), which implies that any further small gain in dry density may lead to large gains in strength.

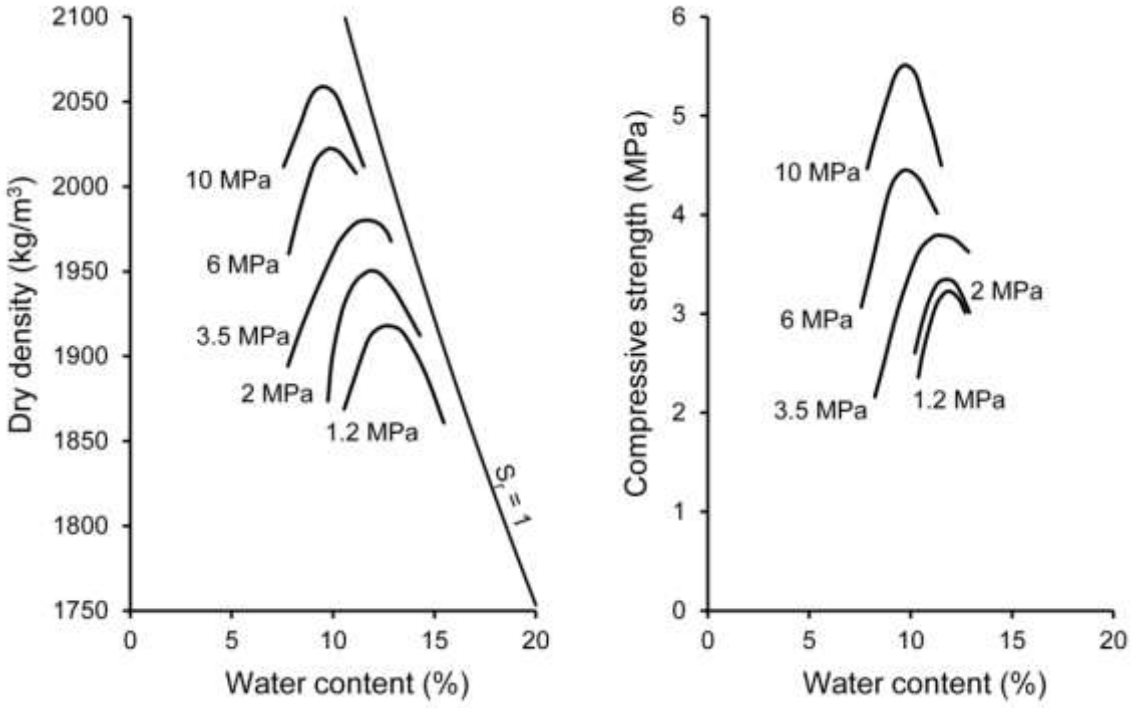

Figure 2.13. Compaction curves and variation of compressive strength with water content and compaction pressure (after Olivier and Mesbah, 1986)

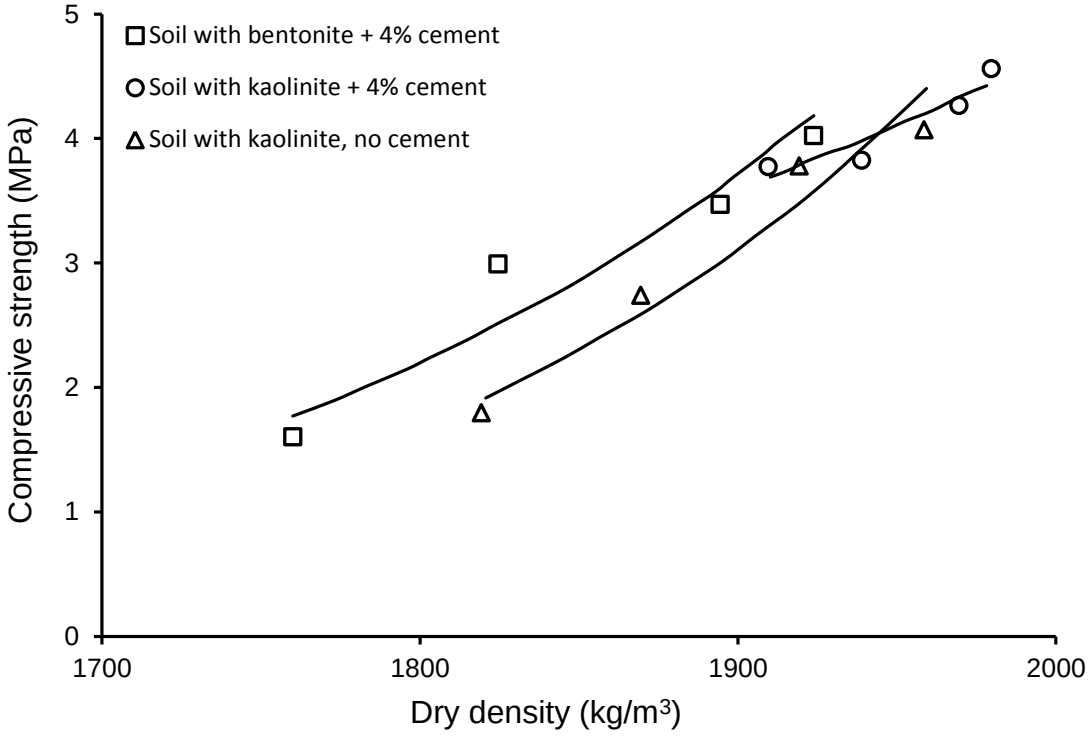

Figure 2.14. Variation of compressive strength with dry density (after Morel et al., 2007)

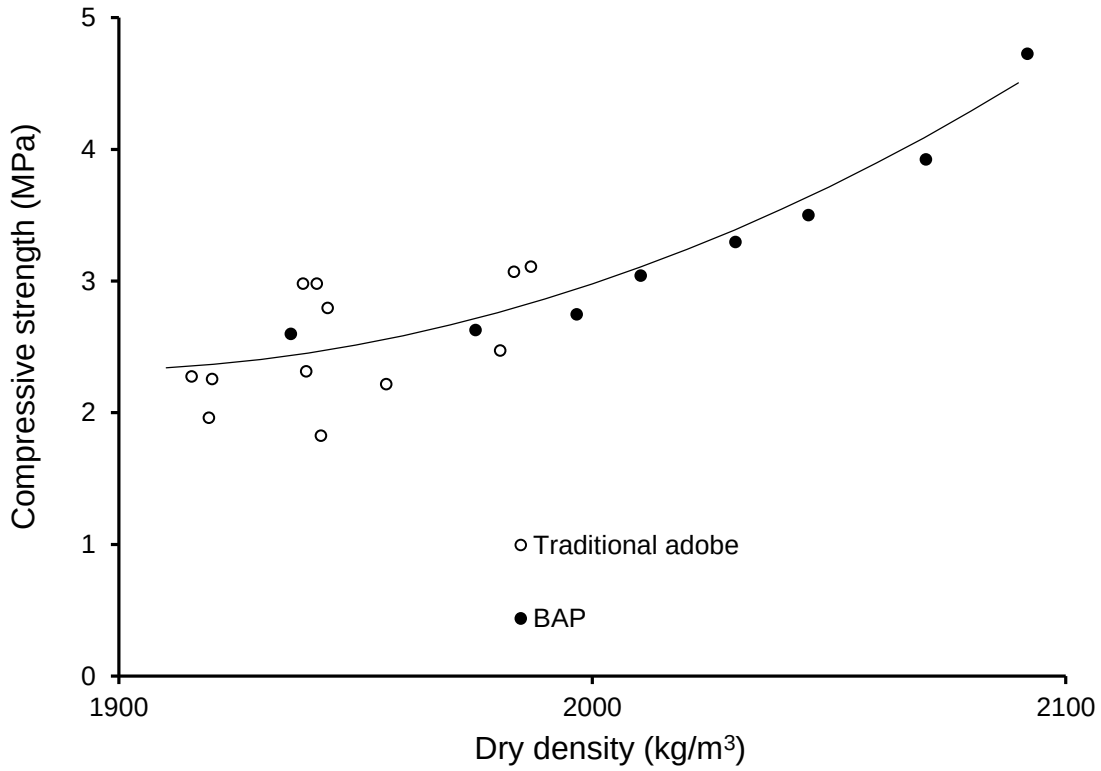

Figure 2.15. Variation of compressive strength with dry density (after Kouakou and Morel, 2009)

In the present work, an innovative hypercompaction procedure has been devised to increase the dry density of the material and hence to improve mechanical performance. This compaction procedure as well as results from mechanical tests are presented and discussed in Chapters 3 and 5, respectively.

2.2.4 Effect of ambient humidity and temperature on compressive strength

The inner and outer surfaces of a building envelope are usually exposed to very different ambient conditions, which may lead to gradients of temperature, humidity and suction across earthen walls. To date, no study has been undertaken about the effect of hygro-thermal gradients on the mechanical performance of earthen structures, with the only exception of few targeted investigations on the effect of humidity and temperature on strength and stiffness.

Bui et al. (2014) tested the effects of moisture content on the compressive strength of the three earthen materials whose properties have already been presented in Table 2.1.

They found that for moisture contents below 4% (which is a typical value of moisture content in equilibrium with atmospheric conditions) compressive strength remains constant. When moisture content was greater than 4%, compressive strength decreases quickly for all tested materials. Moreover, stabilisation by natural hydraulic lime reduced the sensibility to water of the earthen material. In comparison with earth A and earth C, the stabilised earth B showed a smaller decrease of compressive strength as water content increased. On the other hand, stabilisation with low percentages of natural hydraulic lime does not lead to an improvement of mechanical performance (Figure 2.16).

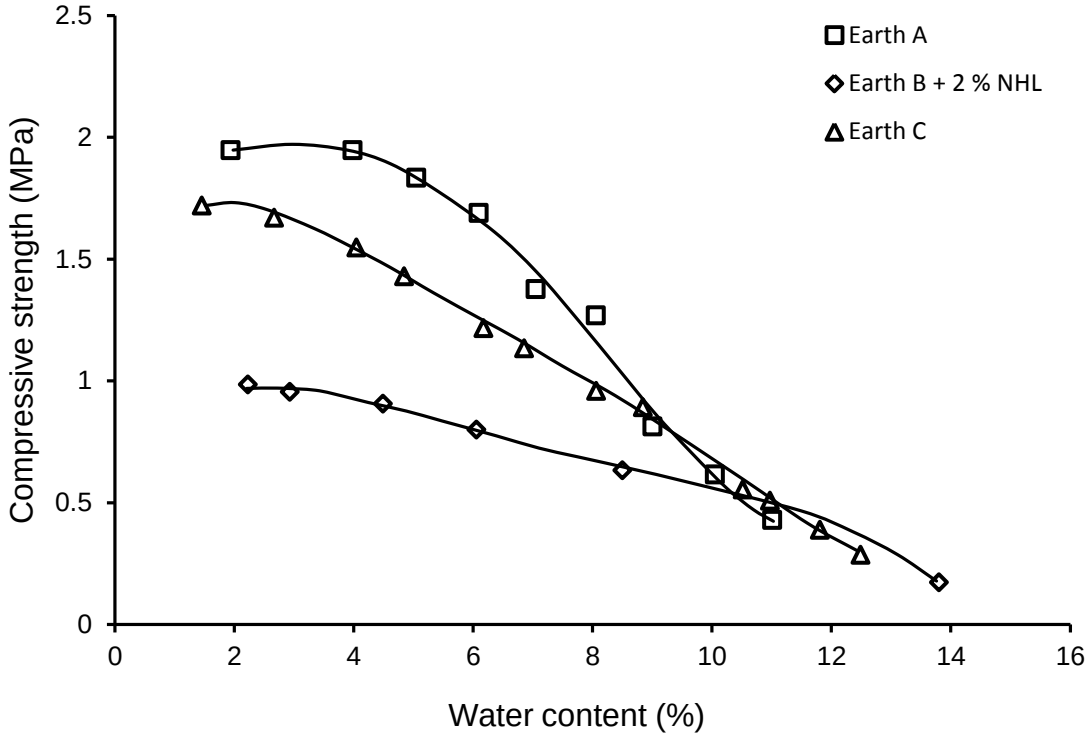

Figure 2.16. Variation of compressive strength with water content (after Bui et al., 2014)

Dierks and Ziegert (2002) showed that unconfined compressive strength of earthen materials reduces significantly as ambient humidity increases. This is shown in Figure 2.17, where the original measurements of relative humidity by Dierks and Ziegert (2002) have been converted in suction values by means of Kelvin equation assuming a constant ambient temperature of 25 °C. Inspection of Figure 2.17 indicates that, for this particular material, the compressive strength reduces from about 5.7 MPa at a humidity of 5% (suction of 405 MPa) to about 2.3 MPa at a humidity of 95% (suction of 7 MPa).

This means that environmental conditions must be duly accounted during design of earthen structures.

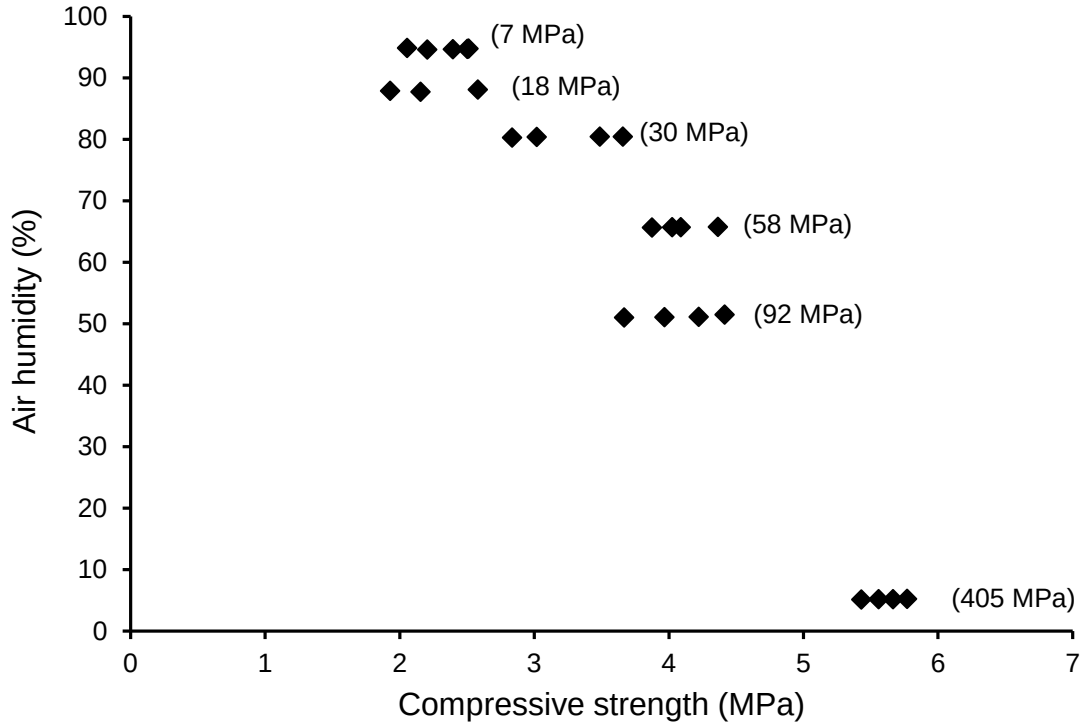

Figure 2.17. Variation of compressive strength with air humidity and suction (after Dierks and Ziegert, 2002)

Similar results were obtained by Beckett and Augarde (2012), who investigated the unconfined compressive strength of raw earth samples equalised at different levels of temperature (15, 20, 30 and 40 °C) and relative humidity (30, 50, 70 and 90%). The tests were performed on the same two earth mixes, i.e. mix 5:1:4 and mix 7:1:2, described in Section 2.1.1. Figure 2.18 indicates that strength is always larger for the earth mix with lower clay content and it increases with decreasing humidity and increasing temperature. On the basis of these results, Beckett and Augarde (2012) concluded that "lower clay content materials should be considered for rammed earth construction in order to provide sufficiently strong materials in more humid conditions".

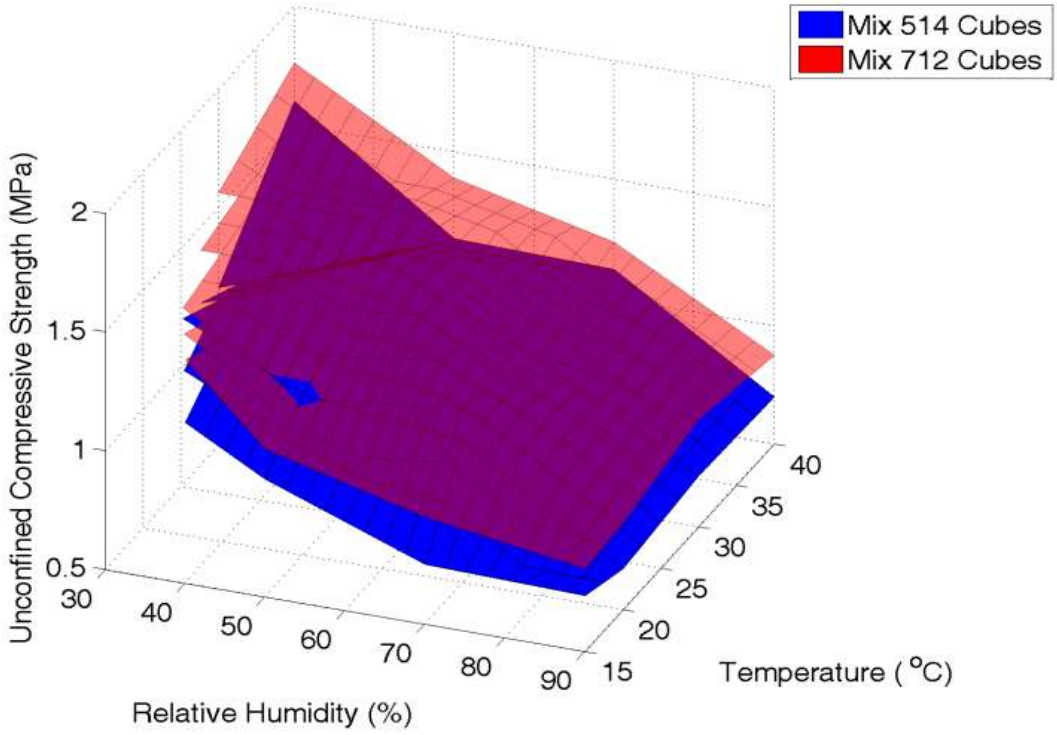

Figure 2.18. Variation of compressive strength with relative humidity and temperature (Beckett and Augarde, 2012)

By assuming thermodynamic equilibrium, the pore water suction can be calculated from the imposed values of temperature and humidity via Kelvin law. The domain of temperature and humidity investigated by Beckett and Augarde (2012) can therefore be reduced to a suction range from 14 MPa to 174 MPa. The unconfined compressive strength is re-plotted against soil suction in Figure 2.19 for both soil mixes. Although mix 7:1:2 showed higher compressive strength than mix 5:1:4, all data are here fitted by a single interpolating linear relationship. Figure 2.19 also shows the results obtained by Bui et al. (2014), already presented in Figure 2.16, and additional data from Jaquin et al. (2009). The data by Beckett and Augarde (2012) exhibit lower values of strength compared to Bui et al. (2014) and Jaquin et al. (2009). This result is particularly interesting because the samples tested by Beckett and Augarde (2012) and Bui et al. (2014) are very similar in terms of both dry density and particle size distribution, which means that any difference in strength must be attributed to either mineralogy or sample size.

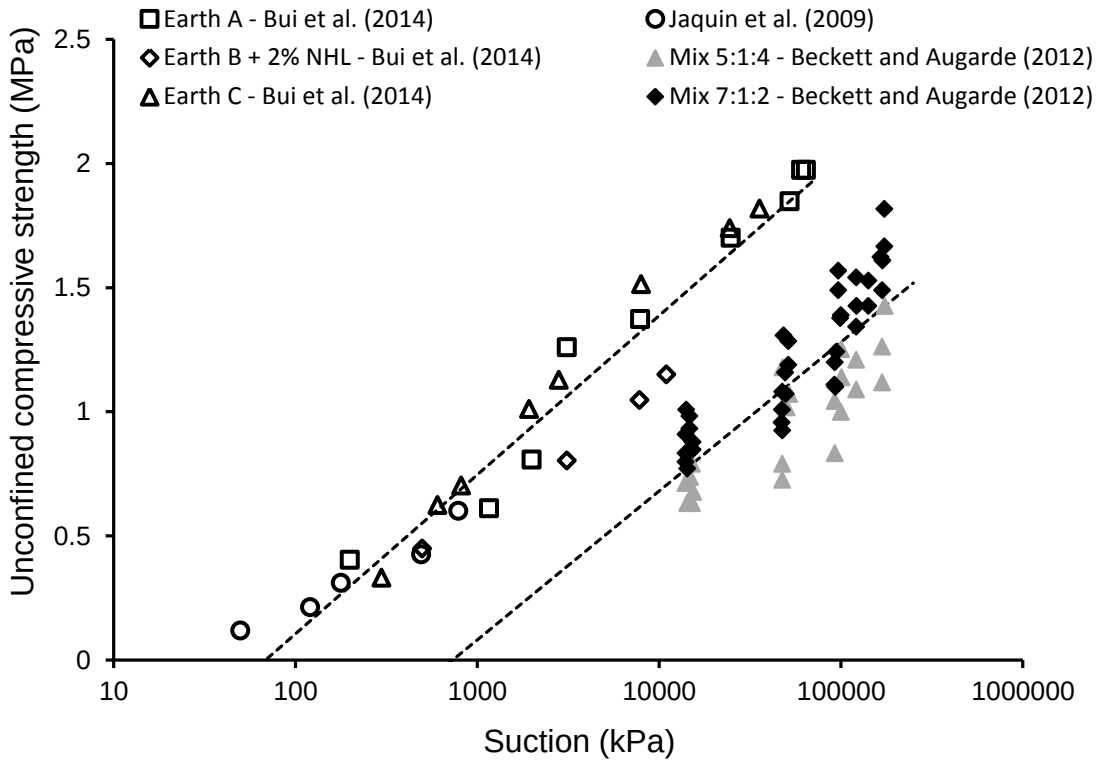

Figure 2.19. Variation of compressive strength with suction: comparison between Bui et al. (2014), Jaquin et al. (2009) and Beckett and Augarde (2012)

In this thesis, the mechanical behaviour of unstabilised and stabilised earthen samples has been investigated at different levels of relative humidity and the relevant results are presented and discussed in Chapter 5.

Raw earth has attracted the interest of civil engineers and architects also because of its capacity of regulating hygrothermal conditions inside buildings through exchanges of vapour with the surrounding environment. The next section focuses on the moisture buffering capacity of earthen materials by reviewing some of the most relevant studies in the literature.

2.3 Moisture buffering capacity

Building materials can adsorb and desorb water vapour, thus reducing extreme fluctuations of indoor humidity and improving health and comfort of occupants. The capacity of adsorbing/releasing water vapour is described by the Moisture Buffering Value of the material. Rode et al. (2005) defined the Moisture Buffering Value at three distinct levels: material level, system level and room level.

- At material level, the moisture buffering capacity is theoretically defined based on individual properties of every material component
- At system level, the moisture buffering capacity is obtained assuming the material as homogeneous and is experimentally determined according to the interactions with the surrounding environment
- At room level, the moisture buffering capacity is dependent on both building and furnishing materials. Moisture load, ventilation rate and others indoor climate factors influence the overall moisture buffering characteristics.

Rode et al. (2005) also proposed a theoretical and a practical definition of the moisture buffering capacity.

The theoretical definition is based on the determination of basic material characteristics (water vapour permeability, dry density, porosity, sorption isotherm). This method provides a measurement of the ideal moisture buffering value MBV_{ideal}.

The practical definition is instead:

> *"The practical Moisture Buffering Value MBV indicates the amount of water that is transported in or out of a material per open surface area, during a certain period of time, when it is subjected to variations in relative humidity of the surrounding air. When the moisture exchange during the period is reported per open surface area and per %RH variation, the result is the $MBV_{practical}$. The unit for $MBV_{practical}$ is kg/m^2 %RH"*

The determination of $MBV_{practical}$ is obtained by subjecting samples to cyclic variations of relative humidity at constant temperature. High and low levels of relative humidity are alternated to simulate daily changes of indoor climate. Several testing procedures have been proposed that differ for the humidity levels applied and the duration over which humidity levels are maintained. In all cases, the $MBV_{practical}$ is determined as follows

$$MBV_{\text{practical}} = \frac{\Delta m}{S\ \Delta\%RH} \tag{2.2}$$

Where, Δm is the variation of sample mass owed to the change in relative humidity, S is the exposed surface and $\Delta\%RH$ is the difference between the high and the low levels of relative humidity.

Rode et al. (2005) also proposed a specific procedure to determine the practical Moisture Buffering Value (MBV). This procedure is based on performing asymmetric cycles of relative humidity inside a climatic chamber: 8 hours of high relative humidity (75%) are followed by 16 hours of low relative humidity (33%). The choice of relative humidity levels can affect the measurement of MBV, thus tests should be performed in a range that is relevant to the chosen application. Moreover, relative humidity cycles must be performed at a constant temperature (usually the chosen temperature is 23°C). Samples should have an exposed area higher than 0.01 m^2. The MBV test is considered completed when the last three cycles become stable, i.e. the moisture uptake at high humidity is equal to the moisture release at low humidity. Following this procedure, three institutions (Technical University of Denmark (DTU), Norwegian Building Research Institute (NBI) and Technical Research Centre of Finland (VTT)) determined the practical MBV of different building materials in the frame of the NORDTEST project. In Figure 2.20, each bar represents the average MBV measured on three samples of the same material over three stable cycles. The thin vertical lines indicate the standard deviation.

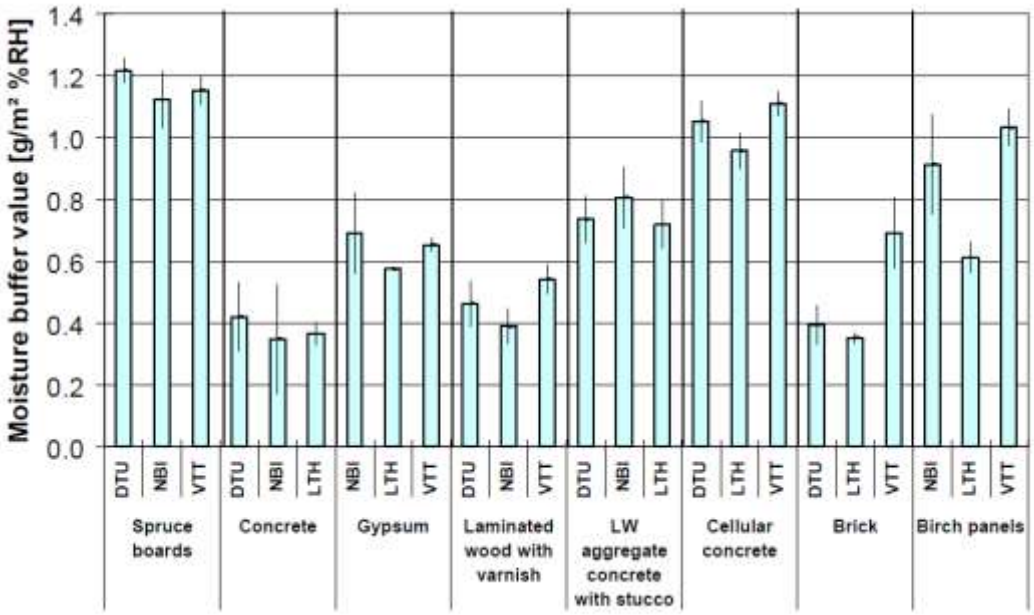

Figure 2.20. MBV measured by DTU, NBI and VTT measured on different construction materials (Rode et al., 2005)

It is remarkable that different laboratories obtained very similar values of MBV for all tested materials, thus indicating that the test procedure leads to meaningful and repeatable results. Untreated spruce boards and cellular concrete showed a good

capacity to buffer humidity while bricks and concrete performed poorly, showing a MBV lower than 0.4 g/m^2 %RH.

Rode et al. (2005) also classified building materials in five different categories depending on their MBV. These categories are summarised in Table 2.3.

Table 2.3. Ranges for MBV categories

Moisture buffering capacity	MBV_{MIN}	MBV_{MAX}
Negligible	0	0.2
Limited	0.2	0.5
Moderate	0.5	1.0
Good	1.0	2.0
Excellent	2.0	…

McGregor et al. (2014) measured the moisture buffering capacity of unstabilised and stabilised compressed earth blocks. Stabilisation was obtained by adding Portland cement CEM I, air lime CL90 or dissolved NaOH (Sodium Hydroxide) to the soil mix. In the case of cement and lime, a stabiliser content of 4% and 8% per dry weight was added. According to the indications given by Davidovits (2011) on geopolymer composition, 3% per dry weight of dissolved NaOH was added to the mix. Samples were statically compacted by using a press with a capacity of 50 kN inside a standard Proctor mould.

McGregor et al. (2014) determined the MBV of unstabilised and stabilised earthen samples by performing different cycles of relative humidity. The cycles of relative humidity used by McGregor et al. (2014) are variations of the test procedures proposed by the NORDTEST project, the norm ISO 24353 (2008) and the Japanese Industrial Standard (2002), as summarised in Table 2.4.

Table 2.4. Testing conditions: humidity control environment (McGregor et al., 2014)

RH (%)	Time step (h)
85/50	8/16
75/53	8/16
75/53	12/12

Figure 2.21 shows that the cycle 85%(8h)/50%(16h) provides the highest MBV compared with the other two cycles. This is due to the large interval of relative humidity which corresponds to large variations of moisture content inside the material as also

shown by the sorption/desorption isotherms in McGregor et al. (2014). The lowest MBV is obtained for the cycle where the relative humidity of 75% is kept for only 8 hours. Because the MBV is dependent on the test procedure (i.e. humidity levels, time), a comparison between different materials is only possible, if the same test procedure is adopted.

Regardless of test procedure, unstabilised earthen materials exhibited the highest MBV (Figure 2.21). In particular, the effect of cement and lime stabilisation is very similar while NaOH stabilisation induced the largest reduction of MBV.

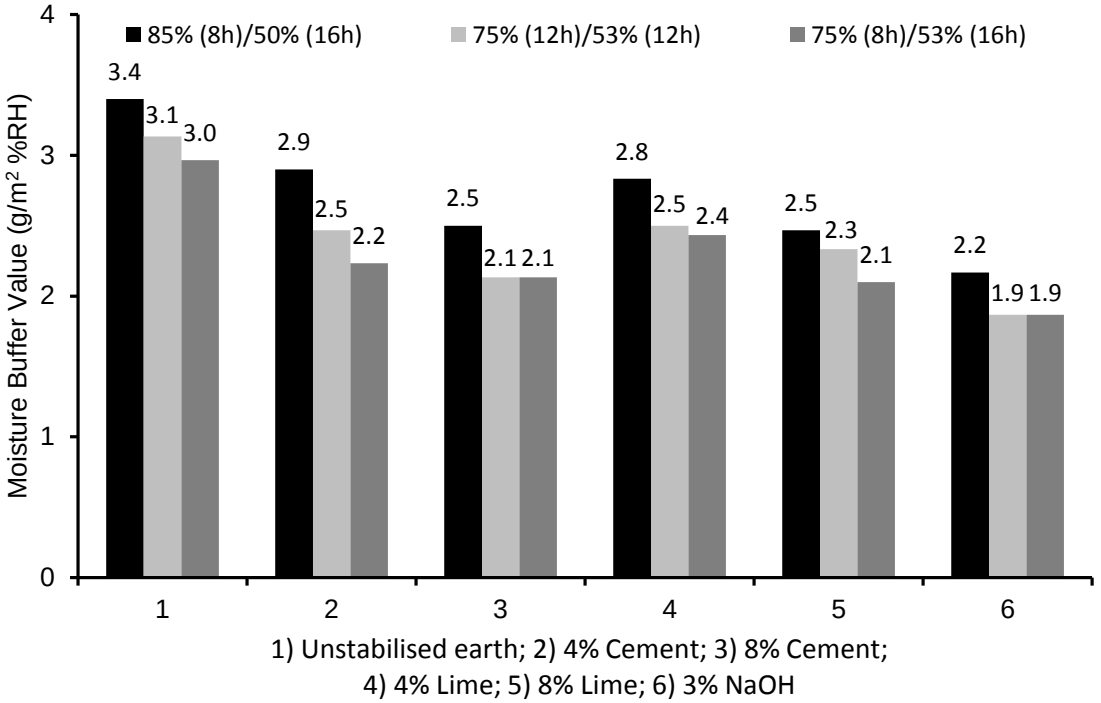

Figure 2.21. MBV measured on unstabilised and stabilised earthen samples: comparison between different test procedures (after McGregor et al., 2014)

McGregor et al. (2016) reviewed the moisture buffering capacity of various earthen materials. They observed that earth plasters have a moisture uptake that ranges from 30 to 70 g/m^2 which is well above that of more traditional plasters such as lime or gypsum plasters (Figure 2.22). McGregor et al. (2016) remarked that compressed earth bricks perform better than earthen plaster with a moisture sorption that ranges from 60 to 160 g/m^2. This is probably due to the presence of a small fraction of swelling clays in the earth bricks. On the contrary, earthen plasters cannot contain any swelling clay because the swelling/shrinkage upon wetting/drying would induce cracking.

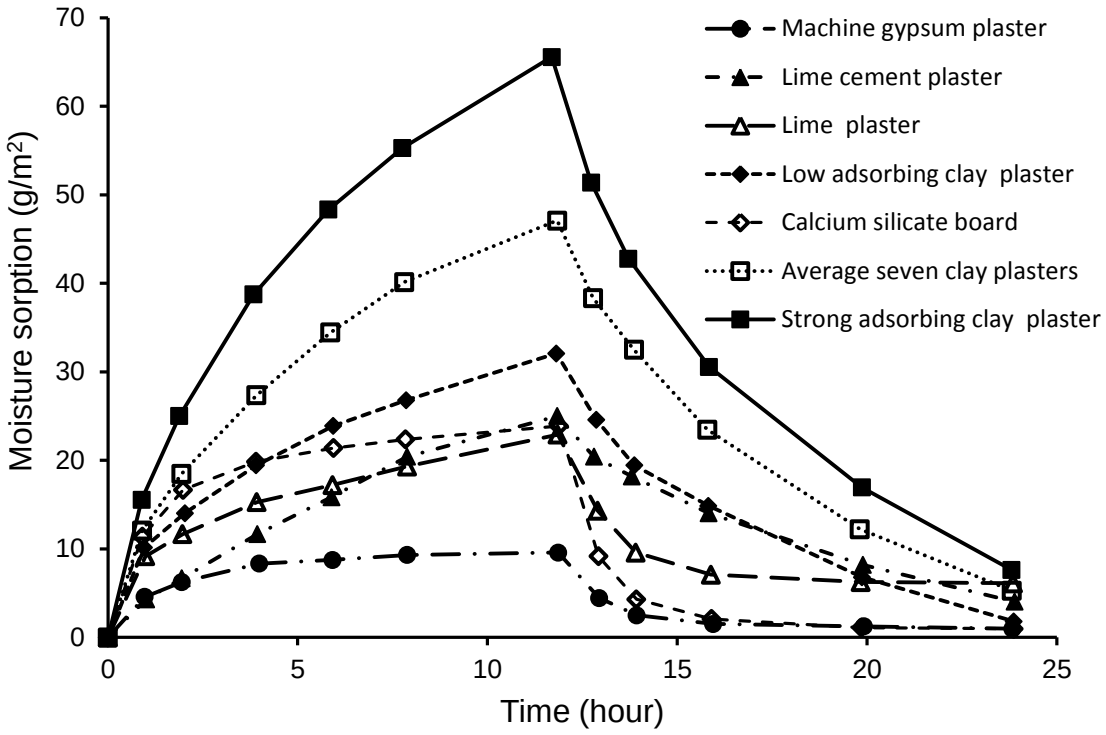

Figure 2.22. Moisture sorption of various building materials (after Eckermann and Ziegert, unpublished work 2006)

In this thesis, the moisture buffering capacity of unstabilised and stabilised earthen samples is assessed by determining the corresponding MBV as further discussed in Chapter 6.

2.4 Durability properties

The high moisture buffering capacity of raw earth is due to its hydrophilic character. This property, which is beneficial in terms of hygroscopic performance, implies on the other hand a limited durability against water infiltration. In particular, the capacity of raw earth to withstand water erosion must be carefully determined.

Specific tests have been devised to determine the durability of earthen materials and some of them are described below.

Wearing test. According to the norm ASTM D559-03 (2012), earthen blocks are immersed in water for 2 minutes, removed and then dried at 105 °C for 24 hours. After drying, eighteen wire brush strokes of about 13 N force are applied to each side of the

block and four strokes to each end of the block. The wearing performance of an earthen block is determined as the dry mass loss after 12 wetting – drying cycles.

Spray erosion test. According to New Zealand standards NZS 4298 (1998), this test consists in spraying the face of an earthen sample with a jet of water for one hour and measuring the resulting erosion depth. The jet of water is applied at constant pressure of 0.05 MPa from a nozzle that is placed at 0.47 m from the sample. The exposed area of the specimen corresponds to a circle of 150 mm diameter. Earthen blocks are then classified in five different classes depending on erosion depth. Others standards propose different procedures that vary for duration of the test, pressure of the water jet, distance of spraying, exposed area and erosion tolerance criteria.

Drip test. According to the standards UNE 41410 (AENOR, 2008) , this test consists in releasing 500 ml of water in 10 minutes from a height of 1 m on a sample that is inclined of 27° respect of the horizontal. If erosion is not deeper than 10 mm, the brick is suitable for construction.

The German norm DIN 18945 (2013) proposes a categorisation of earthen bricks into the following four different classes in relation to their response to water penetration:

Table 2.5. Classes of compressed earth bricks

Application	Class
External wall exposed to natural weathering	Ia
Coated external wall exposed to natural weathering	Ib
External wall not exposed to natural weathering – Internal wall	II
Dry applications	III

In order to establish the class of an earthen brick, the German norm DIN 18945 (2013) proposes the three following durability tests:

Immersion test. This test allows a first qualitative assessment of the material durability. Earthen samples are weighed prior to testing and then dipped in water for 10 minutes. The mass loss is determined by filtering the residual material from water. It is then dried at 40 °C for 24 hours, left at the atmosphere and weighed. Material loss is determined as the ratio between the mass of the filtered material and the initial mass of the sample.

Contact test. This test reproduces the application of a mortar joint or a coating on earthen bricks. For this purpose, an absorbent cloth (cellulose) is dipped in water and

then placed on the visible face of the brick. The applied amount of water must correspond to 0.5 g/cm^2. Samples are then stored for 24 hours in a sealed container on a rack above water. Then, the absorbent cloth is removed and bricks are exposed to atmospheric conditions for 2 days. After this, an examination of the bricks is performed to detect cracks and/or permanent deformations owed to swelling.

Suction test. This test determines the response of earthen blocks when exposed to a temporary excess supply of water. This condition occurs for example in exterior timber-frame walls during driving rains, with water collecting between the wooden frame and the earthen infill. For suction test, three earth block halves are equalised under standard hygro-thermal conditions (T = 23±2 °C; RH = 50±5%) until constant mass. Then, fired bricks are placed in a pan forming a continuous plane. The pan is then filled with water up to 1-5 mm below the upper edge of the fired brick. A layer of an absorbent cloth is laid on top of the fired bricks. Earthen blocks are subsequently placed on the absorbent cloth, thus starting the suction test. During testing, water is adsorbed by the earthen blocks and extra water must be added to keep the same level inside the pan. Samples are visually assessed at 30 min, 3h and 24h after the beginning of the test to detect cracks and permanent deformations owed to swelling.

Results from these three durability tests provide the necessary data to classify earthen bricks according to the norm DIN 18945 (2013). Criteria to classify earthen bricks are summarised in Table 2.6.

Table 2.6. Compressed earth bricks: results from durability tests

Class	**Immersion test** Mass loss (%)	**Contact test**	**Suction test**
Ia	≤ 5%	No cracks and no permanent swelling deformations	≥ 24 h
Ib	≤ 5%		≥ 3 h
II	≤ 15%		≥ 0.5 h
III	No requirement	No requirement	No requirement

Generally, unstabilised earthen materials show a weak behaviour under natural weathering and are often stabilised with hydraulic binders (e.g. cement or lime). However, the use of hydraulic binders increases production costs and overall carbon footprint and the earth material can no longer be considered recyclable. Furthermore, stabilisation reduces moisture buffering capacity as demonstrated by McGregor et al.

(2014). Because of this, several studies have focused on more efficient stabilisation methods.

In partial contradiction with McGregor et al. (2014), Kebao and Kagi (2012) stated that earthen materials maintain their hydrophilic nature even if stabilised with cement or lime. Nevertheless, water infiltration leads to other problems such as mould growth and efflorescence. These authors therefore identified silicone-based water-repellent admixtures as the most effective solution. These admixtures are capable of avoiding liquid water infiltration without affecting water vapour permeability. Also, surface appearance is not modified. Silicone-based water repellent admixtures contain silane and siloxane that react with the soil substrate by creating a layer of hydrophobic nanomolecular polysiloxane within the capillaries (Figure 2.23). Due to this chemical bonding, the polysiloxane layer becomes part of the substrate, thus assuring long term durability.

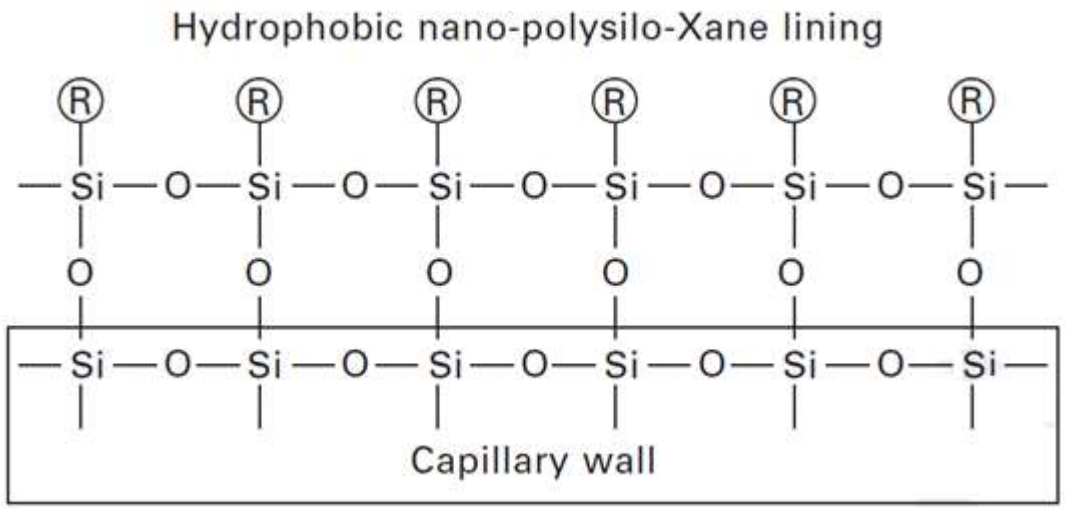

Figure 2.23. Molecular structures of polysiloxane (Kebao and Kagi, 2012)

Kebao and Kagi (2012) tested a silicone-based water repellent admixture on a cement stabilised rammed earth. They observed that an addition of 0.05% of silicone admixture reduced water absorption by 80% in comparison with the untreated material (test performed according to DIN 52617, 1987). It also improved the performance of the material against wind driven rain and rising damp.

Kebao and Kagi (2012) also suggested surface treatment as an effective technique to confer good durability to earthen materials. Acrylic or latex emulsions are rather common film forming treatments that reduce drastically water vapour permeability.

They modify the surface appearance of earthen materials due to the formation of a thin film. This film can however be damaged by UV radiation or harsh natural weathering, thus implying a poor long term durability. In alternative, Kebao and Kagi (2012) indicated a silicone-based water repellent sealing as the best suited treatment. A silicon-based sealer presents small molecular size and can easily penetrate earthen materials, thus forming a thick water repellent layer. This treatment is therefore less sensitive to natural weathering and a longer life span is achieved. Figure 2.24 shows that water absorption of a treated rammed earth substrate is considerably reduced compared to an untreated substrate.

Kebao and Kagi (2012) measured also the water vapour transmission by blowing air through both treated and untreated substrates. They observed that vapour permeability is not significantly affected by the silicone sealer treatment (Figure 2.25).

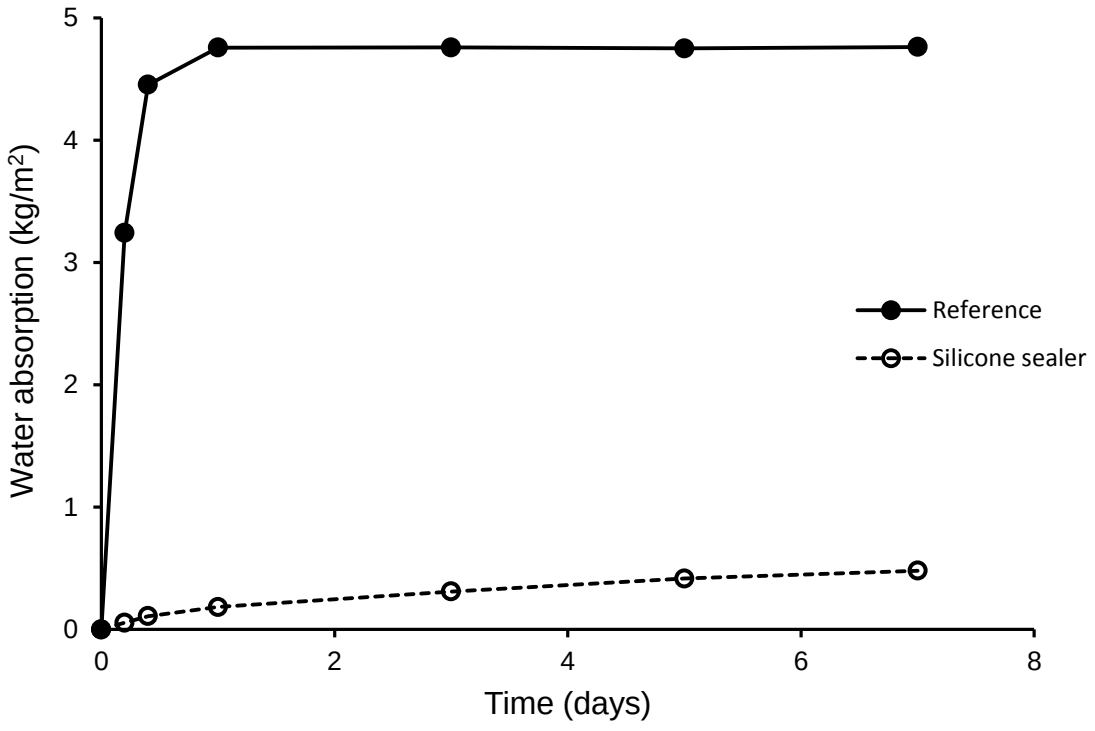

Figure 2.24. Water absorption of rammed earth substrate (after Kebao and Kagi, 2012)

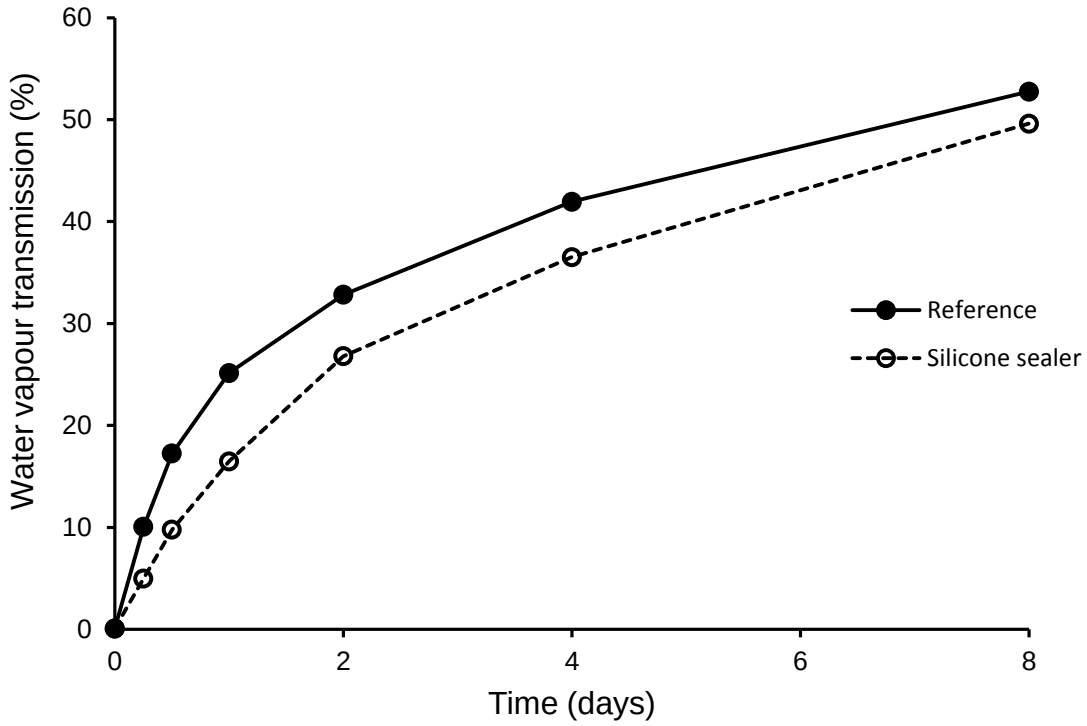

Figure 2.25. Water vapour transmission of rammed earth substrate (after Kebao and Kagi, 2012)

Alkaline activation is another alternative method for stabilising earthen materials. This method consists in dissolving and transforming clay minerals in non-swelling binding materials by using alkaline solutions. The most common alkaline activators are $Ca(OH)_2$, NaOH and KOH.

Elert et al. (2015) proposed alkaline activation to consolidate existing earthen buildings. They compacted adobe earthen blocks (4 x 4 x 4 cm^3) with a soil/water mass ratio of 3. These samples were then impregnated for 20 minutes in three different alkaline solutions: 1) 0.025 mol/L $Ca(OH)_2$, 2) 5 mol/L NaOH and 3) 5 mol/L KOH. After impregnation, samples were stored for 50 days in plastic bags to simulate an in-situ consolidation treatment. Plastic bags were then opened and the samples were left at the atmosphere (T ~ 20 °C, RH ~ 45%) until a constant mass was reached. Samples were subsequently immersed in water for a prolonged period of time. Elert et al. (2015) observed that the $Ca(OH)_2$ treatment did not improve water resistance and samples treated with this solution exhibited complete disintegration after 2.5 h. Conversely, samples treated with NaOH and KOH showed higher water resistance by withstanding significant erosion for almost 48 h.

Another study by Slaty et al. (2015) investigated the durability of a kaolinitic clay mixed with silica sand and activated with a NaOH solution. The kaolinite (74% SiO_2, 26% Al_2O_3) was not thermally activated, i.e. it was not previously converted into metakaolin. Slaty et al. (2015) compacted the earthen mix (kaolinitic clay 42.0%, silica sand 42.0%, NaOH 6.7%, water 9.3%) into a cylindrical mould (50 x 25 mm) at a static pressure of 16 MPa.

After compaction, samples were stored in an oven at 80 °C for 24h and subsequently subjected to a modified wearing test where they were immersed in water for 24 h followed by oven drying at 40 °C for 24 h. This process was repeated for 5, 10, 25, 50 and 100 cycles. After each set of cycles, 3 samples were taken to measure mass, dimensions and compressive strength. Slaty et al. (2015) observed that the compressive strength reduced from 40 MPa for oven dried samples to about 20 MPa after 5 wetting – drying cycles. After the fifth cycle, compressive strength remained constant, thus implying that the material strength remains stable under humid conditions.

In the present study, water based silane-siloxane emulsion and alkaline activation have been adopted as the methods to stabilise compressed earth bricks. Durability of the stabilised material has been assessed according to the three tests prescribed by the German norm DIN 18945 (2013). The relevant results are discussed in Chapter 7.

3

Material and methods

This chapter describes the main geotechnical properties of the tested material as well as the compaction procedures followed to manufacture both small cylindrical samples and compressed earth bricks. The chapter concludes by presenting the different stabilisation methods adopted to improve material durability.

3.1 Material characterisation

The soil used in the present work has been provided by the brickwork factory "Nagen" from the region of Toulouse in France. This soil was chosen among five different materials provided by five different brickwork factories (Barthe, Bouisset, Capelle, Nagen, Saves) based on compressive strength tests performed by the laboratory LMDC (Toulouse, TERCRUSO project). The selected material showed the highest compressive strength, as indicated in Table 3.1 (TERCRUSO, 2013).

Table 3.1. Compressive strength of different materials tested by LMDC (Toulouse)

	Barthe	Bouisset	Capelle	**Nagen**	Savès
Compressive strength (MPa)	4.3	3.6	4.5	5.1	3.0

3.1.1 Grain size distribution

The grain size distribution has been determined by both wet sieving and sedimentation in compliance with the norms XP P94-041 (AFNOR, 1995) and NF P 94-057 (AFNOR, 1992). Figure 3.1 shows the grain size distribution of the soil (thick line with markers) obtained as the average of two independent measurements. Figure 3.1 presents also the lower and upper limits of the particle size distribution as prescribed by three different guidelines for the manufacture of compressed earth bricks (AFNOR, 2001; CRATerre-EAG, 1998; MOPT, 1992).

Inspection of Figure 3.1 indicates that the grain size distribution lies close to the finer limit of the admissible region. As observed by Jaquin et al. (2008) and Beckett and Augarde (2012), finer soils are able to retain more water than coarser soils under the same hygro-thermal conditions, thus resulting in a stronger hygroscopic behaviour. However, a larger fine fraction may weaken mechanical characteristics and undermine durability.

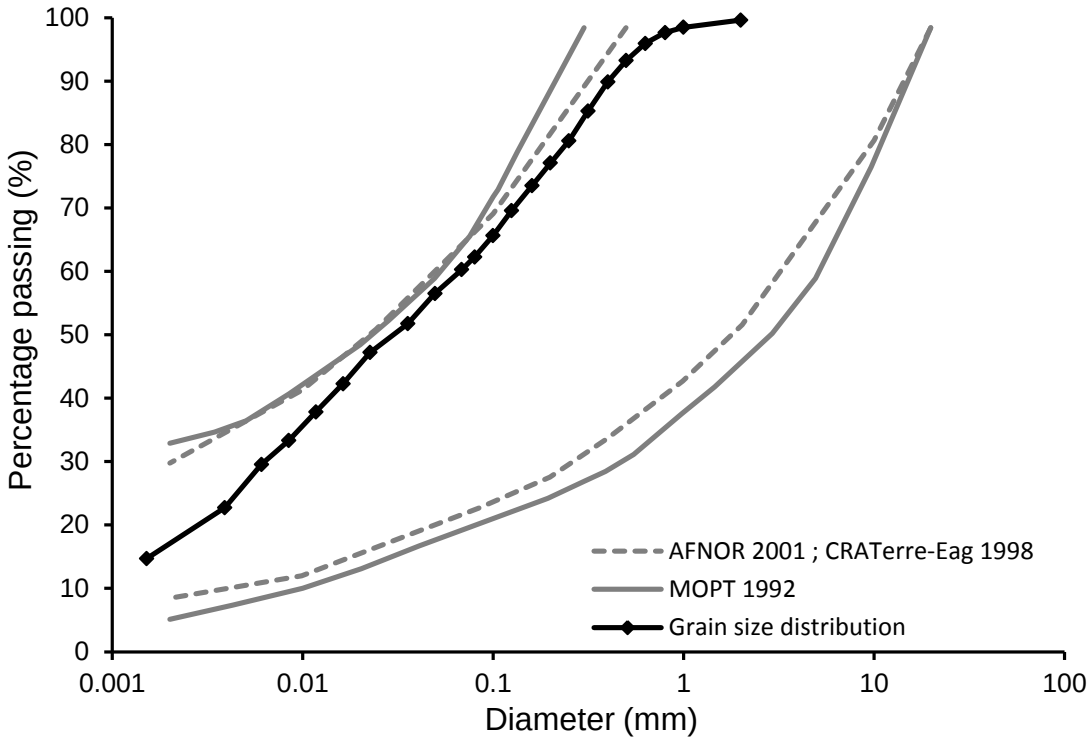

Figure 3.1. Grain size distribution of the tested soil

3.1.2 Plasticity and specific gravity of soil solids

In unstabilised compressed earth, the fine soil fraction acts as a binder of larger grains and must therefore satisfy specific plasticity requirements to ensure adequate bonding.

The plasticity properties of the fine fraction (i.e. of the soil fraction smaller than 400 µm) have been measured in agreement with the norm NF P94-051 (AFNOR, 1993). Liquid limit, plastic limit and plasticity index have been determined as the average of four independent tests. Figure 3.2 shows that the fine fraction of the tested soil is classified as inorganic clay of medium plasticity according to the Unified Soil

Classification System USCS ASTM D2487-06 (2011) and falls within the admissible region for compressed earth bricks (AFNOR, 2001; CRATerre-EAG, 1998; Houben and Guillad, 1994).

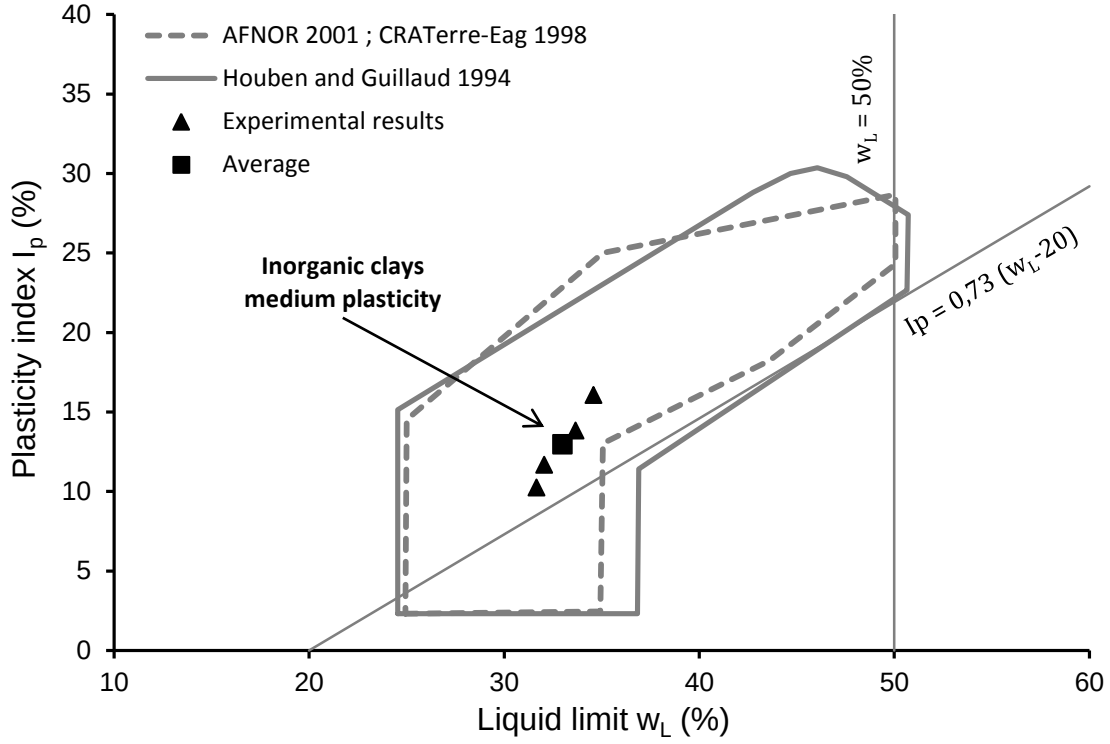

Figure 3.2. Plasticity properties of the tested soil in relation to the admissible region for compressed earth bricks

The specific gravity of soil grains G_s has been determined by means of the pycnometer test according to the norm NF P 94-054 (AFNOR, 1991) and has been calculated as the average of three measurements.

Finally, the clay activity (A), defined as the ratio between the plasticity index and the clay fraction (i.e. the fraction smaller than 2 µm), is equal to 0.79. This classifies the clay fraction as normally active (Skempton, 1953) which is consistent with mineralogy information from the soil provider that indicates a predominantly illitic material with a small quantity of montmorillonite. Illite is a three-layers clay with good bonding characteristics and a limited swelling potential upon wetting, which makes it particularly suited to raw earth construction (Dierks and Ziegert, 2002).Table 3.2 summarises the main properties of the tested soil.

Table 3.2. Main material properties

Grain size distribution		
Gravel	> 2 mm	0.4 %
Sand	0.063 – 2 mm	40.4 %
Silt	0.002 – 0.063 mm	42.9 %
Clay	< 0.002 mm	16.3 %
Plasticity properties		
Liquid limit, w_L (%)		33.0 %
Plastic limit, w_P (%)		20.1 %
Plasticity index, I_p (%)		12.9 %
Activity A (-)		0.79
Specific gravity of soil grains		
G_s (-)		2.66

3.2 Compaction procedures

This section describes the compaction procedure followed during manufacture of cylindrical samples. The main objective of these procedures is to increase material density, thus improving mechanical performance. A comparison with Proctor standard compaction is also presented.

3.2.1 Hypercompaction method: cylindrical samples

The compaction method adopted in this work relies on the following geotechnical principles:

- The stress applied to a soil volume coincides with the effective stress acting on the solid skeleton only if the pore fluid is allowed to drain and the excess pore pressures generated during loading are dissipated, thus leading to consolidation of the soil.
- The dry density of a soil volume increases as compaction energy increases. Therefore, higher compaction pressures generally correspond to improved mechanical properties.

Consistent with the above principles, the adopted compaction method applies a relatively high pressure for a sufficiently long time to allow dissipation of excess pore pressures. This is different from current manufacturing practice where much lower compaction stresses are applied for relatively short times.

For this first part of the study, small cylindrical samples (instead of full size bricks) were produced to facilitate manufacturing and to avoid the presence of corners which could result in stress concentration during compaction. Cylindrical samples of 50 mm of diameter and 100 mm high were compacted at the three pressure levels of 25 MPa, 50 MPa and 100 MPa. Sample dimensions were fixed to obtain a representative volume of material with an aspect ratio of 2. This implies that, during mechanical tests, the effects of friction between the sample and press plates can be neglected (Ciancio and Gibbings, 2012). The lowest compaction pressure of 25 MPa is comparable to that of the most powerful presses currently available on the market (e.g. MecoPress from MecoConcept, Toulouse). The other two values of 50 MPa and 100 MPa are obtained by a geometrical progression with a ratio of two and are significantly higher than the pressure levels applied during current production of earth bricks.

Prior to compaction, 500 grams of dry soil were mixed with the desired amount of water by means of an electrical planetary mixer for at least 15 minutes (Kouakou and Morel, 2009). This time is sufficient to ensure good homogeneity of moisture throughout the soil mix. The moist soil was subsequently placed inside two plastic bags to prevent loss of water and left to rest for at least one day to allow equalisation of water pressures and redistribution of moisture inside the soil. After this, the moist soil was placed inside a cylindrical mould of 50 mm diameter, where it was vertically compacted at the required pressure by using a load-controlled Zwick/Roell Amsler HB250 press with a capacity of 250 kN (Figure 3.3).

A careful design of the compaction mould was necessary to satisfy the following two requirements:

- The mould must be strong enough to withstand the high lateral pressures exerted by the compressed soil.
- The mould must allow water and air to drain as easily as possible during loading. As the pore volume reduces during compression, soil voids may become water saturated with consequent generation of excess pore water pressures. In order for the applied stress to be converted into effective stress, these excess pore water pressures must be dissipated during a consolidation phase when water drains out under constant load. The duration of the consolidation phase depends on the permeability and stiffness of the compacted soil but also on the length of water drainage paths.

Figure 3.3. Zwick /Roell Amsler HB250 press and compaction mould

The mould used in this work consists of a hollow stainless steel cylinder with an external diameter of 170 mm, an internal diameter of 50 mm and a height of 200 mm (Figures 3.4a and 3.4b). The mould thickness is therefore equal to 60 mm, which is enough to withstand the lateral pressure exerted by the soil during compaction with a good margin of safety. The soil is vertically compressed inside the mould by two cylindrical aluminium pistons acting at the top and bottom of the sample. This double-piston compression reduces the effect of friction between the mould and the sample, thus increasing uniformity of stress levels inside the soil. Two perforated aluminium disks are also placed between the top and bottom surfaces of the sample and the respective pistons to facilitate drainage of pore water during consolidation. Each disk is perforated by 17 circular holes of 2 mm diameter. Filter papers are located between the soil and the perforated disks, as well as between the perforated disks and the pistons in order to further help water drainage. Finally, eight longitudinal grooves are cut along the lateral surfaces of the two pistons to create a preferential path for water drainage

between the outer surface of the pistons and the inner surface of the mould (Figures 3.4a and 3.4b).

The above design eases drainage of pore water during compaction and accelerates consolidation time. The pistons and the perforated disks have a diameter of 49.9 mm, which is only slightly smaller than the mould diameter of 50 mm. They therefore fit tightly inside the mould with a tolerance of about 0.05 mm, which is small enough to prevent any extrusion of soil during compaction.

The procedure for assembling the mould and compacting the soil is detailed as follows:

- The mould is seated on the bottom plate of the Zwick press. A solid aluminium disk (49.9 mm diameter and 10 mm thick), a filter paper, a perforated disk (49.9 mm diameter and 10 mm thick) and another filter paper are inserted, in this sequence, at the bottom of the mould.
- The moist soil is scooped inside the mould in four layers, with each layer equal to one fourth of the total mass of the mix. In order to reduce the height of the soil inside the mould, a small compaction stress of about 5 MPa is applied to each layer before adding the next amount of soil. It is important to scratch the upper surface of the last compacted layer before adding the next amount of soil in order to ensure good adherence between layers.
- A filter paper, a perforated disk (49.9 mm diameter and 10 mm thick), another filter paper and a piston (49.9 mm diameter and 90 mm high) are placed, in this sequence, on top of the soil.
- About 80% of the target compaction pressure is applied to the soil for few seconds in order to make sure that the sample sticks to the inner surface of the mould. This is necessary so that the mould can be subsequently lifted without causing the soil to fall out.
- The entire system is turned upside down inside the Zwick press and the solid aluminium disk is replaced with a piston (49.5 mm diameter and 60 mm high). Figure 3.4a shows the equipment in this configuration just before the start of the double compaction.
- A compaction pressure is applied to the soil at a rate of 5 MPa/s until the target value is attained. The target pressure is then kept constant while vertical displacements are recorded until the end of consolidation.

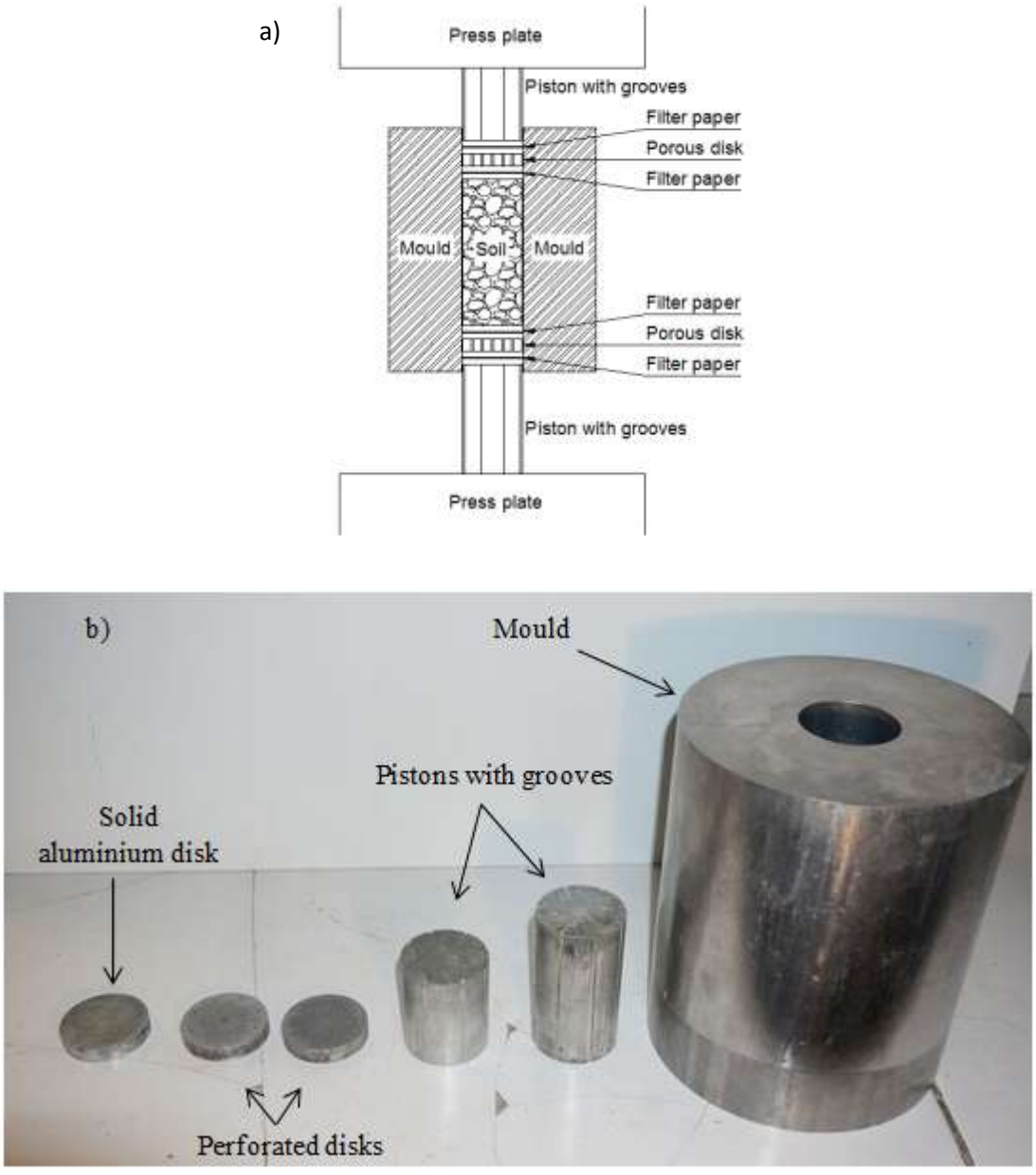

Figure 3.4. Compaction system: a) vertical cross section of experimental set-up during double compaction and b) mould and pistons

The duration of consolidation increases as water content and compaction pressure increase. Consolidation is assumed to be complete when the vertical displacement rate falls below a tolerance of 0.01 μm/s. This rate is measured as the slope of the straight line that fits the final hour of the consolidation curve relating displacement to time (Figure 3.5).

Figure 3.5 also shows the graphic determination of the time t_{90} corresponding to 90% of primary consolidation according to the Taylor method (Taylor and Merchant, 1940). According to this method, the slope of the secant line intercepting the consolidation curve at 90% of primary consolidation (thick line in Figure 3.5) is obtained by

multiplying the slope of the tangent to the consolidation curve at the origin (dotted line in Figure 3.5) by a factor of 1.15.

Inspection of Figure 3.5 indicates that 90% of primary consolidation is attained after few minutes of consolidation. The tolerance of 0.01 μm/s has therefore been chosen to be less than 0.25% of the average displacement rate measured during primary consolidation corresponding to the slope of the secant line in Figure 3.5 (about 4 μm/s). This ensures the occurrence of all primary consolidation and also a large portion of secondary consolidation.

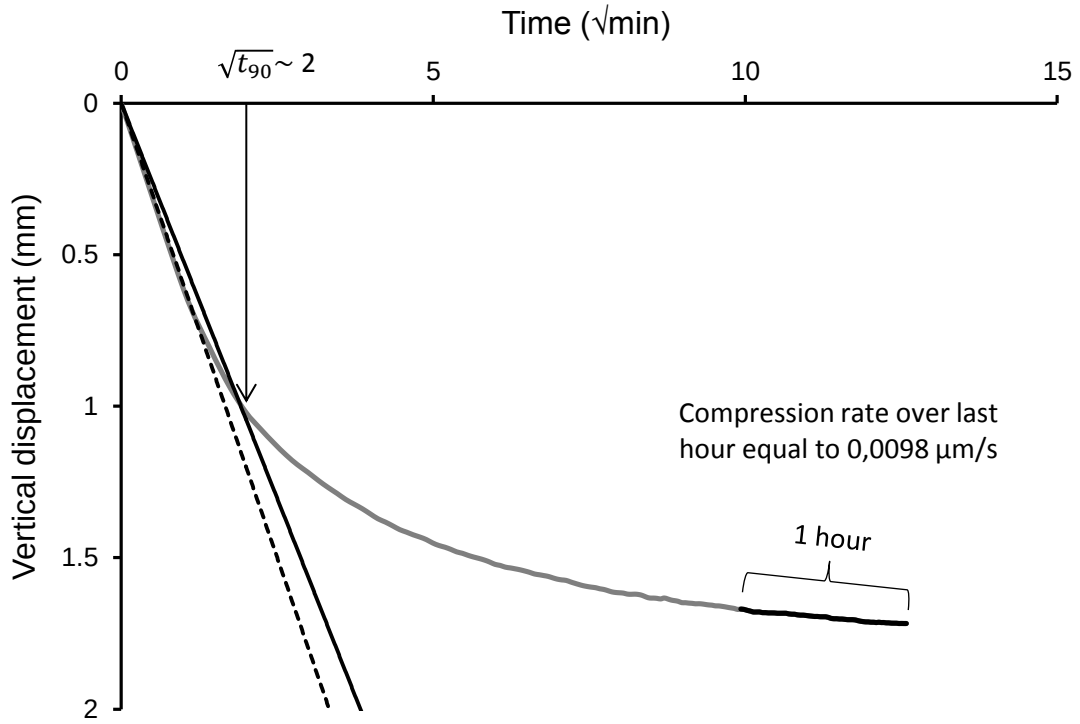

Figure 3.5. Typical vertical displacement versus square root of time during consolidation

After compaction, each sample was cut to a height of 100 mm by trimming excess soil from both top and bottom. The water content of the trimmed soil was measured as specified in the norm NF P 94-050 (AFNOR, 1995) by drying it in an oven at 105 °C until weight became constant. Generally, the values of water content obtained from the top and bottom extremities of the sample were very similar suggesting that moisture was uniform across the entire specimen. The water content of the sample was then taken as the average of the top and bottom values.

3.2.2 Proctor standard

Samples prepared according to the proposed “hypercompaction” method, based on the application of very large static pressures to the soil, were compared with samples compacted according to the Proctor standard, which is the reference for geotechnical structures such as dams and embankments.

Proctor compacted samples were manufactured in compliance with the norm NF P 94-093 (AFNOR, 1999). A fixed mass of 2250 grams of dry soil was mixed with the desired amount of water by means of a planetary mixer for at least 15 minutes and then stored for at least one day in two plastic bags. The moist soil was subsequently compacted in a standard Proctor mould in three layers. Each layer was compacted by 25 blows of a 2.490 kg hammer falling from a fixed height of 305 mm. After compaction, a cylindrical specimen of 50 mm diameter was cored from the larger Proctor sample. The cored specimen was then cut down to a height of 100 mm by trimming the excess soil from the top and bottom extremities. The remaining soil from the larger Proctor sample was used to determine the water content. Three samples of about 50 grams each were taken at three different heights of the original Proctor sample and dried at 105 °C until weight became constant (AFNOR, 1995). The water content was then determined as the average of these three measurements.

Figure 3.6 shows that cored samples have higher dry density than the original Proctor samples. This is due to the friction between the soil and the metallic tube, which produces further compaction of the material during coring. The sample compacted at the optimum water content exhibits the largest increase in dry density due to coring while the wettest and driest samples show the smallest increase of dry density.

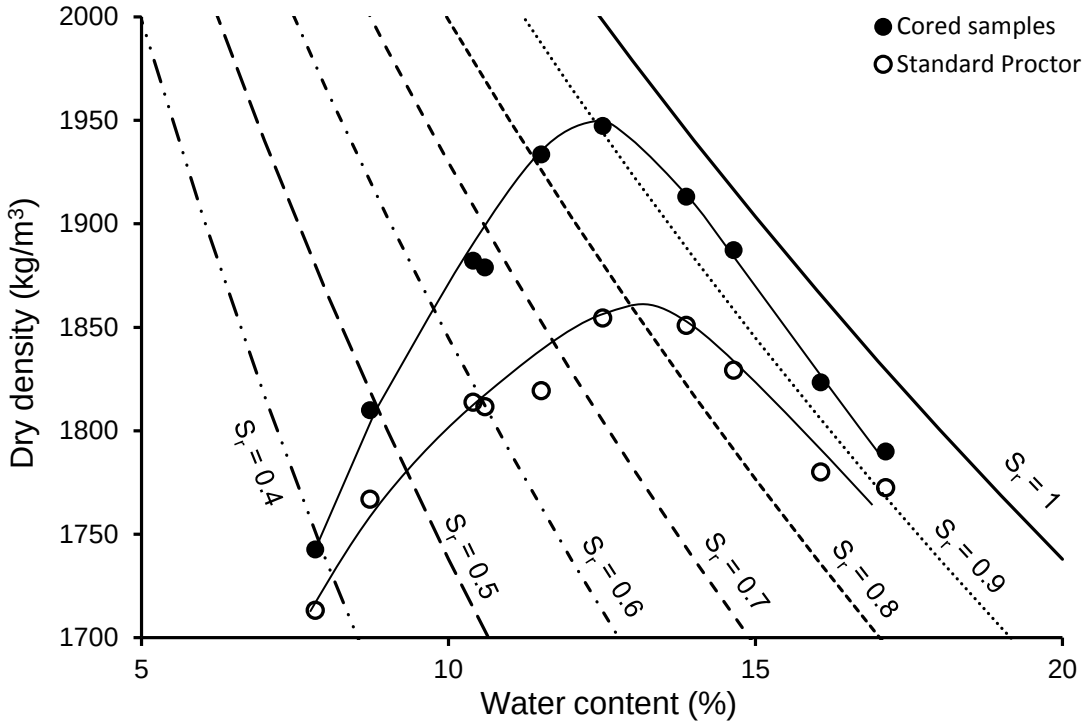

Figure 3.6. Compaction curves of Proctor samples and cored samples

3.2.3 Compaction curves

For all specimens, three diameter measurements were taken at different heights and three height measurements were taken at different angles. The volume of the sample was then calculated from the average values of diameter and height. The mass of the sample was measured by using a scale with a resolution of 0.01 g. Based on the measured values of mass, water content, volume and specific gravity, it was possible to calculate bulk density, dry density, porosity and degree of saturation.

Table 3.3 shows the properties of all specimens: sample code, water content w, bulk density ρ_b, dry density ρ_d, porosity n and degree of saturation S_r. Samples compacted at high pressures are identified by a code Sxx – CSyy – Wzz, where xx is the sample number, yy is the compaction stress in MPa and zz is the percentage water content after compaction, e.g. S03 – CS50 – W6.4 is specimen number 3 compacted at a pressure of 50 MPa with a water content of 6.4%. Similarly, samples compacted according to the Proctor standard are identified by a code PSxx – Wzz where xx is the sample number and zz is the percentage water content after compaction.

It can be remarked from Table 3.3 that porosity reduces from about 0.30 for samples compacted according to Proctor standard to about 0.15 for samples compacted at a pressure of 100 MPa.

Table 3.3. Properties of samples after compaction

Sample	w (%)	ρ_b (kg/m^3)	ρ_d (kg/m^3)	n (-)	S_r (%)
S01 – CS25 – W10.7	10.7	2235	2019	0.242	89.2
S02 – CS25 – W9.8	9.8	2285	2081	0.218	93.2
S03 – CS25 – W9.0	9.0	2319	2128	0.201	95.1
S04 – CS25 – W9.0	9.0	2317	2126	0.202	94.7
S05 – CS25 – W8.7	8.7	2328	2142	0.196	95.0
S06 – CS25 – W8.5	8.5	2318	2136	0.198	91.7
S07 – CS25 – W7.0	7.0	2254	2107	0.209	70.5
S08 – CS25 – W6.3	6.3	2236	2103	0.210	63.0
S09 – CS25 – W9.4	9.4	2289	2092	0.215	91.7
S10 – CS25 – W7.4	7.4	2296	2138	0.198	80.1
S11 – CS25 – W7.0	7.0	2241	2094	0.214	68.6
S01 – CS50 – W7.2	7.2	2353	2194	0.176	89.8
S02 – CS50 – W6.2	6.2	2329	2193	0.177	76.9
S03 – CS50 – W6.4	6.4	2342	2201	0.174	81.1
S04 – CS50 – W7.2	7.2	2358	2200	0.174	90.9
S05 – CS50 – W7.0	7.0	2363	2208	0.171	90.4
S06 – CS50 – W6.9	6.9	2358	2206	0.172	88.5
S07 – CS50 – W7.5	7.5	2355	2191	0.178	92.5
S08 – CS50 – W6.6	6.6	2366	2220	0.167	87.8
S09 – CS50 – W6.3	6.3	2361	2221	0.166	84.2
S10 – CS50 – W5.6	5.6	2325	2202	0.174	71.0
S11 – CS50 – W5.3	5.3	2295	2179	0.182	63.5
S01 – CS100 – W6.5	6.5	2386	2240	0.159	91.6
S02 – CS100 – W6.3	6.3	2385	2244	0.158	89.6
S03 – CS100 – W5.9	5.9	2382	2249	0.156	85.2
S04 – CS100 – W5.2	5.2	2387	2270	0.148	79.6
S05 – CS100 – W5.4	5.4	2388	2266	0.150	81.8
S06 – CS100 – W5.6	5.6	2367	2241	0.159	79.1
S07 – CS100 – W4.7	4.7	2364	2258	0.152	69.6
S08 – CS100 – W5.4	5.4	2390	2268	0.149	82.3
S09 – CS100 – W6.2	6.2	2385	2246	0.157	88.7
S10 – CS100 – W4.8	4.8	2368	2260	0.152	71.4
PS01-W7.8	7.8	1879	1743	0.346	39.3
PS02-W8.7	8.7	1968	1810	0.320	49.2
PS03-W10.4	10.4	2078	1882	0.293	66.7
PS04-W10.6	10.6	2078	1879	0.295	67.6
PS05-W11.5	11.5	2156	1934	0.274	81.1
PS06-W12.5	12.5	2191	1948	0.269	90.5
PS07-W16.1	16.1	2116	1823	0.316	92.9
PS08-W13.9	13.9	2179	1913	0.282	94.3
PS09-W14.6	14.6	2164	1888	0.291	94.7
PS10-W17.1	17.1	2096	1789	0.328	93.3

For each compaction effort, the experimental values of dry density are plotted against the corresponding water contents in Figure 3.7 together with the respective interpolating curves. For each compaction curve, the optimum water content is defined as the water content that corresponds to the highest dry density. As the compressive energy increases from Proctor compaction to static compaction at 25 MPa, 50 MPa and 100 MPa, the optimum water content becomes progressively smaller while the corresponding dry density increases progressively. This means that, as compression effort increases, the compaction curve shift towards the theoretical point at which all porosity is erased and the dry density becomes equal to the density of the solid particles (i.e. G_s). As shown by Figure 3.7, the optimum dry density increases less than linearly with compaction pressure, i.e. the increase in dry density from 25 MPa to 50 MPa is greater than the increase in dry density from 50 MPa to 100 MPa. An unfeasibly high pressure would therefore be necessary to attain the theoretical "no porosity" point.

Samples compacted at higher water contents (points on the right branch of the curves in Figure 3.7) correspond to values of degree of saturation equal or higher than 90%. In these samples, a good proportion of pores becomes saturated during compaction, as confirmed by the observation of water drainage occurring between the piston and the mould at bottom and top of the specimen (this also confirms the efficiency of double compaction). Conversely, no water drainage was observed during compaction of the drier samples (points at the optimum and at the dry of optimum of the curves in Figure 3.7), for which the degree of saturation is lower than 90%. Since no water drainage was observed during compaction of the samples at the optimum water content, perforated disks were no longer necessary and were therefore removed from the compaction mould. This means that both the lower and upper pistons applied the load directly on the soil.

The optimum samples compacted without perforated disks show a higher value of maximum dry density, which is equal to 2320 kg/m^3, compared to that of the samples compacted with perforated disks, which is equal to 2270 kg/m^3. This is due to the fact that, during compaction a small amount of soil is extruded between the perforated disks and the inner wall of the mould, thus generating friction and reducing the load applied to the soil. Moreover, the maximum dry density of 2320 kg/m^3 is the highest value registered in the literature for an unstabilised earthen material.

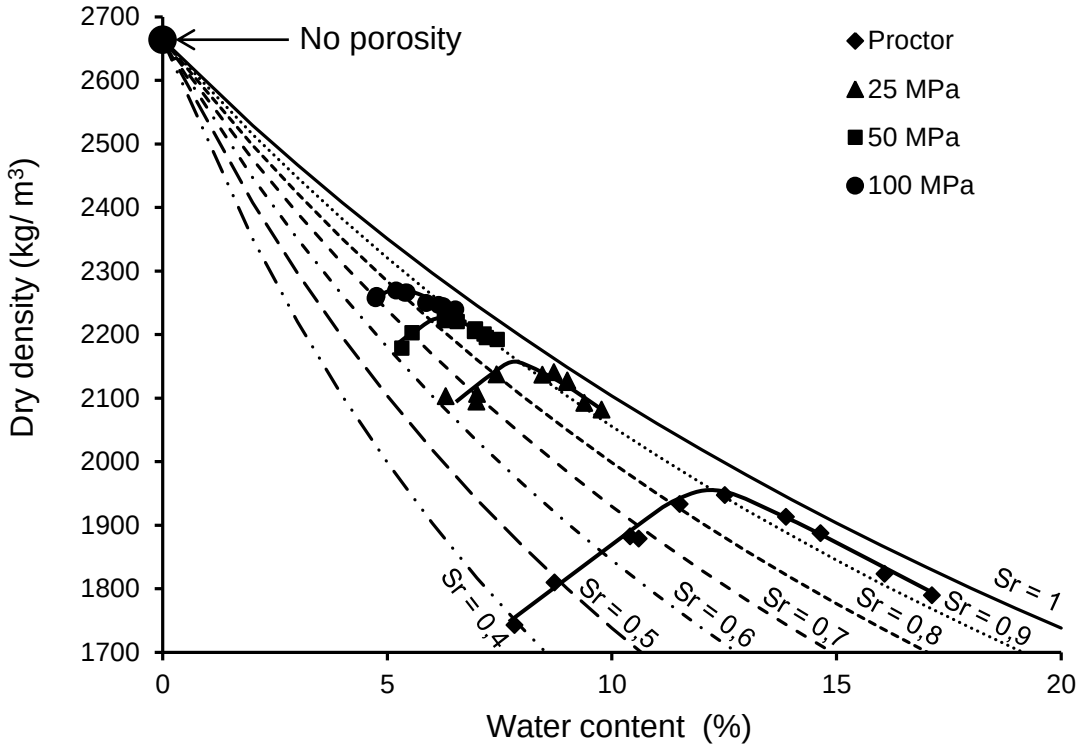

Figure 3.7. Compaction curves at 25, 50 and 100 MPa together with standard Proctor

3.2.4 Equalisation

After compaction, all samples were equalised inside a climatic chamber under a constant temperature of 25 °C and a relative humidity of 62%. Equalisation took typically 15 days and was considered complete when the mass of the samples changed less than 0.1% over at least one week. This preliminary equalisation stage was necessary to eliminate the potential influence of different hygroscopic conditions on the measured mechanical properties of the material (Beckett and Augarde, 2012; Bui et al., 2014). As shown in Figure 3.8, during equalisation, all samples experienced desaturation and shrinkage as water content reduced to about 3.5% and dry density increased, especially for the wetter samples. The specimens compacted at the highest pressure of 100 MPa show very similar values of dry density at the end of equalisation (Figure 3.8). This suggests that application of a high compaction pressure reduces the dependency of the material properties after equalisation on the compaction water content, thus resulting in better quality control of the final product. On the contrary, samples manufactured at smaller pressures show, after equalisation, variable values of dry densities depending on the water content at the time of compaction.

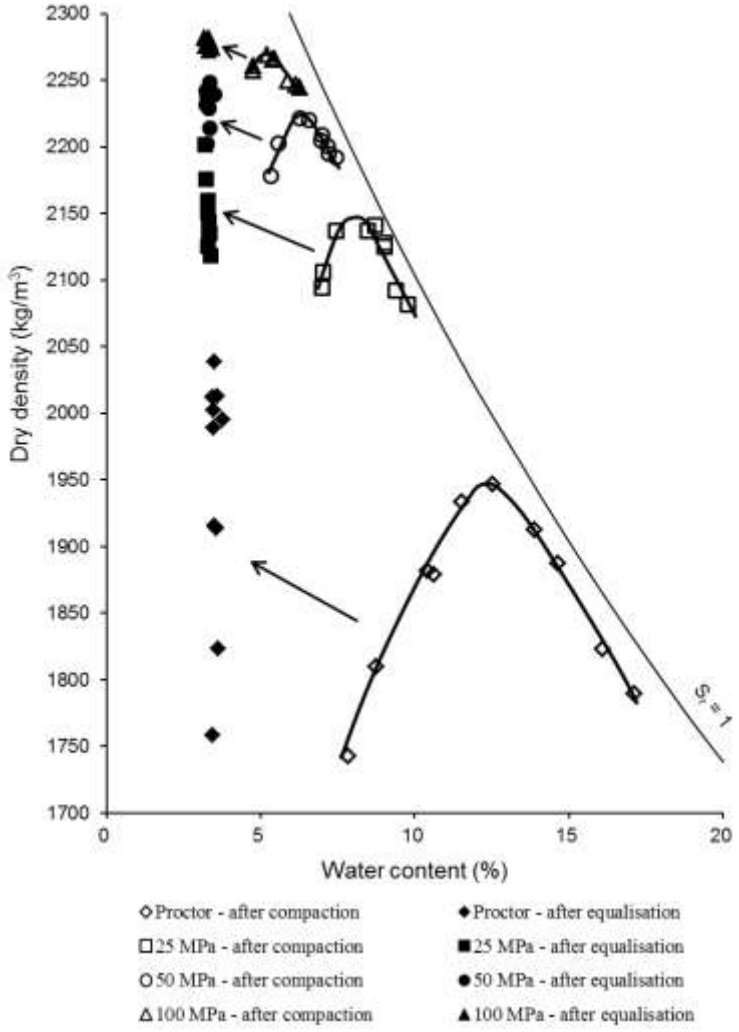

Figure 3.8. Changes in dry density and water content during equalisation

3.3 Hypercompaction method: brick scale

Cylindrical samples were used to assess the effect of high-pressure compaction on the hydro-mechanical behaviour of the earthen material at the element scale. This compaction procedure was then extended to manufacture earth bricks, which is the main objective of the present work. Bricks were manufactured at the optimum water content and a compaction pressure of 100 MPa.

3.3.1 Press and compaction mould

Compared to cylindrical samples, bricks present a considerably larger surface on which the compaction load acts. The application of a pressure of 100 MPa to a relatively large brick face requires a more powerful press than the one used for the fabrication of

cylindrical samples. Therefore, the press 3R RP 3000 TC/TH with a load capacity of 3000 kN was used in this work (Figure 3.9).

The maximum height between the top and bottom plates of the press dictated the size of the compressed earth bricks which were limited to 200 x 100 x 50 mm^3. Even though compressed earth bricks have generally larger size, e.g. 295 x 140 x 90 mm^3 according to Rigassi (1995), the dimensions chosen in the present work are similar to those of standard fired clay bricks, e.g. 215 x 102.5 x 65 mm^3 according to BS 3921 (1985).

The laying surface (i.e. the surface that is loaded during compaction and subsequent service life) is equal to 20000 mm^2 and it is therefore necessary to apply a load of 2000 kN to attain a compaction stress of 100 MPa.

Figure 3.9. 3R 3000 TC/TH compression press.

3.3.2 Compaction procedure

Prior to compaction, 2300 grams of dry soil were mixed with 120 grams of water by means of a planetary mixer for at least 15 minutes. This corresponds to the optimum water content of the cylindrical samples compacted at 100 MPa (w_{opt} = 5.2%). As with the cylindrical samples, after mixing, the moist soil was stored in two plastic bags for at least 24 hours in order to prevent loss of water and to ensure redistribution of moisture inside the soil. After this, the soil was placed inside the mould where it was double compacted by using the 3R RP 3000 TC/TH press.

The mould inside which the earthen bricks were compacted represents an original piece of equipment that was designed and manufactured during the present project in collaboration with the company 3R Recherches & Realisations Remy S.A.S. (Figure 3.10). It consists of four separated parts: two parts parallel to the longest dimension of the brick (pieces 1 and 2) and two parts parallel to the shortest dimension (pieces 3 and 4). These four parts are made of high resistance steel (AFNOR designation: 40 CMD 8) to withstand the high lateral pressures exerted by the compacted soil. Two bolts M42 (quality 12.9) are used to assembly the mould together (Figure 3.10).

The indentations in parts 1 and 2 were included to impede the rotation of parts 3 and 4 during assembly but also to unload the two bolts from the shear stress owed to the soil pressure acting on parts 3 and 4. During compaction, the two bolts are therefore mainly subjected to traction.

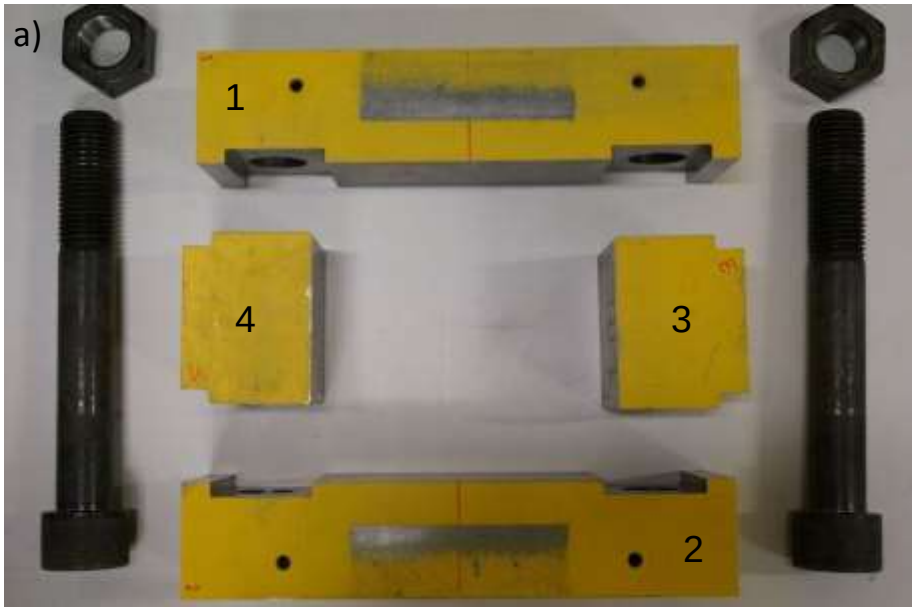

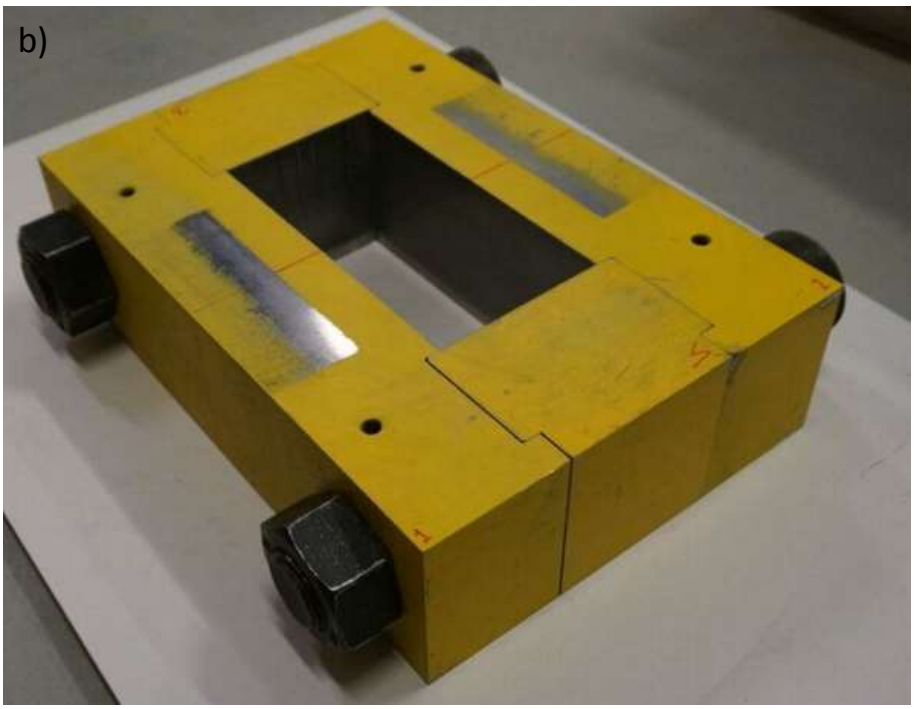

Figure 3.10. Compaction mould: a) disassembled b) assembled

The moist soil is vertically compressed inside the mould by means of two aluminium pistons acting at the top and bottom of the brick. Both pistons have a cross section of 199.8 mm x 99.8 mm while the inner dimension of the mould is 200 mm x 100 mm. This gives a tolerance of about 0.1 mm, which is twice that of the hollow cylindrical mould. This higher tolerance allows only limited extrusion of the soil between the pistons and inner mould walls during compaction but eases considerably the assembly of the mould without damaging the aluminium pistons.

Similar to the cylindrical samples, the double compaction process reduces the effects of friction between the brick and the mould, thus increasing stress uniformity inside the soil. The mould does not include any specific water drainage system because the soil is compacted at the optimum water content, which means that no water drainage takes place during compaction as discussed earlier. The procedure for assembling the mould, compacting the soil and demoulding the brick is detailed as follows:

- The lower piston is seated on the bottom plate of the press together with four spacers that are 10 mm shorter than the piston (Figure 3.11a). Each spacer is used to support one of the four parts of the mould.
- The four parts that constitute the mould are positioned on top of the spacers so that parts 3 and 4 fit inside the indentations of parts 1 and 2. All four pieces are assembled together by slightly tightening the two M42 bolts. In this condition,

the lower piston penetrates inside the mould for 10 mm (Figures 3.11b and 3.11c).

- The moist soil is scooped inside the mould and distributed as uniformly as possible (Figure 3.11d).
- The upper piston is then placed on top of the soil and a pressure of 80 MPa is applied for few seconds so that the soil sticks to the inner surface of the mould (Figure 3.11e). This is necessary to ensure that the spacers can be subsequently removed without causing the mould to fall (the support exerted by the spacers is replaced by the support exerted by friction at the interface between the brick and the mould).
- A compaction pressure is applied at a rate of 0.17 MPa/s until the target value of 100 MPa is attained and maintained constant for one hour. This time was considered sufficient for consolidation based on previous experience on small cylindrical samples. In this configuration, both pistons are loaded by the same force and double compaction of the soil is therefore achieved (Figure 3.11f).

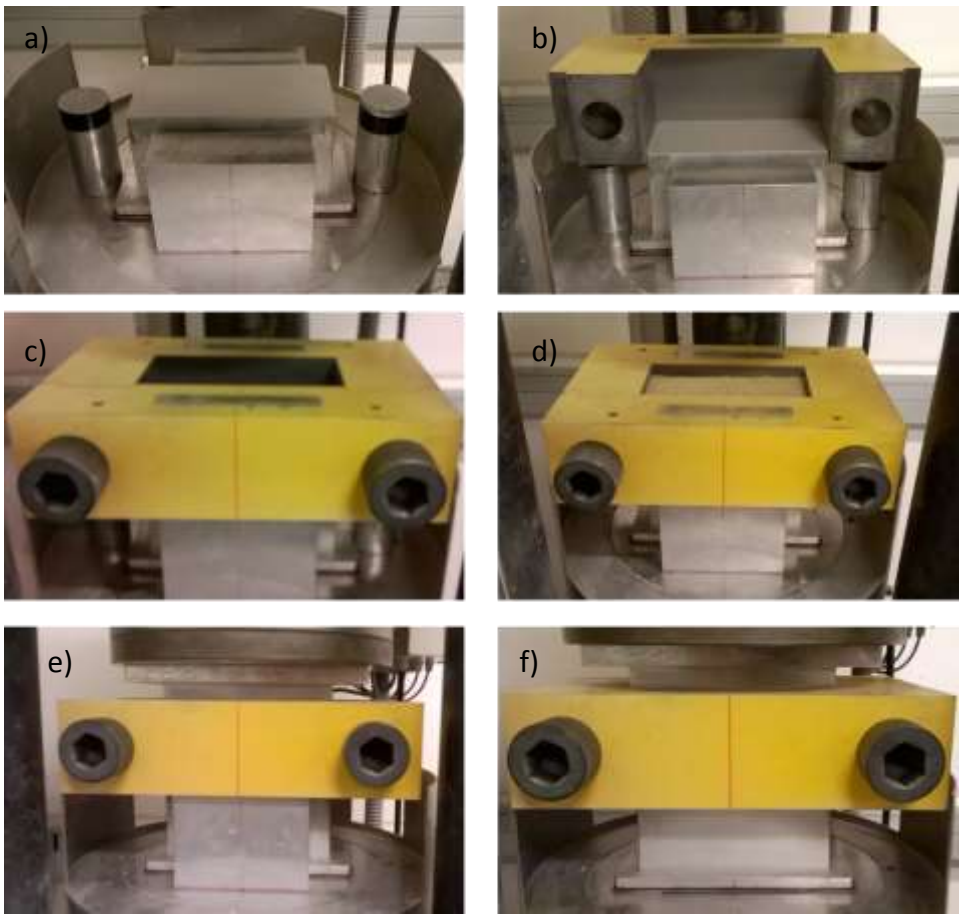

Figure 3.11. Double compaction of earth brick

- After compaction, the bottom press plate and the mould seating on it are lowered to create a space to fit two aluminium spacers on top of parts 1 and 2. A load is then applied again to the spacers to gently push the mould down until the brick is fully demoulded (Figure 3.12).

Figure 3.12. Brick demoulding phase

A total of 40 bricks were compacted by means of the above fabrication method. After compaction, earth bricks were stored at room temperature of 25 °C for a period of two weeks before compressive strength tests were performed. Table 3.4 summarises the main properties of all compressed earth bricks after equalisation. The acronyms SD and CV refer to the standard deviation and coefficient of variation of all measured properties. It can be noted that the dry density of the compressed earth bricks is on average higher than that of the cylindrical samples. This is due to the fact that bricks have a volume to lateral surface ratio higher than cylindrical samples, which reduces the effects of lateral friction during compaction.

Table 3.4. Main properties of all compressed earth bricks after equalisation at T = 25 °C

	w (%)	**ρ_b (kg/m^3)**	**ρ_d (kg/m^3)**	**n (-)**	**S_r (%)**
Minimum	2,3	2378	2310	0,122	44,4
Maximum	3,2	2399	2339	0,133	58,9
Average	2,8	2390	2325	0,127	51,4
SD	0,2	5,5	6,1	>0,1	3,9
CV (%)	7,1	0,2	0,3	>0,1	7,6

3.4 Stabilisation methods

In this section, the stabilisation methods adopted to improve durability of cylindrical earthen samples are presented and discussed.

A preliminary evaluation of the durability of unstabilised earth compacted to 100 MPa at the optimum water content was performed by means of immersion tests in compliance with the German norm DIN 18945 (2013). This test consist in dipping samples in water for ten minutes and measuring the corresponding mass loss (see Section 2.4).

Unstabilised earth exhibited very limited durability with a mass loss of 70% after ten minutes of immersion.

After these results, stabilisation was considered indispensable to improve durability. Earthen samples were stabilised by substituting soil water with different solutions of hydrophobic products at different concentrations. In the first part of this experimental campaign, the following four hydrophobic additives were tested:

- Potassium silicate Marque blanche (commercial name)
- Hydrofuge 64 (commercial name)
- Silane-siloxane emulsion GPE50P (commercial name)
- Plasticure (commercial name)

The exact compositions of the above hydrophobic additives have not been disclosed by the commercial providers. For stabilised cylindrical samples compacted at 100 MPa, the optimum solution content is assumed to be 5.2% which is the same as the optimum water content of the unstabilised cylindrical samples compacted at the same pressure. Prior to compaction, 500 grams of dry soil were mixed with 5.2% of a solution of water and the above mentioned products with variable concentrations. Table 3.5 summarises the composition of all solutions added to the soil mix.

After compaction, the stabilised samples were stored at room temperature of 25 °C until a constant mass was reached. Subsequently, immersion tests were performed to evaluate the effects of stabilisation on durability. The mass loss after immersion is plotted in Figure 3.13 against the corresponding percentage of hydrophobic additive. The same figure also indicates the limits between different brick classes according to the norm DIN 18945 (2013). Inspection of Figure 3.13 shows that all samples presented a mass

loss higher than 15%. This means that all samples fall in the Class III category, which is only suitable for dry applications according to the German norm DIN 18945 (2013). In particular, Hydrofuge 64 and potassium silicate Marque blanche do not improve significantly the durability of the material. Plasticure increases water resistance up to a percentage of 0.54% but, if the additive concentration is increased further, the material response does not improve significantly. These three additives were therefore discarded for further testing.

Table 3.5. Composition of tested additive solutions (first campaign)

	Additive (% Dry mass)	**Water** (% Dry mass)	**Solution content** (% Dry mass)
Untreated sample	0	5.20	5.20
Hydrofuge 64	1.35	3.85	5.20
	2.7	2.50	5.20
Potassium silicate Marque blanche	0.27	4.93	5.20
	0.81	4.39	5.20
	1.35	3.85	5.20
	2.7	2.50	5.20
Plasticure	0.14	5.06	5.20
	0.27	4.93	5.20
	0.40	4.80	5.20
	0.54	4.66	5.20
	0.81	4.39	5.20
	1.08	4.12	5.20
	1.62	3.58	5.20
	2.15	3.05	5.20
Silane-siloxane emulsion GPE50P	0.14	5.06	5.20
	0.27	4.93	5.20
	0.40	4.80	5.20
	0.54	4.66	5.20
	0.81	4.39	5.20
	1.08	4.12	5.20
	1.62	3.58	5.20
	2.15	3.05	5.20

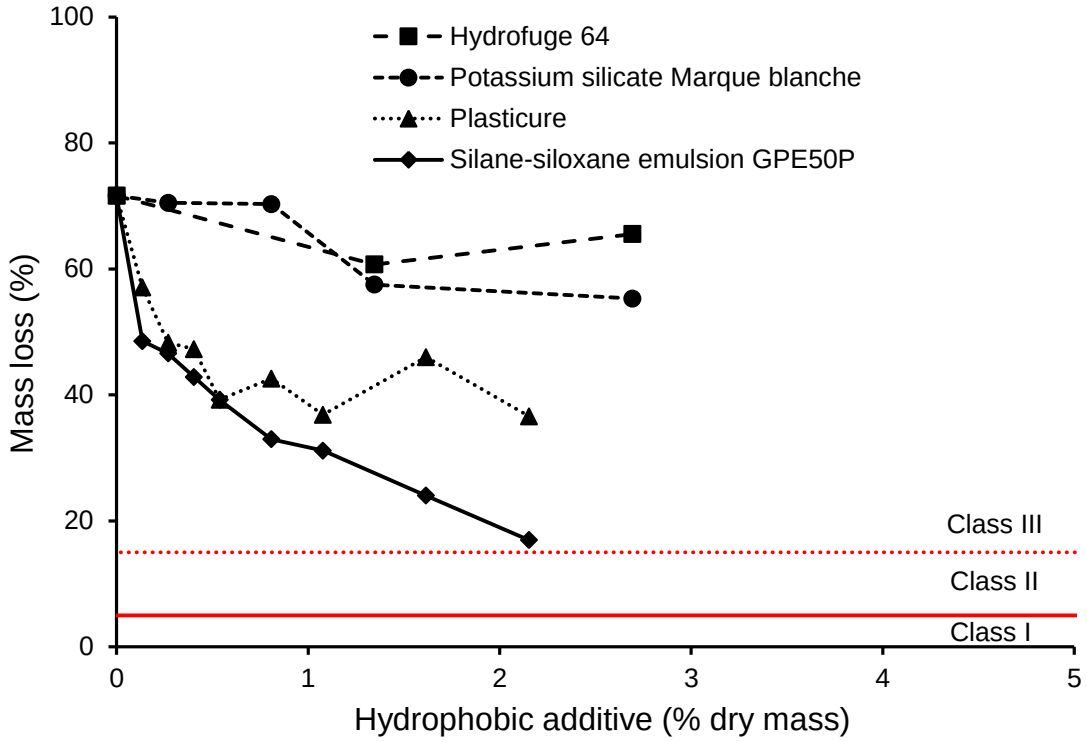

Figure 3.13. Results from the first campaign of immersion tests

The durability of samples stabilised with the silane-siloxane emulsion GPE50P consistently improved with increasing additive concentration. It is therefore expected that higher concentrations of silane-siloxane emulsion may further enhance durability. On the basis of this evidence, a second testing campaign was performed where samples were compacted with higher concentrations of the silane-siloxane emulsion. Moreover, a number of samples were manufactured by mixing the silane-siloxane emulsion with a water based solution of sodium hydroxide (NaOH). Sodium hydroxide was selected to facilitate alkaline activation of earthen materials by transforming clay minerals in non-swelling binding products. Among various alkaline activators such as $Ca(OH)_2$ and KOH, sodium hydroxide is indicated as the strongest one (Elert et al., 2015; Cheng and Saiyouri, 2015; Slaty et al., 2015). Table 3.6 summarises the composition of all solutions added to the dry soil during this second testing campaign.

Table 3.6. Composition of tested additive solutions (second campaign)

Silane-siloxane emulsion (% Dry mass)	**Water** (% Dry mass)	**NaOH Solution** (% Dry mass)	**NaOH solution concentration** (mol/L)	**Total liquid content** (% Dry mass)
0	5.20	-	-	5.20
0.14	5.06	-	-	5.20
0.27	4.93	-	-	5.20
0.40	4.80	-	-	5.20
0.54	4.66	-	-	5.20
0.81	4.39	-	-	5.20
1.08	4.12	-	-	5.20
1.62	3.58	-	-	5.20
2.15	3.05	-	-	5.20
3.23	1.97	-	-	5.20
4.31	0.89	-	-	5.20
5.20	0	-	-	5.20
0	-	5.20	1	5.20
0.54	-	4.66	1	5.20
1.08	-	4.12	1	5.20
2.15	-	3.05	1	5.20
4.31	-	0.89	1	5.20
0	-	5.20	2	5.20
0.54	-	4.66	2	5.20
1.08	-	4.12	2	5.20
2.15	-	3.05	2	5.20
4.31	-	0.89	2	5.20
0	-	5.20	4	5.20
0.54	-	4.66	4	5.20
1.08	-	4.12	4	5.20
2.15	-	3.05	4	5.20
4.31	-	0.89	4	5.20
0	-	5.20	8	5.20
0.54	-	4.66	8	5.20
1.08	-	4.12	8	5.20
2.15	-	3.05	8	5.20
4.31	-	0.89	8	5.20

Figure 3.14 shows the results from the immersion tests performed on samples stabilised by solutions of silane-siloxane emulsion and sodium hydroxide at different concentrations. Inspection of Figure 3.14 indicates that samples compacted with high concentrations of silane-siloxane emulsion show limited mass loss. Also, the addition of

the NaOH solutions helps reducing material erosion as their concentration increases from 1 mol/L to 2 mol/L. However, further increases of NaOH concentration (i.e. 4 mol/L and 8 mol/L) are no longer effective but actually have a detrimental effect on durability.

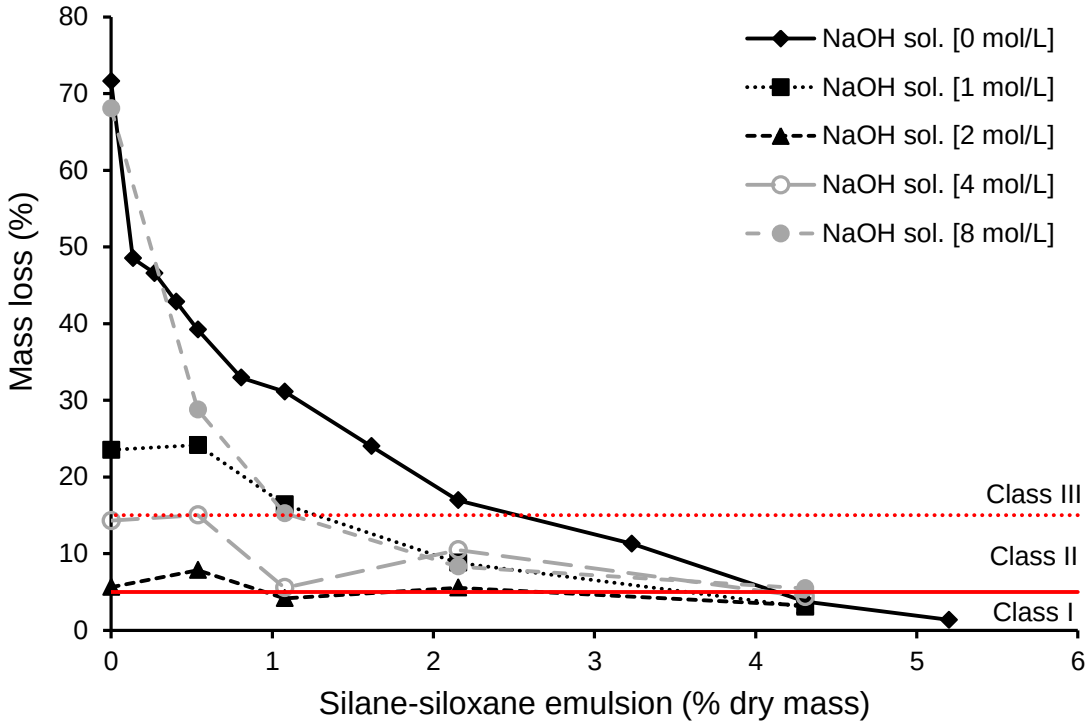

Figure 3.14. Results from the second campaign of immersion tests.

After these tests, the following three different additive compositions were selected for further testing:

- 5.2% silane-siloxane emulsion (mass loss of 1.36% - class I)
- 5.2% NaOH solution at 2 mol/L concentration (mass loss of 5.64% - class II)
- 1.08% silane-siloxane emulsion + 4.12% NaOH solution at 2 mol/L concentration (mass loss of 4.18% - class I)

Samples with the above compositions will be tested to analyse mechanical behaviour (Chapter 5) and moisture buffering capacity (Chapter 6). Durability properties will also be further investigated by performing contact tests and suction tests according to the norm DIN 18945 (Chapter 7).

3.5 Final remarks

In this chapter material properties and methodologies for sample preparation have been presented. The main results can be summarised as:

- Geotechnical properties of the base soil were determined including the grain size distribution and material plasticity in the context of existing recommendations for compressed earth bricks (see Sections 3.1.1 and 3.1.2).
- An innovative hypercompaction method was presented. This method includes three main characteristics: 1) the application of high compaction stresses to increase material density, 2) the use of a double compaction procedure to increase stress uniformity across the height of the sample and 3) the design of a compaction mould with pore water drainage paths to facilitate soil consolidation (see Section 3.2.1).
- The criterion chosen to define the end of consolidation coincides with the measurement of a displacement rate below 0.01 μm/s over a period of at least one hour. This assures that compressed samples experience the whole primary consolidation and a large share of secondary consolidation (see Section 3.2.1).
- Cylindrical earthen samples were compacted at the three pressure levels of 25 MPa, 50 MPa and 100 MPa and at different water contents. For each compaction curve, the highest dry density corresponds to the optimum water content. Also, the dry density increases less than linearly with compaction stress (see Section 3.2.3).
- Samples compacted with the proposed hypercompaction method showed a much higher dry density compared to the Proctor standard (see Section 3.2.3).
- Drainage of water was observed from both the bottom and the top of the mould during compaction of samples prepared at higher water contents. This confirmed the efficiency of the double compaction procedure. No water drainage was observed during compaction of the samples prepared at the optimum water content. For these samples, the water drainage system of the compaction mould was unnecessary (see Section 3.2.3).
- Samples compacted at 100 MPa showed very similar properties after equalisation regardless of the compaction water content. This indicates that the application of a high compaction pressure can result in better quality control of the final product (see Section 3.2.4).

- The hypercompaction method was extended to manufacture compressed earth bricks of dimensions 200 x 100 x 50 mm^3. Forty compressed earth bricks were manufactured according to this method in order to determine their compressive strength. The dry density of the bricks is slightly higher than that of cylindrical samples compacted at the same pressure and water content. This is due to the higher volume to lateral surface ratio of bricks compared to cylindrical samples, which reduces the effect of friction and hence increases compaction efficiency (see Section 3.3.2).
- Unstabilised samples showed poor durability during water erosion tests and hence stabilisation was considered indispensable. Immersion tests were performed to select the stabilisation method the gives the best results in terms of durability against water infiltration. Based on these tests, it was concluded that the following three additives offered the most promising performance when mixed with the dry soil prior to compaction:
    - silane-siloxane emulsion (5.2% by dry mass of soil)
    - NaOH solution at 2 mol/L concentration (5.2% by dry mass of soil)
    - silane-siloxane emulsion (1.08% by dry mass of soil) + NaOH solution at 2 mol/L concentration (4.12% by dry mass of soil)

These compositions were the object of further investigation in the following part of the work .

4

Microstructural analysis

This chapter presents the results from mercury intrusion and nitrogen adsorption porosimetry tests. These two techniques are complementary since they investigate two different pore size ranges: mercury intrusion porosimetry detects pore sizes between 10^1 nm and 10^5 nm, while smaller pores down to 2 nm can be analysed by nitrogen adsorption. The main objective of these tests was to assess the effect of the hypercompaction procedure on the microstructural properties of earthen samples.

4.1 Mercury intrusion porosimetry tests

As already discussed in Section 2.1.4, mercury intrusion porosimetry (MIP) tests are based on the principle that a non-wetting fluid, such as mercury, can be intruded into a porous media only if sufficient pressure is applied. Assuming that pores are cylindrical, the smallest pore diameter d_{pore} intruded by mercury for a given pressure difference ΔP across the mercury interface can be calculated by means of Washburn equation:

$$\Delta P = \frac{4\,\gamma \cos\theta}{d_{pore}} \tag{4.1}$$

where γ is the mercury surface tension and θ is the mercury contact angle. A surface tension of 485 dyn/cm and a contact angle of 147° are assumed as suggested by Diamond (1970) for illitic soils.

MIP tests are also based on the assumption that pores are connected to the sample surface either directly or through larger pores. Pores that do not match this assumption are named "ink-bottle" pores (Moro and Böhni, 2002). The presence of these pores affects the measured pore size distribution, though more reliable results can be obtained by performing multiple intrusion-extrusion cycles.

MIP tests were performed in this work by means of a Micromeritics AutoPore IV Mercury Porosimeter. Each test consists of two stages: a low pressure stage (to measure pores with diameter between 10^4 nm and 10^5 nm) and a high pressure stage (to measure pores with diameter between 10^1 nm and 10^4 nm). The low pressure stage can be performed in two different ports at the same time. One single chamber is instead available for the high pressure stage (Figure 4.1).

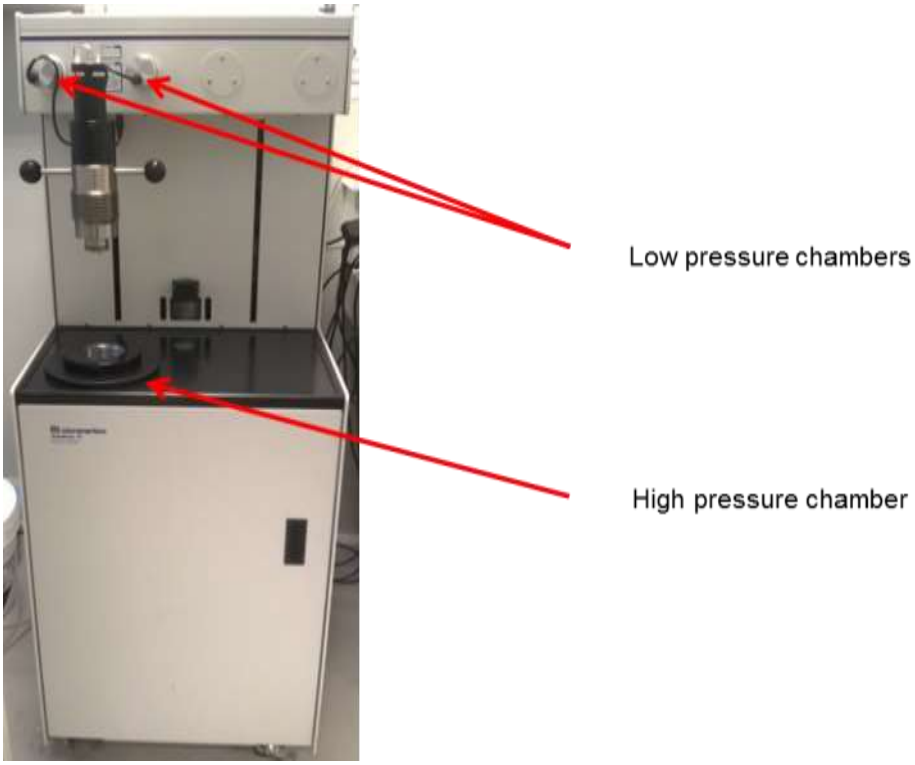

Figure 4.1. Micromeritics AutoPore IV Mercury Porosimeter

4.1.1 Sample preparation and testing procedure

MIP tests were performed on small samples of about 4 grams (about 1.5 cm^3) taken from the cylindrical specimens compacted according to the Proctor standard (AFNOR, 1999) and at static pressures of 25 MPa, 50 MPa and 100 MPa (see Section 3.2.1). Samples were equalised for a week at a temperature of 25°C and a relative humidity of 62% to avoid any change of material fabric caused by the variable environmental conditions inside the laboratory.

After equalisation and prior to MIP tests, all soil water was removed to avoid errors in the measurement of pore volume. For this purpose, samples could have been oven dried but this would have changed the original pore size distribution as observed by Diamond (1970). Freeze drying was therefore adopted because this procedure impacts much less on material fabric compared to oven drying (Delage and Pellerin, 1984; Romero et al., 1999; Cuisinier and Laloui, 2004; Simms and Yanful, 2004; Sasanian and Newson, 2013). Samples were initially dipped in liquid nitrogen (-196 °C) for few minutes until boiling reduced and then placed under vacuum at a temperature of -50°C for at least two days. During immersion in liquid nitrogen, the pore water freezes instantaneously becoming amorphous ice with a negligible change in volume, which avoids deformation of soil fabric. Then, under vacuum, the frozen water sublimates from the solid phase into the gas phase. This procedure was performed by using the freeze-drier Crios from the company Cryotec (Figure 4.2).

Figure 4.2. Freeze-drier Crios (Cryotec)

After freeze-drying, samples were placed inside a penetrometer that was then inserted inside the low pressure chamber (compressed air chamber) of the MIP equipment. Prior to mercury intrusion, the gas pressure was lowered inside the penetrometer in order to evacuate any residual moisture and air from the soil pores. Evacuation must be performed slowly in order to avoid any aspiration of the material. This stage was considered completed when the target pressure of 50 µmHg (corresponding to an absolute pressure of 6.7 kPa) was attained and kept constant for at least five minutes.

After evacuation, the penetrometer was filled with mercury at low pressure. The first data point is generally taken at a pressure of 4 kPa or higher (Giesche, 2006). Readings at lower pressures are possible but not reliable since the head-pressure of mercury must be taken into account (a height of 1 cm mercury column corresponds to a pressure of 1333 Pa). In this study, the first data point was taken at a pressure of 10 kPa (i.e. pore diameter of 6×10^4 nm). The low pressure stage terminates when pressure attains a value of 200 kPa (i.e. pore diameter of 7×10^3 nm).

After the low pressure stage, the penetrometer was transferred to the high pressure chamber (compressed oil chamber) for the subsequent stage. During the high pressure stage, pressure was first increased up to 207 MPa (i.e. pore diameter of 1×10^1 nm) to intrude the pores and then decreased back to 360 kPa to perform extrusion. The change from low to high pressure affects measurements because of differences between pressure transducers and testing environments, i.e. air versus oil (Giesche, 2006). This is taken into account by correcting raw data as explained in the next section.

4.1.2 Processing of raw data

The change between low and high pressure stages affects the measurement of pore volume because of differences in pressure transducers and testing environments between the two chambers. These artificial effects are corrected in the present work as explained in the following.

The raw values of pressure and intruded volume of mercury are directly measured during the test. The pore diameter is then calculated from the measured pressure according to Equation 4.1 while the corresponding pore volume is assumed to coincide with the intruded volume of mercury. During the low pressure stage, the intruded volume of mercury continuously increases as pressure grows and pores with smaller diameters are progressively filled. The derivative of pore volume respect to pore diameter $\mathrm{d}V/\mathrm{d}d_{pore}$ also increases up until the end of the low pressure stage. However, at the beginning of the subsequent high pressure stage, the cumulative intruded volume remains approximately constant as pressure increases, which means that the value of $\mathrm{d}V/\mathrm{d}d_{pore}$ suddenly drops to zero. Only after a further increase of pressure, the derivative $\mathrm{d}V/\mathrm{d}d_{pore}$ begins to grow again and eventually rises above the value measured at the end of the low pressure stage.

The correction of raw data adopted in this work consists in imposing the monotonic increase of the derivative dV/dd_{pore} around the transition point between the low and high pressure stages. This is achieved by neglecting all data points at the beginning of the high pressure stage for which dV/dd_{pore} is lower than the value attained at the end of the low pressure stage (Figure 4.3).

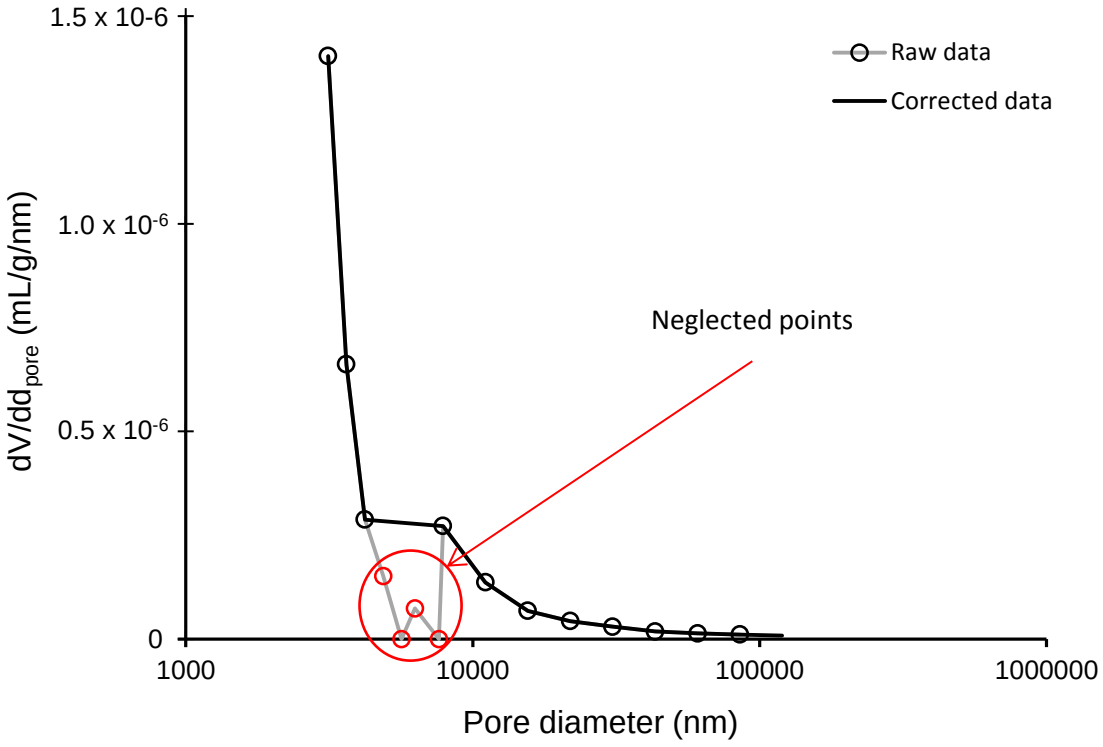

Figure 4.3. Zoomed view at the transition between low and high pressure stages: correction of raw data

After removing these data points, the cumulative intruded volume V_i at the generic point i of the high pressure stage is recalculated from the derivative $(\mathrm{d}V/\mathrm{d}d_{pore})_i$ as follows:

$$V_i = \left(\frac{\mathrm{d}V}{\mathrm{d}d_{pore}}\right)_i \left(d_{pore,i-1} - d_{pore,i}\right) + V_{i-1} \tag{4.2}$$

Porosimetry curves are often presented as semi-logarithmic plots of dV/dlogd_{pore} versus logd_{pore} to improve visualisation over the small pore range. Before plotting these curves, a second correction was made to smooth the measured pore size distribution. This is necessary to better visualise the experimental data especially over the small pore range. The correction consists in replacing the logarithm of the pore diameter log$d_{pore,i}$ and

corresponding derivative $(\mathrm{d}V/\mathrm{d}\log d_{pore})_i$ at the generic point i of the mercury intrusion curve with the respective running averages between points $i-2$ and $i+2$ calculated as follows:

$$\log d_{pore,i} = \frac{\log\left(d_{pore,i+2} * d_{pore,i-2}\right)}{2} \tag{4.3}$$

$$\left(\frac{\mathrm{d}V}{\mathrm{d}\log d_{pore}}\right)_i = \left|\frac{V_{i+2} - V_{i-2}}{\log\left(\frac{d_{pore,i+2}}{d_{pore,i-2}}\right)}\right| \tag{4.4}$$

Figure 4.4 shows that the above corrections result in a pore size distribution curve that is smoother than the raw data but still respects the original trend.

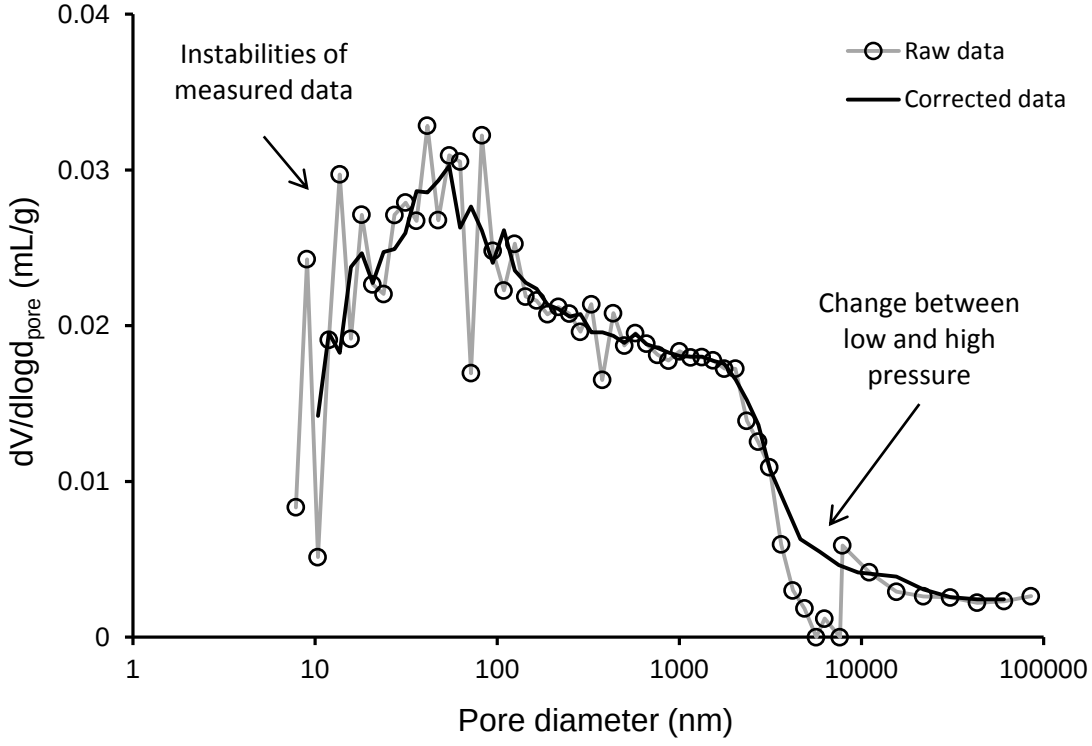

Figure 4.4. Typical result of raw data processing

4.2 Results of mercury intrusion porosimetry tests

4.2.1 Effect of compaction effort

Figures 4.5a and 4.5b show the cumulative volume (intruded and extruded) and the pore size distribution of different specimens compacted at their respective optimum water contents. Inspection of Figure 4.5a indicates that porosity *n* reduces from 21% to 15% as compaction energy increases from the Proctor standard to static compaction at 25 MPa, 50 MPa and 100 MPa. As reported in Section 2.1.4, inter- and intra-aggregate pore volumes as well as the pore diameter that separates the region of the inter-aggregate porosity from the region of intra-aggregate porosity can be determined by comparison between intruded and extruded volumes of mercury (numerical values are reported in Table 4.1).

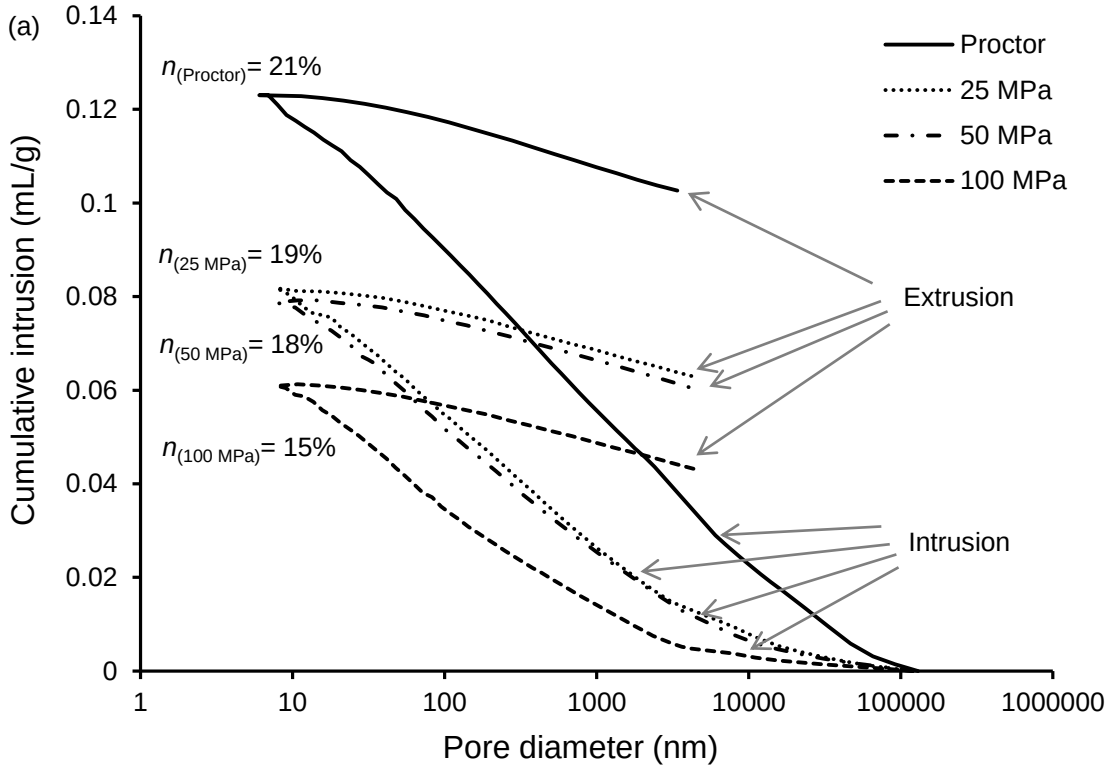

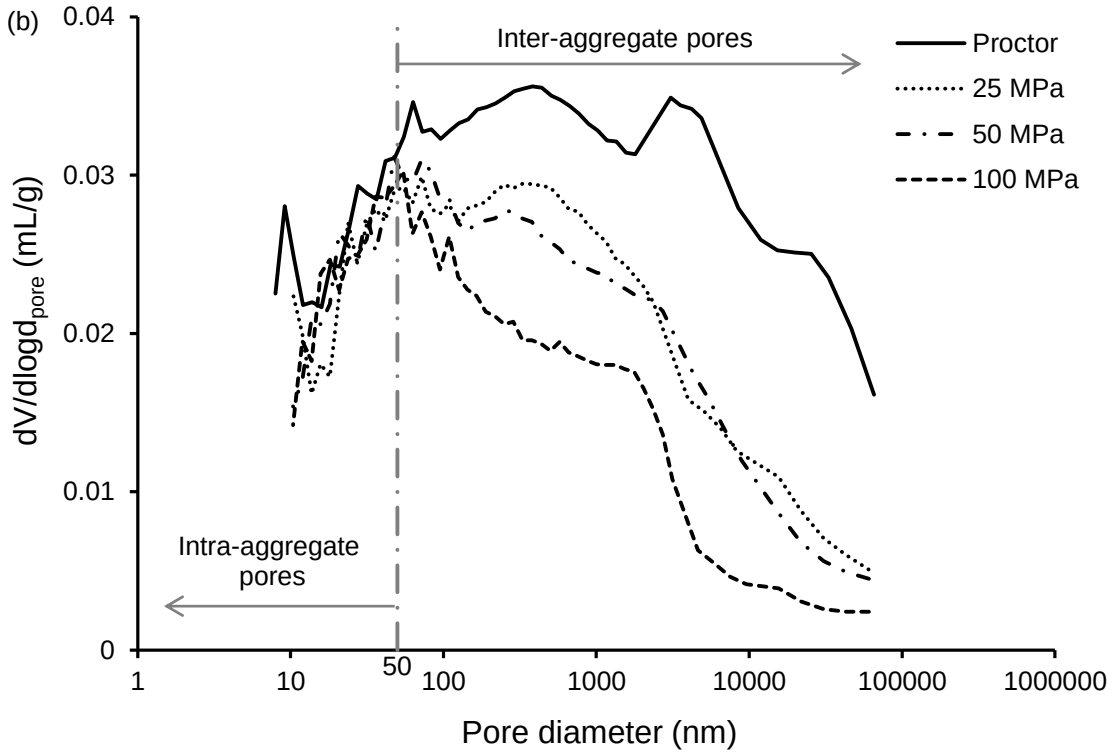

Figure 4.5. Comparison between Proctor standard and hypercompaction: intruded and extruded cumulative volumes (a) and pore size distribution (b)

Table 4.1. Inter- and intra-aggregate pore volumes, pore diameter boundary between inter- and intra-aggregate porosity

	Intruded volume (mL/g)	Inter-aggregate pore volume (mL/g)	Intra-aggregate pore volume (mL/g)	Pore diameter boundary (nm)
Proctor	0.123	0.103	0.020	41
25 MPa	0.082	0.063	0.019	53
50 MPa	0.079	0.060	0.019	53
100 MPa	0.061	0.043	0.018	57

Interestingly, inter-aggregate porosity (i.e. pores with diameter larger than 50 nm) is reduced by a factor of about 2.5 when compaction effort increases from the Proctor standard to a static pressure of 100 MPa (Table 4.1). The influence of compaction effort on intra-aggregate porosity (i.e. pores with diameter smaller than 50 nm) is instead very limited, as shown by the pore size distribution in Figure 4.5b. This is consistent with the results obtained by Simms and Yanful (2004) on compacted tills, by Hoffemann et al. (2007) on compacted bentonite and by Tarantino and De Col (2008) on compacted

kaolin. All these studies concluded that mechanical compaction only affects inter-aggregate porosity while no effects are noticeable on intra-aggregate porosity.

Based on these results, it is expected that compaction effort has a significant influence on the mechanical properties of earthen materials (affected by density and, hence, by inter-aggregate porosity) but has no influence on hygroscopic behaviour (controlled by intra-aggregate porosity). This conclusion, which is based on the above microstructural analysis, is also confirmed by macroscopic tests that will be presented in Sections 5.1 and 6.3.

4.2.2 Analysis of sample homogeneity

Double compaction consists in the application of the same load on both the top and bottom surfaces of the earthen sample. Double compaction reduces the effect of lateral friction on the sample homogeneity as it increases the uniformity of stress levels across the soil (see Section 3.2.1). In order to explore this effect further, MIP tests were performed on small soil specimens taken at different heights of the same sample to analyse homogeneity of material fabric. Figures 4.6a and 4.6b compare the cumulative intruded volume and pore size distribution of small specimens taken at the top, middle and bottom of a cylindrical specimen compacted at 100 MPa with the optimum water content. Specimens taken at the top and bottom extremities of the cylindrical sample show a slightly lower porosity than the specimen taken at middle height. This is caused by the friction between the sample and the mould, which creates a decreasing gradient of compaction stress from the sample extremities, where the load is applied, to the middle. Hence, compaction is slightly more effective at the two extremities of the sample than at the middle, though the difference of porosity measured in this work is not very significant. This result also confirms the importance of double compaction: a larger inhomogeneity of material fabric would be expected if single compaction was performed from only one side of the sample.

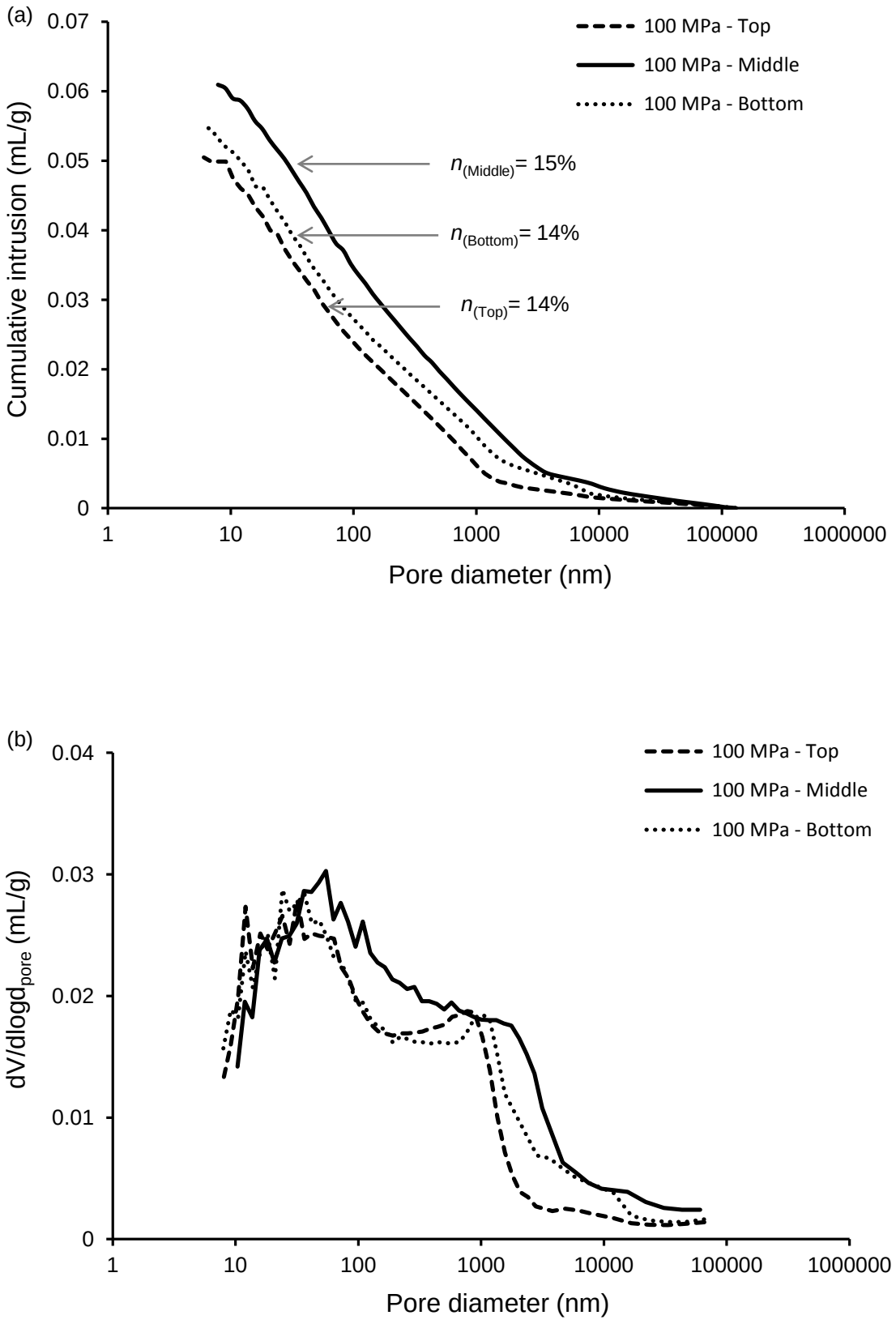

Figure 4.6. Comparison top, middle and bottom height: cumulative volume (a) and pore size distribution (b)

4.2.3 Effect of compaction water content

In Section 3.2.4 it has been shown that cylindrical samples produced with the same compaction effort tend to shrink of different amounts during equalisation at T = 25 °C and RH = 62% depending on their initial water content. These differences tend, however, to reduce as the compaction effort increases from the lowest level corresponding to the Proctor standard up to the highest level corresponding to a static pressure of 100 MPa.

To further explore this aspect, MIP tests were performed to analyse the microstructural properties after equalisation of samples compacted with the same effort at similar densities but different water contents. Figure 4.7 shows the water content and dry density of the two samples compacted according to Proctor standard and the two samples compacted at 100 MPa after compaction (hollow red markers) and after equalisation (full red markers). In each case, the two samples had, after compaction, the same porosity but different water contents corresponding to the dry and wet side of optimum, respectively. In particular, porosity after compaction was equal to 0.32 in the case of the two Proctor samples and 0.15 in the case of the two samples compacted at 100 MPa.

Figures 4.8a and 4.8b compare the cumulative intruded volume and pore size distribution after equalisation of the two Proctor specimens and the two specimens compacted at 100 MPa. Inspection of Figures 4.8a and 4.8b indicates that the two Proctor specimens exhibit different amounts of shrinkage during equalisation, with the specimen compacted wet of optimum shrinking more, and hence attaining a lower porosity, than the specimen compacted dry of optimum. The different porosity is also reflected in the different pore size distribution of these two specimens after equalisation. Conversely, the two specimens compacted at 100 MPa show almost identical pore size distributions after equalisation regardless of compaction water content, which is consistent with data presented in Section 3.2.4 (see Figure 4.7). This result confirms that the application of a high compaction pressure can standardise material properties and reduce fabric variability associated to compaction water content.

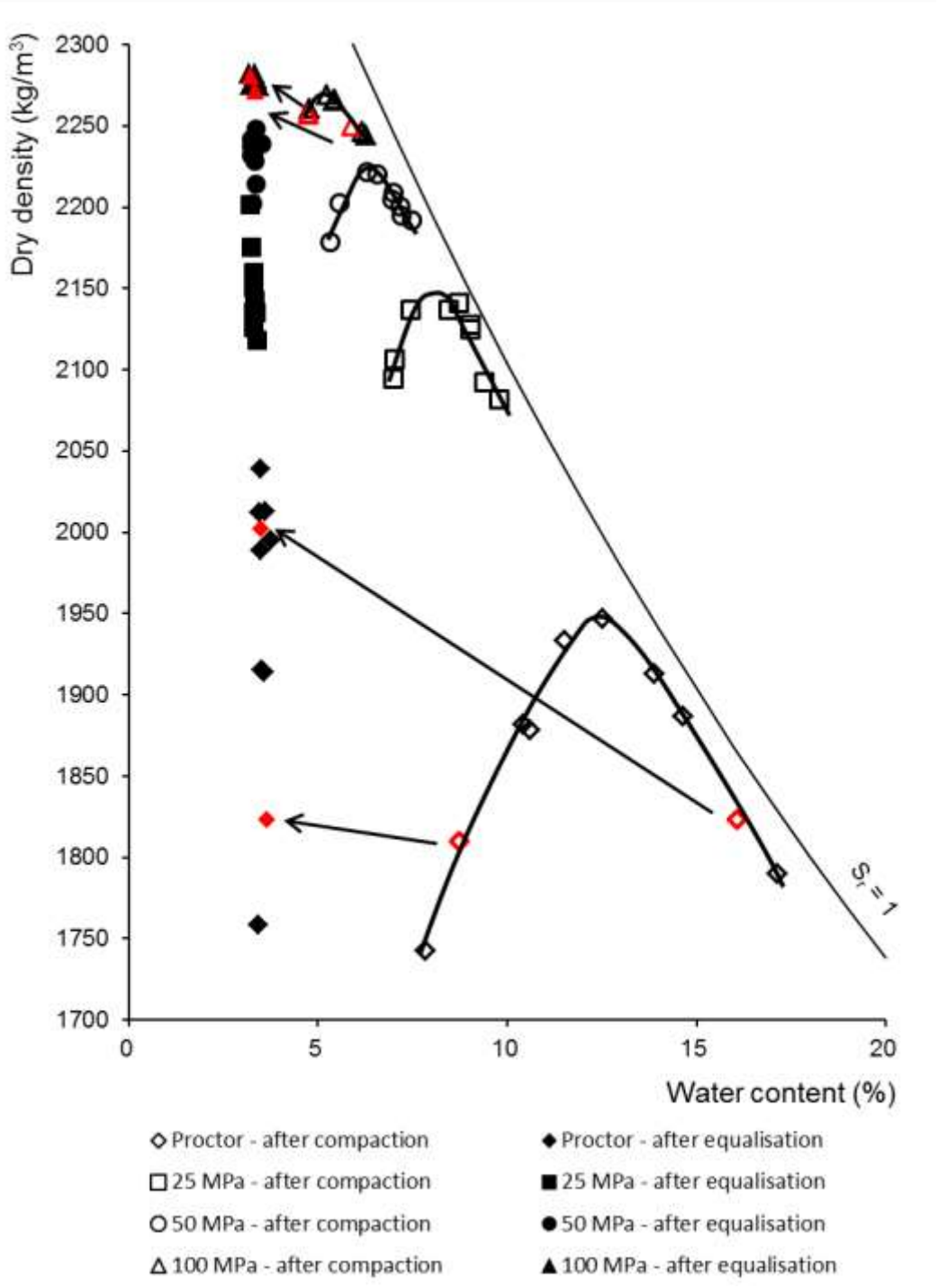

Figure 4.7. Water content and dry density of samples compacted according to Proctor standard and at 100 MPa

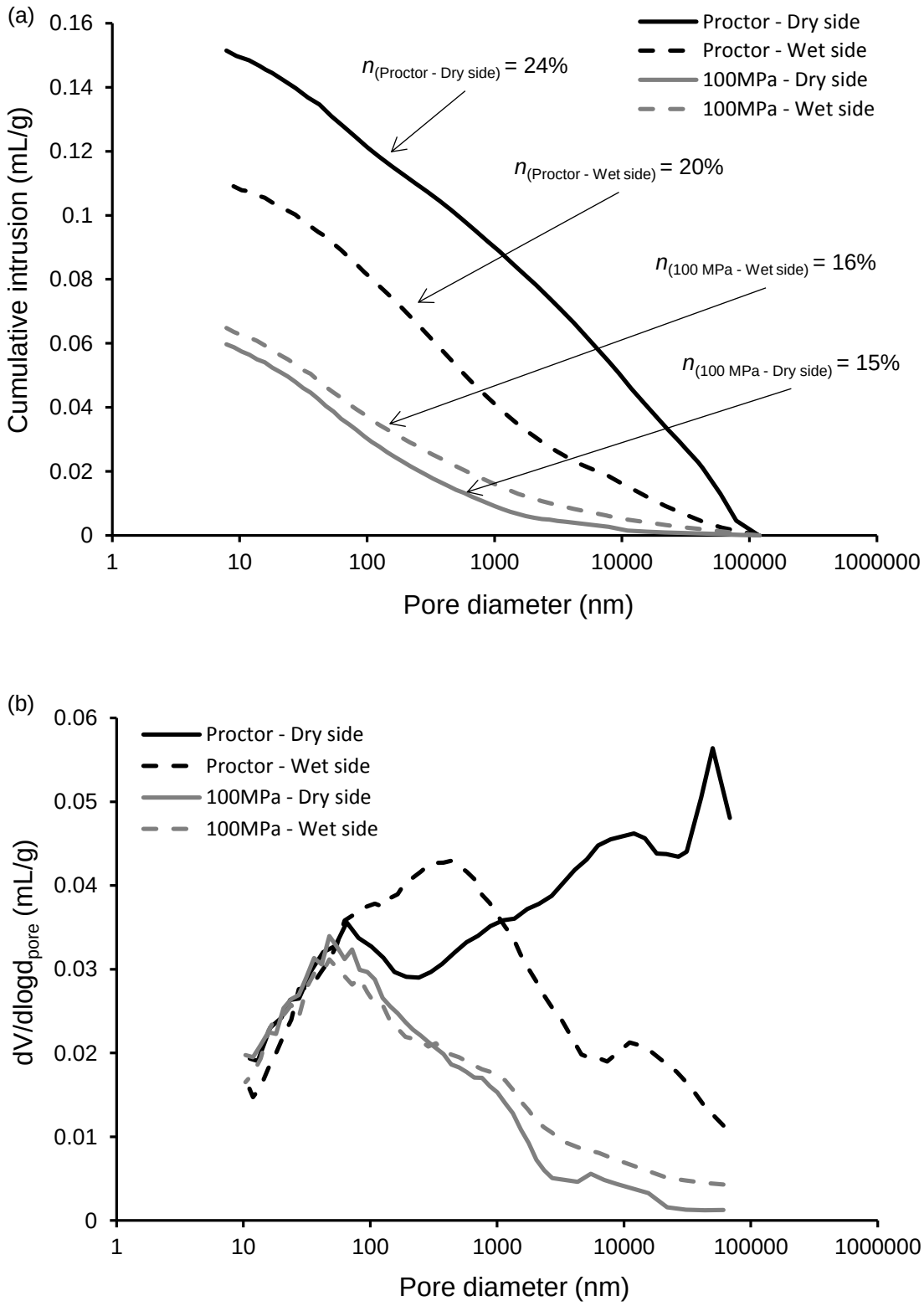

Figure 4.8. Effects of compaction water content. Comparison Proctor standard and 100 MPa: cumulative volume (a) and pore size distribution (b)

MIP tests allow the analysis of pore sizes from 10^5 nm to 10^1 nm, which is the class of pores governing the macroscopic mechanical behaviour of earthen materials. The

hygroscopic behaviour is instead governed by smaller pores with diameter of few nanometers. This smaller pore class can only be detected by nitrogen adsorption tests, which cover the pore size range from 2 nm to 50 nm as discussed in the next section.

4.3 Nitrogen adsorption

4.3.1 Sample preparation and testing procedure

Nitrogen adsorption tests were performed on small specimens of about 1 gram (corresponding to 0.5 cm^3) taken from the compacted cylindrical specimens and equalised at a temperature of 25 °C and a relative humidity of 62% for a week, similarly to the specimens subjected to MIP tests.

Likewise MIP specimens, after equalisation pore moisture was removed by freeze-drying to obtain reliable measurements of specific surface and pore size distribution. Samples were then weighed, inserted inside a penetrometer and connected to a Micromeritics TriStar II Surface Area and Porosity equipment (Figure 4.9) to perform nitrogen adsorption tests. Nitrogen was intruded in the pore network by increasing its pressure at constant temperature of 77 K (- 196 °C) up to its saturation value of 1 atm (absolute) and then decreased to perform extrusion. During testing, the amount of intruded nitrogen was measured to determine isothermal adsorption and desorption curves. From these curves, the specific surface area and pore size distribution was determined by means of the of the BJH model (Barret et al., 1951) as reported in Section 2.1.4.

Figure 4.9. Micromeritics TriStar II Surface Area and Porosity equipment

4.3.2 Effect of compaction effort

Figure 4.10 shows the pore size distribution of specimens compacted at 25 MPa, 50 MPa and 100 MPa at their respective optimum water contents. Inspection of Figure 4.10 confirms that mechanical compaction does not affect intra-aggregate pores, i.e. pores with diameter lower than 50 nm, which is consistent with the results obtained from MIP tests. The pore size distribution curves of the three samples overlap over the entire pore size range. Also, the specific surface of all three samples was measured to be equal to 22 m^2/g. The specific surface is governed by the grain size distribution (0.4% gravel, 40.4% sand, 42.9% silt and 16.3%, as reported in Section 3.1.1) and clay mineralogy (illitic clay, according to the information from the soil provider) of the tested soil.

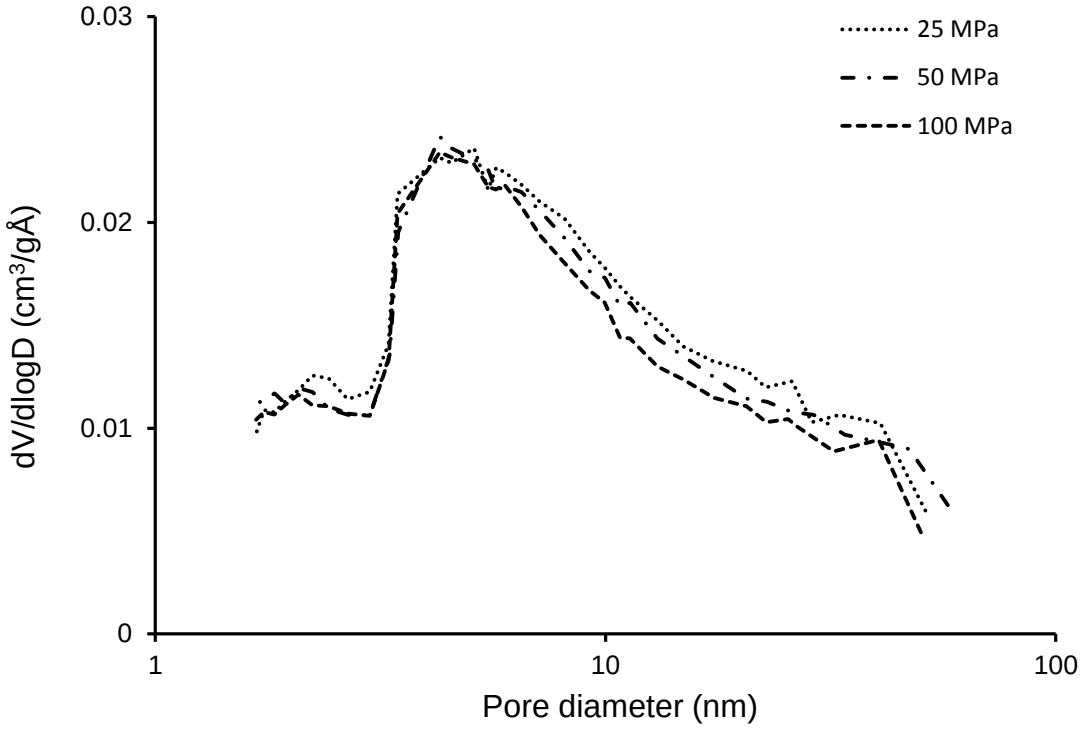

Figure 4.10. Nitrogen adsorption tests. Comparison of pore size distributions between specimens compacted at 25 MPa, 50 MPa and 100 MPa

4.4 Final remarks

MIP and nitrogen adsorption tests were performed to better understand the effects of compaction procedure on material fabric. In particular, it was found that:

- Compaction affects only inter-aggregate porosity with negligible effects on intra-aggregate pores. This was confirmed by both MIP and nitrogen adsorption tests.
- Cylindrical samples are homogeneous and porosity changes only marginally across their height with the two extremities tending to be slightly more compacted than the middle. Double compaction is considered essential to achieve this uniformity of material density. A significantly larger inhomogeneity would be expected if compaction was performed from only one side of the sample.
- At the highest pressure of 100 MPa, the effect of the compaction water content on pore fabric is significantly reduced, thus facilitating the standardisation of material properties during production.

The above outcomes will aid interpretation of the macroscopic mechanical behaviour (presented in Chapter 5) and moisture buffering behaviour (presented in Chapter 6).

5

Mechanical behaviour

This chapter presents results from mechanical tests conducted to measure the stiffness and strength of unstabilised and stabilised earth at the scale of small cylindrical samples and large bricks.

5.1 Effect of density of unstabilised earth

Results from mechanical tests on cylindrical unstabilised samples are presented in this section. The main objective was to determine the effect of the compaction load, and hence of the dry density, on the stiffness and strength of the unstabilised earth. Cylindrical samples were manufactured at the three compaction pressures of 25, 50 and 100 MPa and at different water contents, both on the dry and wet sides of optimum. This resulted in samples with different values of dry density for each compaction pressure depending on the chosen compaction water content. The samples were manufactured according to the compaction method presented in Section 3.2. Note that these samples were manufactured in the early stages of this research and, therefore, perforated disks were always used to help drainage of pore water during compaction (the use of these disks was subsequently abandoned for samples compacted dry of optimum or at the optimum).

Stiffness parameters such as Young modulus and Poisson ratio were measured base on five unconfined loading-unloading cycles. Cycles were performed at a loading rate of 0.005 MPa/s between one ninth and one third of the estimated compressive strength of the material (strength was estimated as the average value of preliminary compression tests on two samples for each compaction level).

Axial displacements were measured between two points along the height of the cylindrical samples at a distance of 50 mm by means of two transducers (i.e. extensometers from Epsilon Technology Corp., Model 3542-050M-005-HT1) placed on diametrically opposite sides. Radial displacements were instead measured by means of a chain fitted around the sample, at its middle height, and connected to a displacement

transducer (i.e. extensometer from Epsilon Technology Corp., Model 3544-150M-060M-ST) as shown in Figure 5.1.

After five loading-unloading cycles, the samples were loaded to failure to determine the unconfined compressive strength.

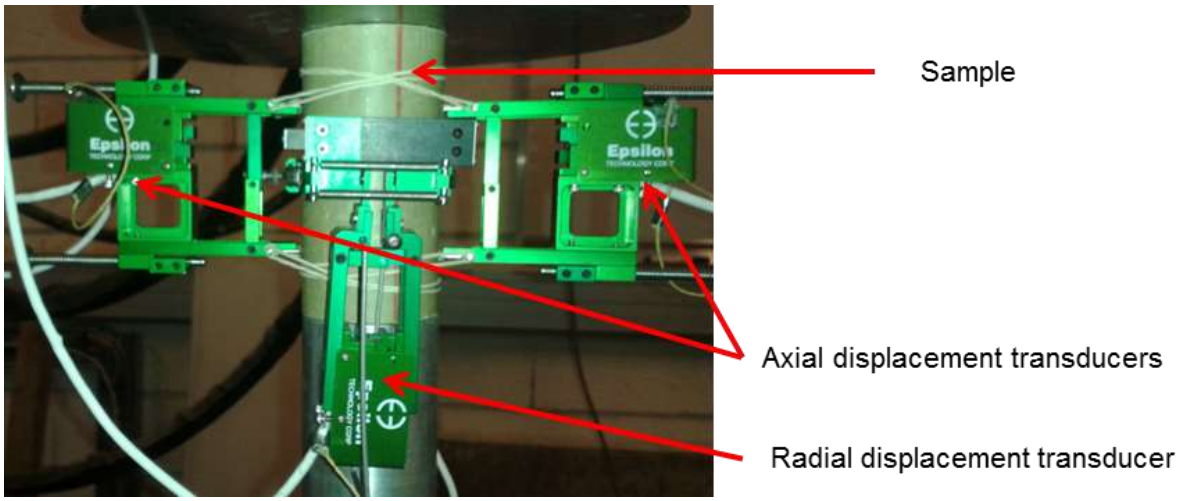

Figure 5.1. Testing set-up for measuring axial and radial displacements

5.1.1 Young modulus

Due to the hysteretic response of the material during cyclic testing (Figure 5.2), the Young modulus and Poisson ratio were determined by considering only the unloading branches of the five cycles. This was based on the assumption that material behaviour is elasto-plastic during loading but essentially elastic during unloading. In particular, the Young modulus was determined as the average slope of the five unloading branches in the axial stress-strain plane.

Figure 5.3 shows the values of the Young modulus plotted against dry density for all specimens. All data are fitted by a unique trendline (thick line) with a relatively narrow standard deviation band (dashed lines). The values of dry density in Figure 5.3 are those after equalisation (see Section 3.2.4, Figure 3.8). Inspection of Figure 5.3 indicates that compaction load has a big influence on the measured values of Young modulus with a variation of one order of magnitude between the specimens compacted at 100 MPa and those compacted according to Proctor standard.

Interestingly, the Young modulus grows more than linearly with increasing dry density. Therefore, any small increase in dry density beyond the current maximum value of 2280

kg/m^3 would produce a significant augmentation of material stiffness. Of course, the dry density cannot be higher than the density of the soil particles. The attainment of this theoretical limit corresponds to the case when porosity becomes equal to zero and would require the application of an extremely large compaction pressure, which is practically unfeasible as discussed in Section 3.2.3.

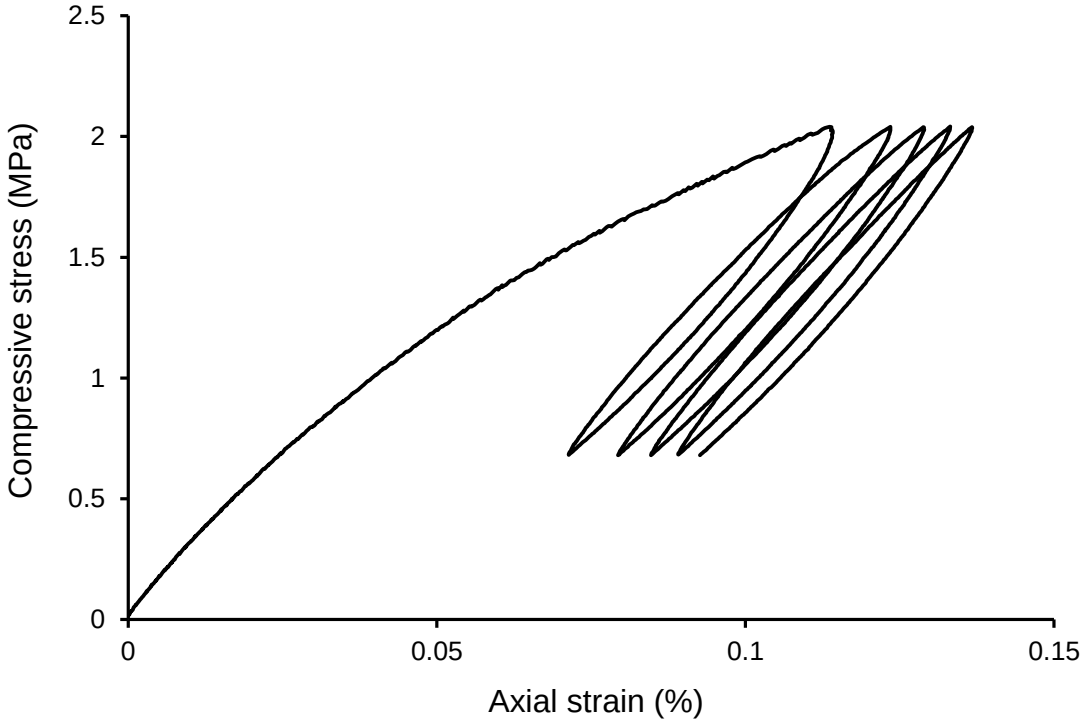

Figure 5.2. Typical cyclic test for measuring stiffness properties (sample S09-CS100-W6.2 – see Table 3.3)

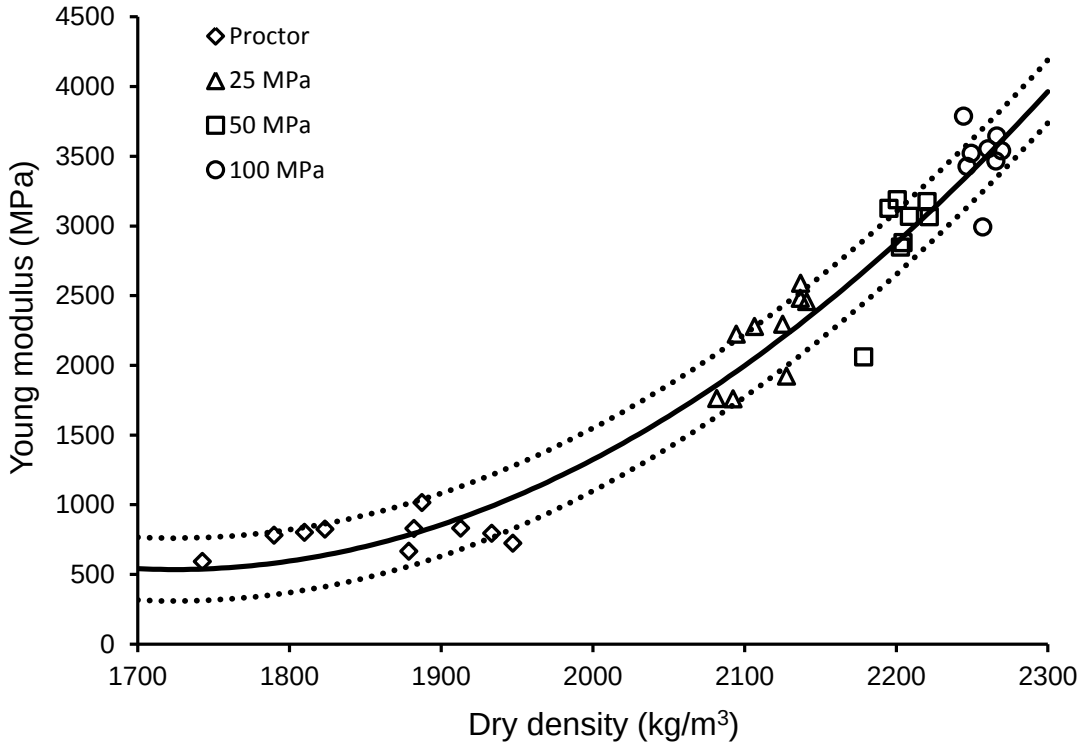

Figure 5.3. Variation of Young modulus with dry density

5.1.2 Poisson Ratio

Similar to the Young modulus, the Poisson ratio was calculated as the average ratio between radial and axial deformations of the five unloading branches. Figure 5.4 shows the variation of the Poisson ratio with increasing dry density.

Inspection of Figure 5.4 indicates that the measured values of Poisson ratio are more scattered than the values of Young modulus, which makes more complicated to establish a clear relationship between Poisson ratio and dry density. This relatively large scatter is most likely due to the experimental technique employed to determine radial displacements which introduce some measurement errors. This is because radial displacements are measured by a circumferential strain gauge which applies a spurious confinement to the sample. Nevertheless, the trend line (thick line) in Figure 5.4 indicates that the Poisson ratio tends to slightly increase as dry density increases. This also indicates a tendency of the material to undergo smaller volumetric changes under a given axial load as the dry density increases.

In Figure 5.4 the labels next to the data points represent the values of water content after compaction. Samples compacted wet of optimum (solid markers) showed generally lower values of Poisson ratio at the same value of dry density, compared to samples compacted dry of optimum (hollow markers). Samples compacted wet of optimum also showed a larger increase of Poisson ratio with dry density compared to samples compacted dry of optimum, for which the Poisson ratio remained about constant.

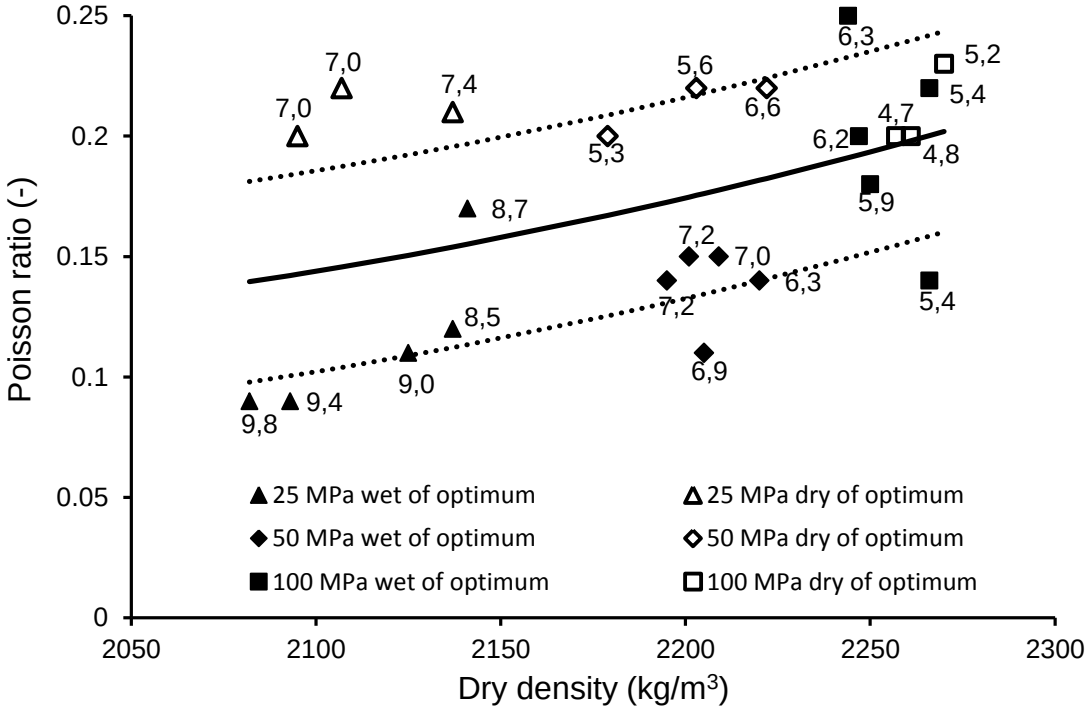

Figure 5.4. Variation of Poisson ratio with dry density

5.1.3 Shear modulus

For isotropic linear elastic materials, the Young modulus, E and Poisson ratio, ν are combined to calculate the shear modulus, G by means of the following equation:

$$G = \frac{E}{2(1+\nu)} \tag{5.1}$$

The assumption of elastic and isotropic behaviour can be considered valid for earthen materials only at low loading levels during service life, as observed by Bui and Morel (2009). Based on this assumption, the values of shear modulus are here calculated by means of Equation 5.1 and plotted in Figure 5.5 against dry density. It can be observed that shear modulus increases about linearly with increasing dry density and this is

mainly due to the large variations of the Young modulus (Figure 5.2) compared to the relatively small changes of Poisson ratio (Figure 5.4).

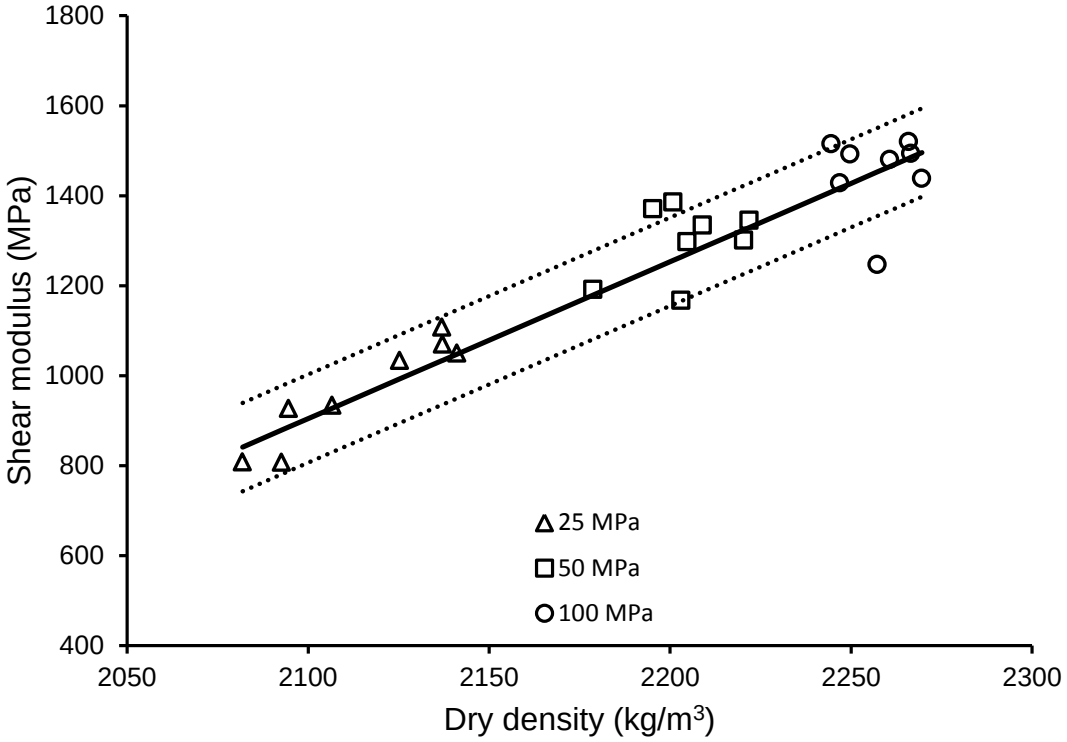

Figure 5.5. Variation of shear modulus with dry density

5.1.4 Compressive strength

As discussed in Section 2.2.2, the unconfined compressive strength is a key property for the design of earth buildings. Strength measurements can be affected by many factors such as test procedure, sample geometry (e.g. aspect ratio) and, of course, material characteristics (e.g. dry density, moisture content, stabiliser content).

Insufficient sample slenderness, associated to the occurrence of friction between the sample and the press plates, can introduce errors in the measurement of compressive strength (Morel et al., 2007; Ciancio and Gibbings, 2012). In this study, the aspect ratio of cylindrical samples was equal to two (samples have a diameter of 50 mm and height of 100 mm), which is considered sufficient to avoid measurement errors. Teflon spray was also smeared on the press plates to reduce friction at the contact between the top and bottom surfaces of the samples and the press plates. Most samples tested in the present study showed sub-vertical failure planes that cut through the top and bottom

surfaces. This corroborates the assumption that the friction between the earth material and the press plates was negligible and did not affect the observed failure mechanism (Figure 5.6).

All unconfined compression tests were performed under a constant displacement rate so that the post peak stress-strain behaviour could also be investigated. Before the main testing campaign, a number of preliminary pilot experiments were performed in which the displacement rate was varied from 0.01 mm/s (Kouakou and Morel, 2009) to 0.001 mm/s, which is the slowest rate that can be applied by the Zwick/Roell Amsler HB250 press. Figure 5.7 shows the results from two compressive strength tests performed with these two limit rates of axial displacement on two samples compacted at the same pressure with similar values of water content and, hence, dry density. The two samples show comparable peak values of compressive strength but a more fragile behaviour is observed during the test performed at the faster rate with the appearance of small instabilities along the loading branch of the stress-strain curve. On the basis of these preliminary results, the slowest displacement rate of 0.001 mm/s was used during the entire testing campaign in order to obtain a regular stress-strain curve without instabilities.

Figure 5.8 shows the variation of the measured peak strength with dry density. Similar to the Young modulus, compressive strength grows more than linearly with increasing dry density. Thus, a small increase of dry density beyond the maximum value measured in this study could lead to a significant augmentation of compressive strength. Remarkably, samples compacted at 100 MPa show a compressive strength that is about ten times higher than that of the Proctor samples.

Figure 5.6. Typical compressive failure mechanism
(sample S10 - CS50 - W5.6 - see Table 3.3)

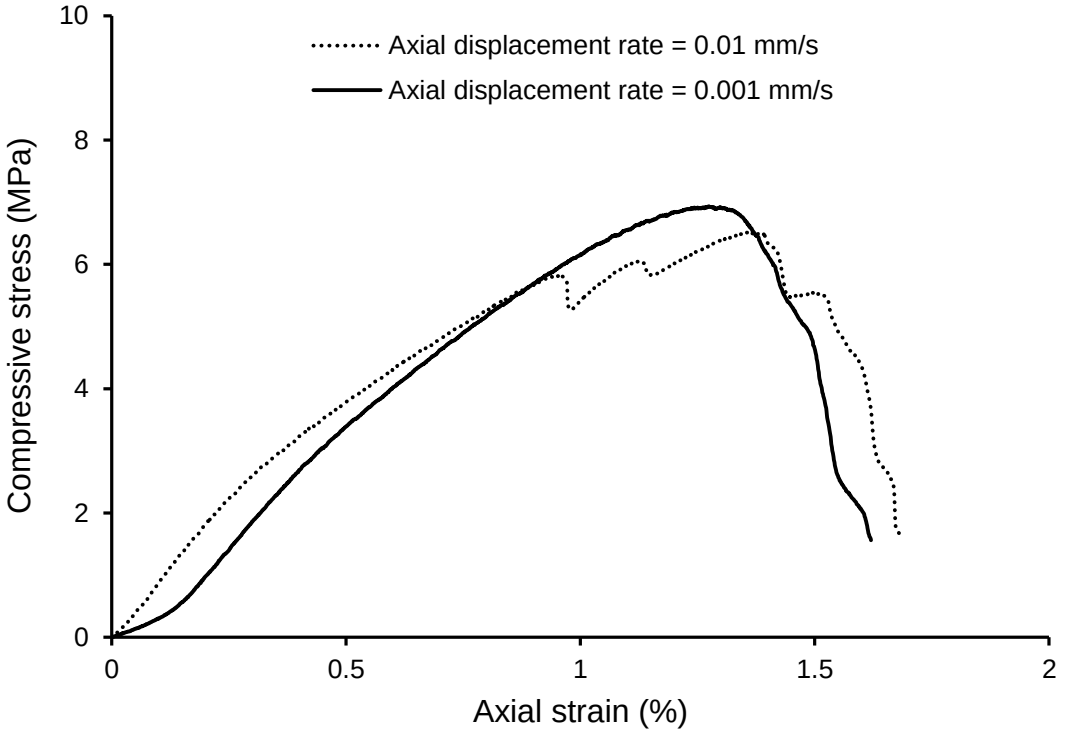

Figure 5.7. Stress-strain curves: tests performed on similar samples but at different displacement rates

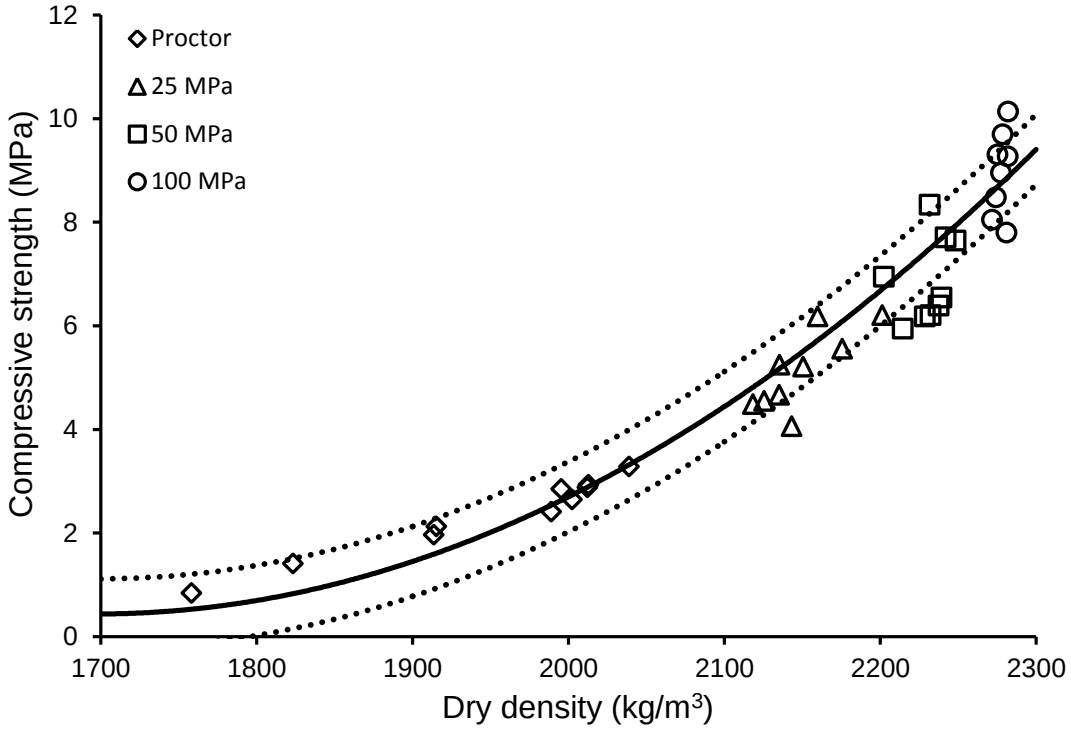

Figure 5.8. Variation of compressive strength with dry density

5.2 Effect of consolidation time of unstabilised earth

The hypercompaction procedure presented in Section 3.2 is based on a consolidation criterion which requires the application of a constant load for more than two hours. This is a very strict requirement which might hinder dissemination of this fabrication method to industrial practice. Further investigation has therefore been undertaken about the effect of consolidation time on mechanical behaviour, with a view of possibly accelerating the fabrication process.

Cylindrical earth samples were compacted at a pressure of 100 MPa with the optimum water content of 5.2% with different consolidation times corresponding to 0.5, 1, 2, 5, 10, 20, 40, 80 and 160 minutes. Subsequently, the samples were equalised at a temperature of 25 °C and at a relative humidity of 62% for two weeks. Figure 5.9 shows the effect of consolidation time on the dry density measured after equalisation. As it can be observed, dry density increases as consolidation time increases. However, a consolidation time of about 20 minutes is enough to attain a value of dry density close to the maximum. This is consistent with the fact that most vertical displacements occur during primary consolidation that is completed after only few minutes (see Section 3.2.1).

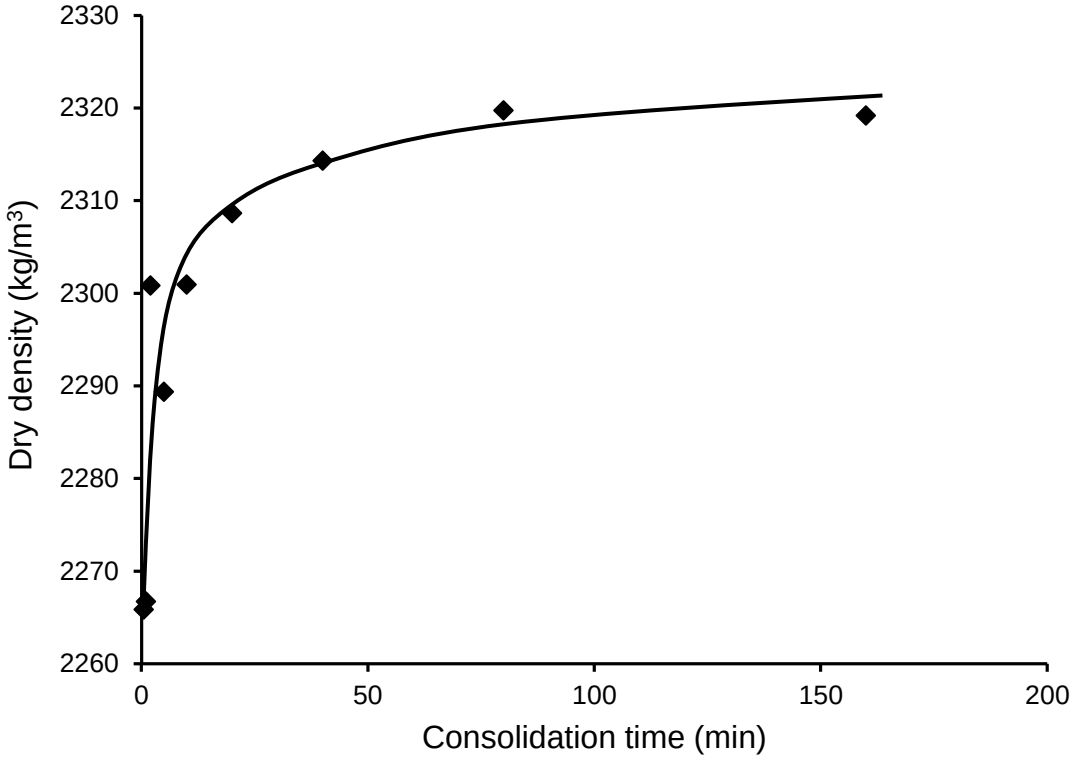

Figure 5.9. Relationship between dry density and consolidation time

The samples were then subjected to loading-unloading cycles to determine the Young modulus and subsequently loaded until failure to determine compressive strength according to the experimental procedure discussed in Sections 5.1.1 and 5.1.4. Figures 5.10 and 5.11 show, respectively, the variation of Young modulus and compressive strength with consolidation time. Inspection of Figures 5.10 and 5.11 indicates that both stiffness and strength increase for larger consolidation times up to approximately 20 minutes but then they tend to stabilise for longer consolidation times. This is also consistent with the changes of dry density shown in Figure 5.9.

From these results, it can be concluded that a shorter consolidation time than that assumed in Section 3.2 can be adopted without significantly affecting the mechanical characteristics of the material. At the same time, inspection of Figures 5.10 and 5.11 suggests that a very short consolidation time of the order of seconds, such as it is often the case in current practice, is not enough to ensure the best mechanical performance.

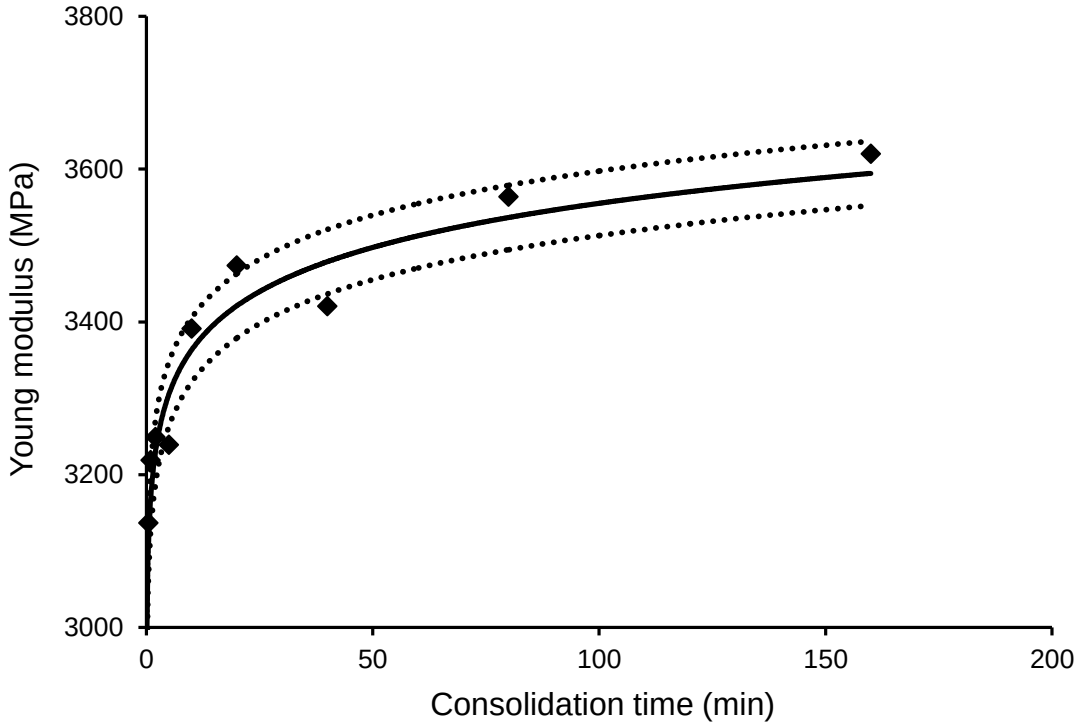

Figure 5.10. Variation of Young modulus with consolidation time.

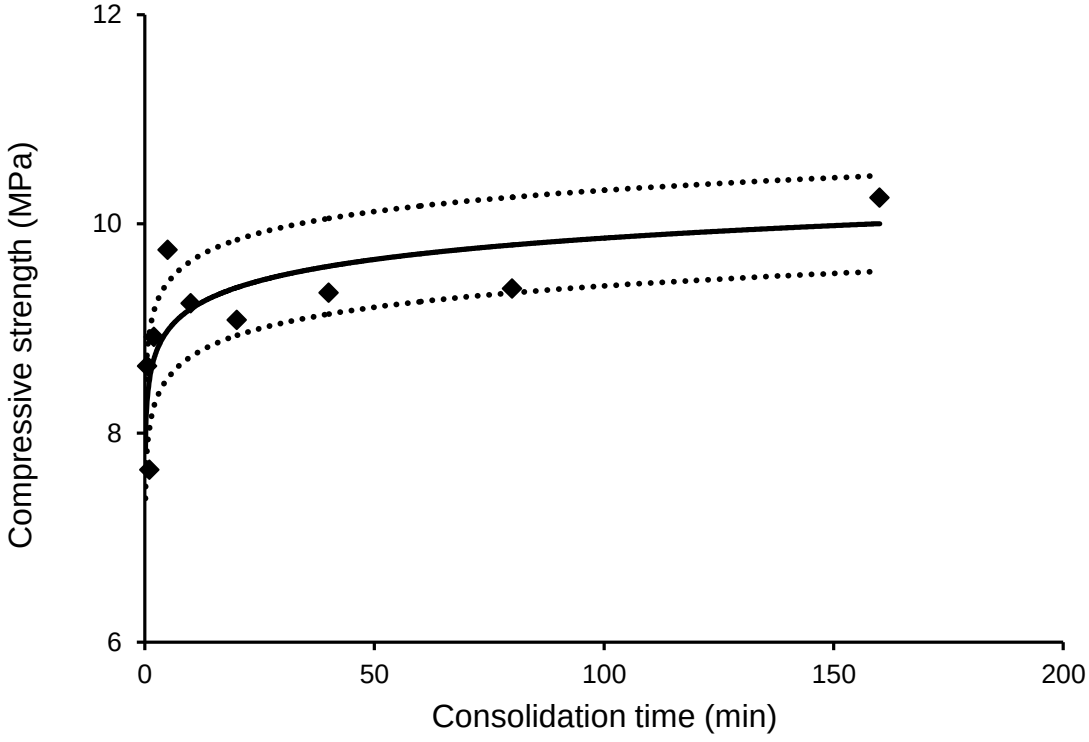

Figure 5.11. Variation of compressive strength with consolidation time.

5.3 Effect of relative humidity

Earth materials show different mechanical properties depending on hygrothermal conditions as shown, for example, by Dierks and Ziegert (2002), Beckett and Augarde (2012) and Bui et al. (2014).

To further explore this aspect, mechanical tests were performed on stabilised and unstabilised cylindrical samples equalised at five different levels of ambient humidity (i.e. 95%, 77%, 62%, 44% and 25%) under a constant temperature of 25 °C. The objective of these tests was to investigate the effect of ambient relative humidity on the stiffness and strength of the material stabilised according to different techniques.

Unstabilised samples were compacted at the optimum water contents for the three pressure levels of 25, 50 and 100 MPa while stabilised samples were only compacted at 100 MPa. Stabilisation was achieved by mixing the base soil with one of the following three liquid additives instead of water (see Section 3.4):

- 5.2% silane-siloxane emulsion
- 5.2% NaOH solution at 2 mol/L concentration
- 1.08% silane-siloxane emulsion + 4.12% NaOH solution at 2 mol/L concentration

The liquid additive content was always equal to 5.2%, which is the same as the optimum water content of the unstabilised samples. As discussed in Section 3.4, the above stabilising additives were selected on the basis of preliminary immersion tests. Since both unstabilised and stabilised samples were compacted at the optimum liquid content, no perforated disks were used to aid drainage during compression (see Section 3.2).

Five sets of six cylindrical samples were fabricated, with each set consisting of three samples of unstabilised earth compacted at the three pressure levels of 25, 50 and 100 MPa, respectively, and three samples of stabilised earth compacted at 100 MPa by using the three different additives. After compaction, each of the five sets was equalised inside a climatic chamber at five different levels of relative humidity, corresponding to 95%, 77%, 62%, 44% and 25%, under a constant temperature of 25 °C. After equalisation, the samples were subjected to mechanical tests to determine the Young modulus and the unconfined compressive strength by using the same experimental procedure described in Sections 5.1.1 and 5.1.4.

For each specimen, dimensions (i.e. diameter and height) and mass were measured after equalisation and just prior to mechanical testing. After the end of the test, a small fragment of about 50 grams was taken from the failed specimen to determine the water content in agreement with the French norm NF P 94-050 (1995). By using the measured values of volume, mass, water content and specific gravity, it was then possible to calculate the bulk density ρ_b, the dry density ρ_d, the porosity n and the degree of saturation Sr of the tested samples.

The values of temperature, T and relative humidity, RH imposed during equalisation can be combined into an equivalent value of total suction, ψ by using Kelvin equation:

$$\psi = -\frac{R\,T}{V_m}\ln(RH) \tag{5.2}$$

where R is the universal gas constant and V_m is the molar volume of water. This allowed to further analyse the variation of both Young modulus and compressive strength with total suction as discussed in the following.

5.3.1 Young modulus and compressive strength of unstabilised earth

Table 5.1 summarises the main properties of the unstabilised samples after equalisation at the five target levels of relative humidity under a constant temperature of 25 °C. At any given value of relative humidity, the three samples compacted at different pressures show similar values of water content. Also, as relative humidity decreases, samples experience desaturation and shrinkage which in turn induce a slight increase of dry density.

Figure 5.12 shows the variation of Young modulus with total suction for the unstabilised samples compacted at the three different pressures. In general it can be observed that stiffness increases as suction increases from 7 MPa to 112 MPa but then tends to level off as suction grows above 112 MPa. For the samples compacted at 25 and 50 MPa, the value of stiffness increases by a factor of about 2.5 as suction grows from the lowest value of 7 MPa to the highest value of 190 MPa. Instead, for the samples compacted at 100 MPa, the stiffness increases by a factor of about 3.1 over the same suction range.

After five loading-unloading cycles, the unstabilised samples were loaded to failure to measure their unconfined compressive strength.

Figure 5.13 shows the variation of the peak compressive strength with suction. Similar to Young modulus, material strength increases as suction increases from 7 MPa to 112 MPa but then tends to stabilise as suction increases further. The progressively smaller increases of both Young modulus and compressive strength with growing suction are in agreement with Fisher (1926) idealised capillarity model. This model shows that the stabilising effect produced by a water meniscus at the contact between two identical spheres grows with suction but tends towards a constant asymptote.

Table 5.1. Properties of unstabilised samples after equalisation at different RH levels

Relative humidity	Ψ (MPa)	Compaction pressure	w (%)	ρ_b (kg/m^3)	ρ_d (kg/m^3)	n (-)	S_r (%)
95 %	7	25 MPa	4.1	2208	2121	0.204	42.7
		50 MPa	4.2	2235	2145	0.195	46.2
		100 MPa	4.1	2334	2242	0.158	58.0
77 %	36	25 MPa	3.9	2212	2129	0.201	41.3
		50 MPa	4.0	2246	2160	0.189	45.6
		100 MPa	3.7	2333	2250	0.155	53.5
62 %	66	25 MPa	3.4	2213	2140	0.197	37.0
		50 MPa	3.3	2243	2171	0.185	38.7
		100 MPa	3.0	2351	2283	0.143	47.8
44 %	112	25 MPa	2.6	2202	2146	0.194	28.7
		50 MPa	2.6	2243	2186	0.179	31.7
		100 MPa	2.5	2360	2302	0.136	42.4
25 %	190	25 MPa	2.2	2195	2148	0.194	24.4
		50 MPa	2.1	2242	2196	0.176	26.2
		100 MPa	2.0	2355	2309	0.133	34.6

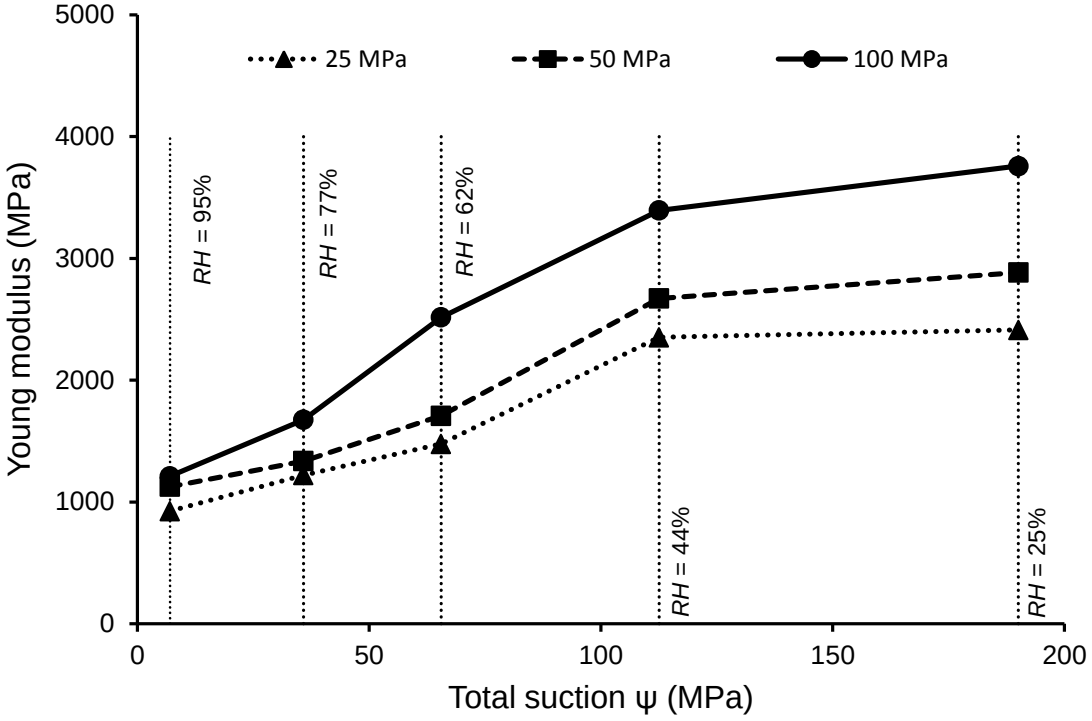

Figure 5.12. Variation of Young modulus with total suction: unstabilised samples

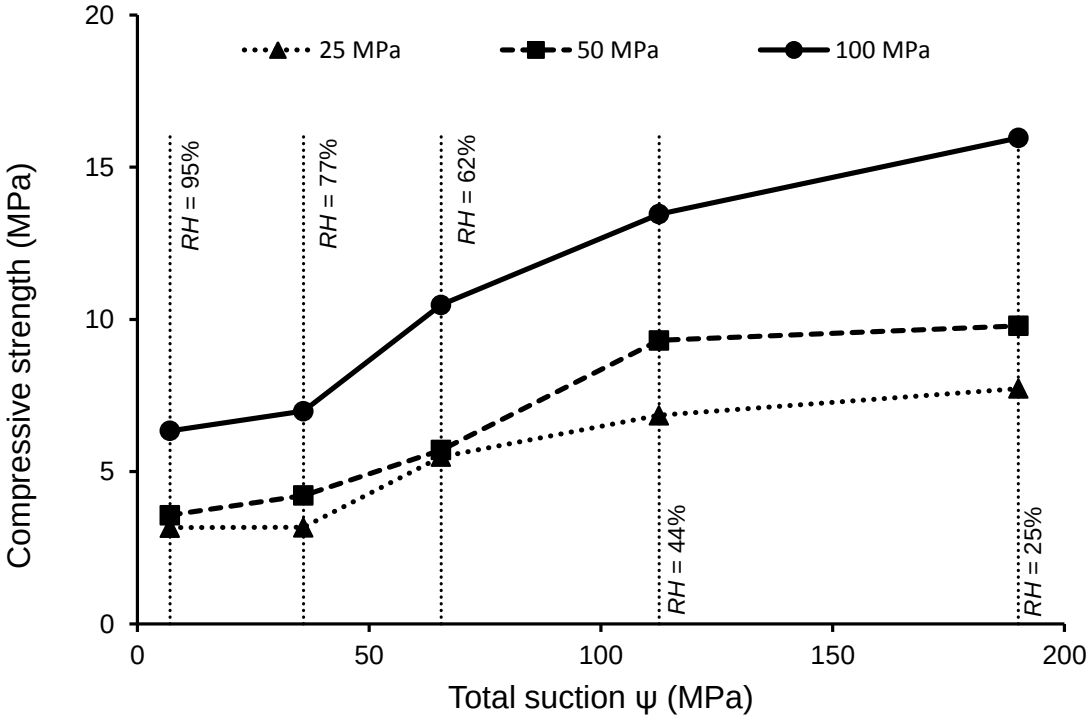

Figure 5.13. Variation of compressive strength with total suction: unstabilised samples

5.3.2 Young modulus and compressive strength of stabilised earth

Table 5.2 summarises the main properties after equalisation of the samples stabilised with the three different liquid additives and compacted at 100 MPa. The corresponding properties of the unstabilised samples compacted at 100 MPa are also reported in Table 5.2 for ease of comparison. After equalisation at a given relative humidity, the three stabilised samples show different values of water content which is probably due to the different tendency of the stabilising additives to evaporate during drying at 105 °C. It can also be noted that dry density in all samples increases as relative humidity decreases, similarly to the unstabilised samples.

Figure 5.14 shows that the increase of Young modulus with growing suction is smaller for stabilised samples than for unstabilised samples. This is probably because the inter-particle bonding produced by capillarity is overridden by that produced by chemical stabilisation. As it will be shown in Chapter 6, this is also consistent with the reduced moisture buffering (i.e. the reduced ability to store/release moisture during variations of ambient humidity) of stabilised samples compared to unstabilised samples. Samples stabilised with the silane-siloxane emulsion and with a mix of NaOH solution and silane-siloxane emulsion always exhibit a lower stiffness than unstabilised samples. The stiffness of the samples stabilised with the NaOH solution is higher than that of unstabilised samples at low suction levels. However, as suction increases above 65 MPa, the Young modulus of stabilised samples remains approximately constant and is therefore surpassed by that of unstabilised samples which continues to grow.

Figure 5.15 shows that the peak compressive strength of both unstabilised and stabilised samples increases with increasing suction. Similar to the Young modulus, stabilised samples show a lower compressive strength than unstabilised samples with the only exception of the samples stabilised with NaOH solution, which show better mechanical characteristics than the unstabilsed samples at low suction levels. In summary, chemical stabilisation appears to have a negative impact on the mechanical properties of hypercompacted earth. This is a rather counterintuitive result but is consistent with what observed by Bui et al. (2014) for conventional earth blocks. A possible explanation is that chemical stabilisers partly inhibit inter-particle bonding due to water capillarity, which in turn limits the improvement of mechanical properties with growing suction.

Moreover, the results suggest that water capillarity is more effective than chemical stabilisation in improving mechanical properties.

Table 5.2. Properties of stabilised/unstabilised samples after equalisation at different RH

Relative humidity	Ψ (MPa)	Sample	w (%)	ρ_b (kg/m^3)	ρ_d (kg/m^3)	n (-)	Sr (%)
95 %	7	Unstabilised	4.1	2334	2242	0.158	58.0
		Silane-siloxane emulsion	3.3	2291	2218	0.167	43.7
		NaOH solution	4.3	2355	2258	0.152	63.7
		NaOH solution + Silane-siloxane emulsion	3.8	2325	2240	0.159	53.5
77 %	36	Unstabilised	3.7	2333	2250	0.155	53.5
		Silane-siloxane emulsion	3.2	2315	2243	0.158	45.4
		NaOH solution	4.0	2362	2271	0.147	61.6
		NaOH solution + Silane-siloxane emulsion	3.5	2331	2252	0.155	51.0
62 %	66	Unstabilised	3.0	2351	2283	0.143	47.8
		Silane-siloxane emulsion	2.8	2327	2264	0.150	42.2
		NaOH solution	3.5	2354	2274	0.146	54.4
		NaOH solution + Silane-siloxane emulsion	3.2	2351	2278	0.145	50.3
44 %	112	Unstabilised	2.5	2360	2302	0.136	42.4
		Silane-siloxane emulsion	2.4	2322	2268	0.149	36.6
		NaOH solution	3.0	2348	2280	0.144	47.4
		NaOH solution + Silane-siloxane emulsion	3.0	2349	2281	0.144	47.5
25 %	190	Unstabilised	2.0	2355	2309	0.133	34.6
		Silane-siloxane emulsion	2.2	2320	2270	0.148	33.7
		NaOH solution	1.8	2337	2296	0.138	29.9
		NaOH solution + Silane-siloxane emulsion	2.0	2342	2296	0.138	33.3

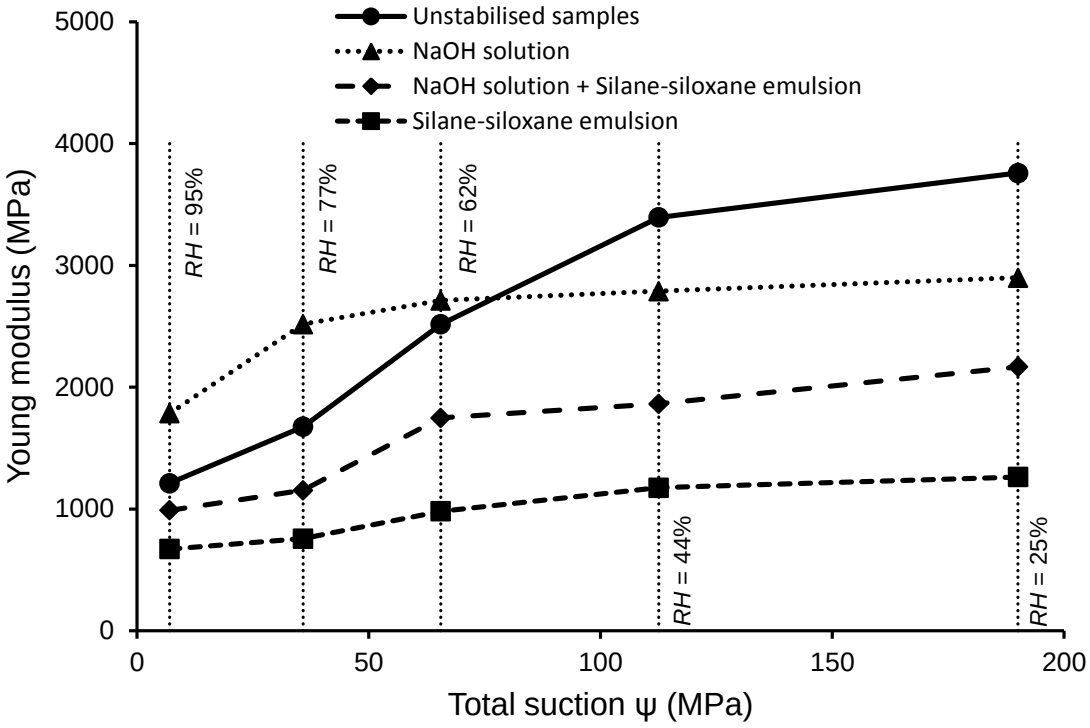

Figure 5.14. Variation of Young modulus with total suction: unstabilised and stabilised samples compacted at 100 MPa

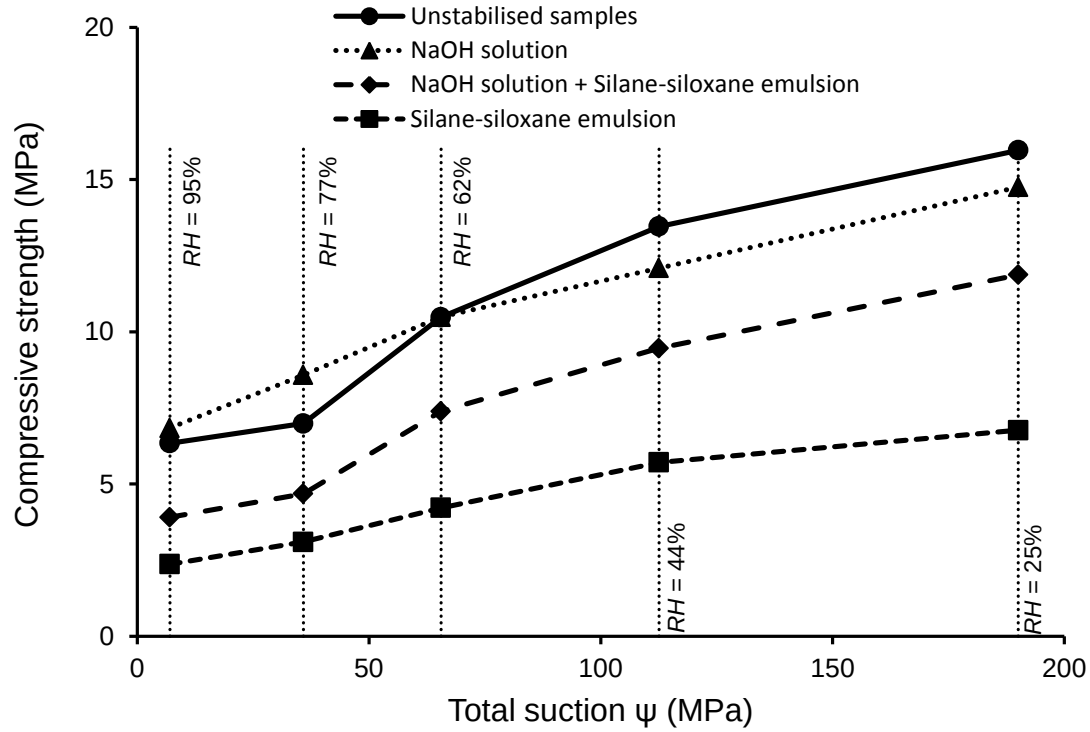

Figure 5.15. Variation of compressive strength with total suction: unstabilised and stabilised samples compacted at 100 MPa

5.4 Compressive strength of compressed earth bricks

The hypercompaction method for fabricating small cylindrical samples has been extended to the production of larger compressed earth bricks.

Earth bricks were therefore compacted at a pressure of 100 MPa and at the optimum water content of 5.2%. The main properties of bricks have been shown in Table 3.4 (see Section 3.3). In particular, it was observed that bricks attained higher dry densities than cylindrical samples owed to their higher volume to lateral surface ratio. Further details about the procedure for the compaction of earth bricks have already been presented in Section 3.3.

The tests presented in this section were performed with the objective of demonstrating that hypercompaction can largely improve the strength of earth bricks compared to conventional manufacturing methods. In addition, the influence of different experimental methods on the measured strength of earth bricks were also explored. In particular, similar to Aubert et al. (2016), multiple measurements of compressive strength were taken by varying brick orientation or using Teflon plates to reduce friction on the loaded surfaces. These tests were performed by using the compression press 3R RP 3000 TC/TH with a load capacity of 3000 kN (Figure 3.9).

In another set of tests, compressive strength was measured along different directions on cubic specimens that were dry-sawn from a brick to investigate the effect of compaction-induced anisotropy. A final set of tests was also performed on samples made of two half-bricks bonded by a cement mortar to analyse the effect of the joint on mechanical characteristics. The above two sets of tests were performed by using the Zwick/Roell Amsler HB250 press with a capacity of 250 kN (Figure 3.3). The use of a different press was necessary because of the lower load at which the smaller dry-sawn bricks failed, which cannot be detected by the press 3R RP 3000 TC/TH used in the other tests.

All compression tests on entire bricks, half-bricks and cubic specimens were run at a constant load rate of 0.08 MPa/s similar to Aubert et al. (2016). Note also that Aubert et al. (2016) tested extruded bricks while in the present work only hypercompacted earth bricks have been investigated.

5.4.1 Effect of aspect ratio

As already discussed in Section 3.3, all earth bricks manufactured in the present work have dimensions equal to 200 x 100 x 50 mm^3. The effect of aspect ratio (i.e. the ratio between the dimension parallel to the loading direction and the minimum dimension of the cross section) on the measured unconfined compressive strength was investigated by varying the orientation of the brick inside the press. In particular, the load was applied along the three directions 1, 2 and 3 perpendicular to the largest, intermediate and smallest faces of the brick, respectively (Figure 5.16), which correspond to three values of aspect ratio equal to 0.5, 2 and 4, respectively.

Figure 5.17 shows the variation of the peak compressive strength with aspect ratio. Each histogram bar represents the average compressive strength measured on six bricks while the thin vertical lines indicate the standard deviation. Inspection of Figure 5.17 indicates that the highest compressive strength is measured when the load is applied on the largest surface of the brick corresponding to an aspect ratio equal to 0.5. This is an expected result due to the friction between the brick and the press plates which strongly confines the sample, thus producing a fictitious increase of strength.

A similar result was obtained by Aubert et al. (2013) who measured a compressive strength higher than 45 MPa for an earth brick tested in similar conditions. They recognised that this extremely high value of compressive strength is an anomaly owed to the low aspect ratio of the brick during testing.

Lower and more realistic values of the unconfined compressive strength were measured when the load was applied along the other two directions, i.e. directions 2 and 3, corresponding to values of aspect ratio equal to 2 and 4, respectively. Compressive strength was similar along both these directions, with a slightly lower value when the load was applied on the intermediate brick surface. This slight difference might be attributable to differences in the failure mechanism between the two cases. A shearing failure mechanism developed when the load was applied along direction 2, corresponding to an aspect ratio of 2, as indicated by the inclined failure surface (Figure 5.18). Conversely, a sub-vertical failure surface, typical of a compressive failure mechanism, was observed when the load was applied along direction 3 corresponding to an aspect ratio of 4 (Figure 5.18).

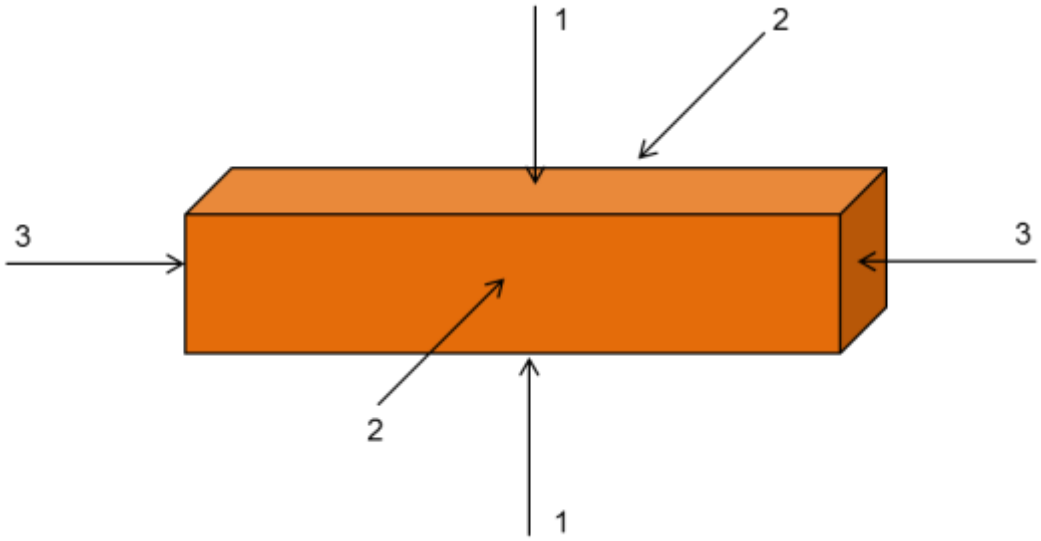

Figure 5.16. Loading directions 1, 2 and 3 perpendicular to the largest, intermediate and smallest brick surfaces

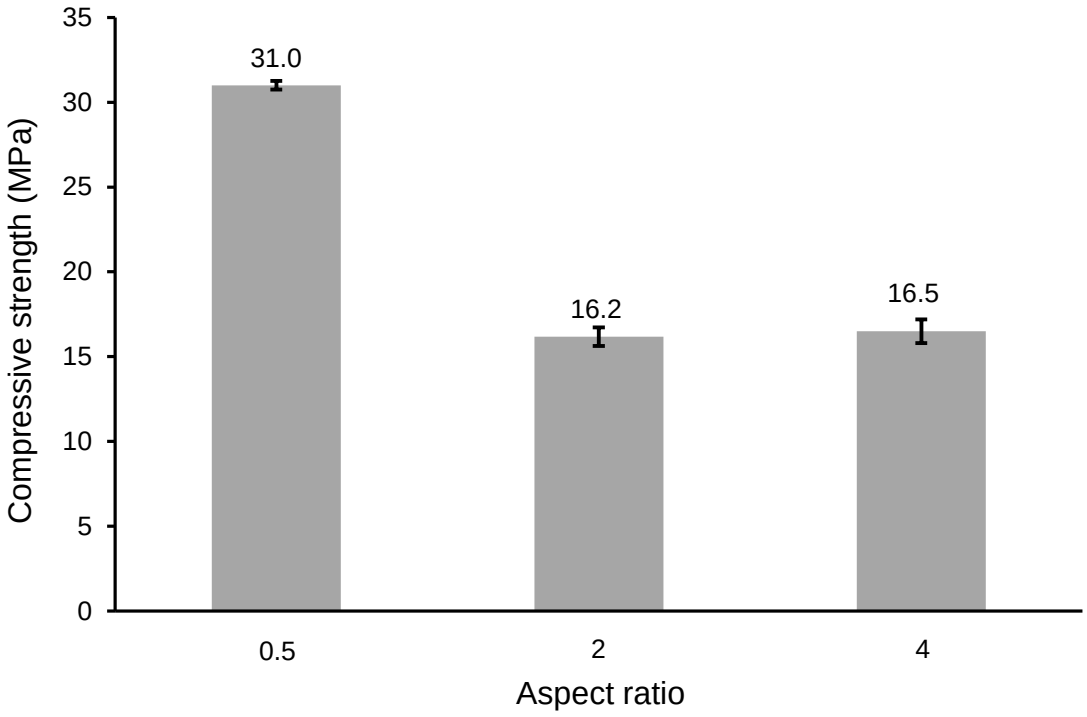

Figure 5.17. Variation of compressive strength with aspect ratio.

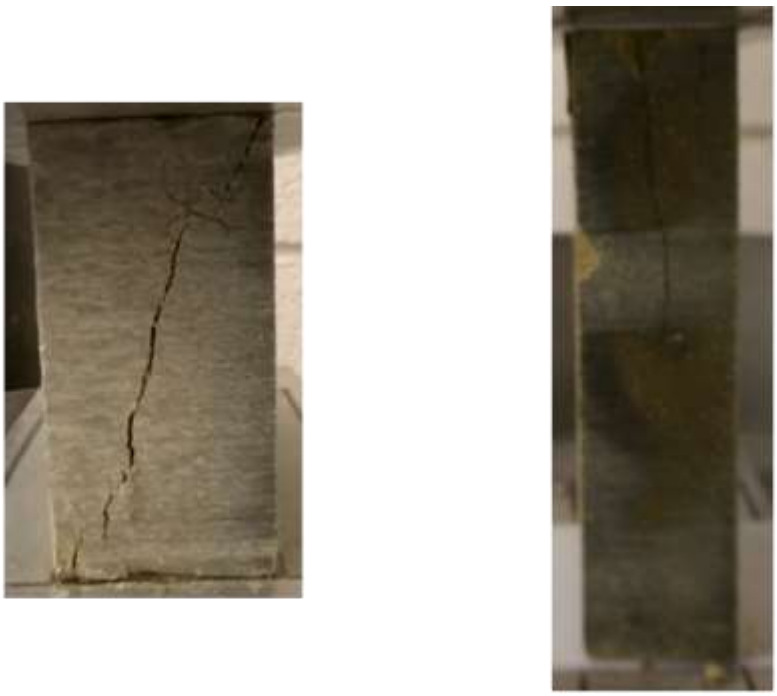

Figure 5.18. Failure mechanisms corresponding to loading directions 2 and 3

5.4.2 Effect of Teflon capping

As suggested by Ciancio and Gibbings (2012), the friction between the sample and the press plates can be reduced during mechanical tests by capping the top and bottom surfaces of the sample with Teflon plates. To explore this further, compression tests were performed on two different sets of six similar bricks. The first set of bricks was capped with Teflon plates while the second set was left uncapped. In all these tests, the load was applied on the smallest surfaces (i.e. along direction 3 corresponding to the largest aspect ratio of 4).

Figure 5.19 shows the average values of compressive strength measured on the two sets of bricks. These values are very similar with a ratio of 0.88 between the average strength of capped and uncapped samples. Dispersion of results is also significantly reduced when samples are capped with Teflon plates as indicated by the smaller standard deviation in this case (Figure 5.19). This result is also in agreement with that of Aubert et al. (2016) who found that samples capped with Teflon plates have an average compressive strength that is between 0.9 and 1.0 times that of uncapped samples.

In summary, the friction between the earth sample and the press plates is reduced by both a high aspect ratio and Teflon capping, which implies that the strength measured

on Teflon capped samples in Figure 5.19 probably provides the most realistic value of unconfined compressive strength for the brick material.

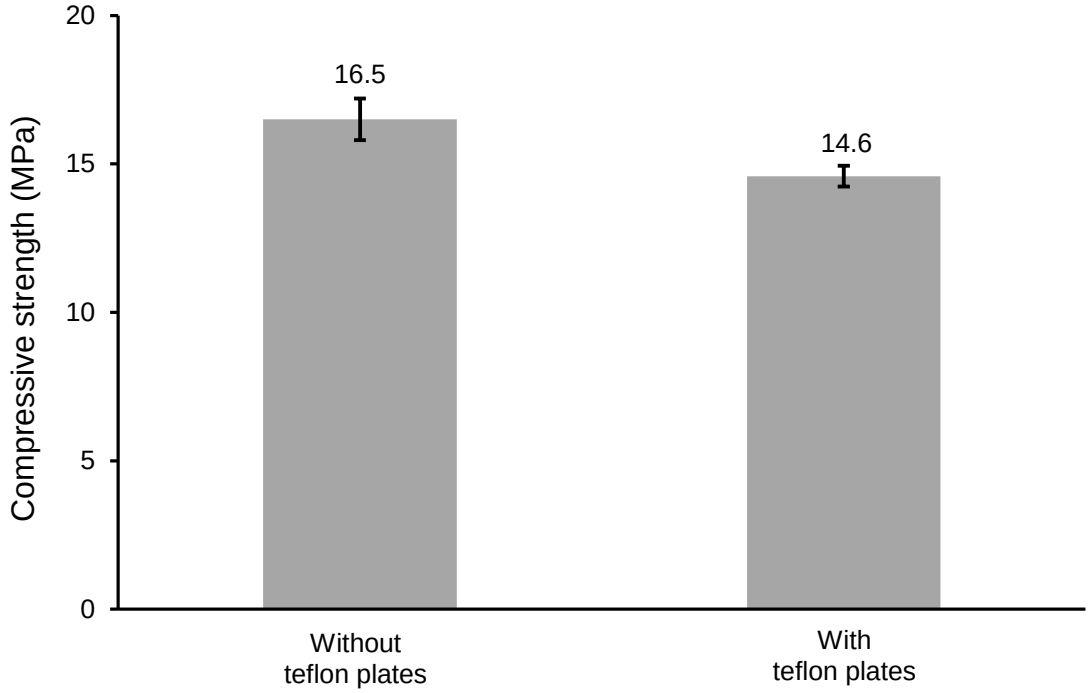

Figure 5.19. Compressive strength of bricks with or without Teflon capping

These results also showed that the process of hypercompaction largely improves mechanical performance of compressed earth bricks. Table 5.3 shows that the compressive strength of hypercompacted bricks is comparable with that of traditional materials such as stabilised compacted earth and standard masonry bricks. For the material tested by Guetlala (1997), compressive strength varies from 5.2 MPa (0% of cement, i.e. unstabilised soil) to 12.9 MPa (10% of cement). In the latter case, the percentage of cement is so high that the "green" prerogatives of earthen materials are almost entirely compromised (Bui et al., 2014).

Note that the compressive strength of unstabilised compressed earth bricks reported in Table 5.3 represents the average value measured on bricks capped with Teflon plates and loaded in the direction perpendicular to the smallest face (aspect ratio equal to 4). This value of compressive strength is also in compliance with the requirements for standard masonry construction according to the norm ASTM C270 (2014).

Table 5.3. Comparison in terms of compressive strength

Material	Compressive strength (MPa)
Compressed earth bricks (present work)	14.6
Compacted stabilised soil (Guetlala 1997)	From 5.2 to 12.9
Standard masonry bricks (ASTM C270, 2014)	From 6.9 to 27.6

5.4.3 Effect of mortar joint

A common experimental procedure for estimating the unconfined strength of earth bricks within a masonry assembly consists in loading two half-bricks connected by a cement mortar or an earth mortar joint until failure (RILEM Technical Committee 164, 1994). In these tests, the load is applied perpendicular to the mortar joint, along the direction of compaction.

In the present work, two sets of six samples consisting of superimposed brick halves were loaded until failure. The two brick halves were obtained from a single brick which was dry-cut by means of an electric circular saw along the direction parallel to the smallest surfaces of the brick. In the first set of tests, the two halves were simply superposed without any mortar, whereas, in the second set, the two halves were stuck together by means of a cement mortar prepared according to the norm NF EN 196-1 (2006). Tests on the mortar-joined samples were performed 28 days after their fabrication, during which the samples were left to cure at a constant temperature of 25°C.

Figure 5.20 shows the average compressive strength measured from the two sets of samples. Inspection of Figure 5.20 indicates that the mortar-joined samples show lower compressive strength than the samples without mortar. This is probably due to the relatively high water content of the cement mortar, which might damage the surface of the unstabilised earth.

Aubert et al. (2016) also found that the compressive strength of mortar-joined half-bricks is lower than that of half-bricks without mortar. In their case, the reduction of compressive strength is however lower than that observed in the present study. This may be due to the fact that, during manufacturing, extruded bricks have higher water contents than compressed bricks and the wet cement mortar can bind better with a moister soil.

The average compressive strength of half-bricks without mortar (Figure 5.20) is also lower than all strength measurements obtained from entire bricks (see Sections 5.4.1 and 5.4.2). This is in agreement with Morel et al. (2007) who argued that the compressive strength of half-bricks tends to underestimate that of entire bricks. This can probably be explained by the process of dry-sawing an intact brick in two halves, which might weaken the material by creating micro-cracks. It can therefore be assumed that unconfined compression tests of entire bricks provide the most realistic assessment of material strength. This is only true, however, if the load is not applied on the laying surface of the brick, as also pointed out by Aubert et al. (2016).

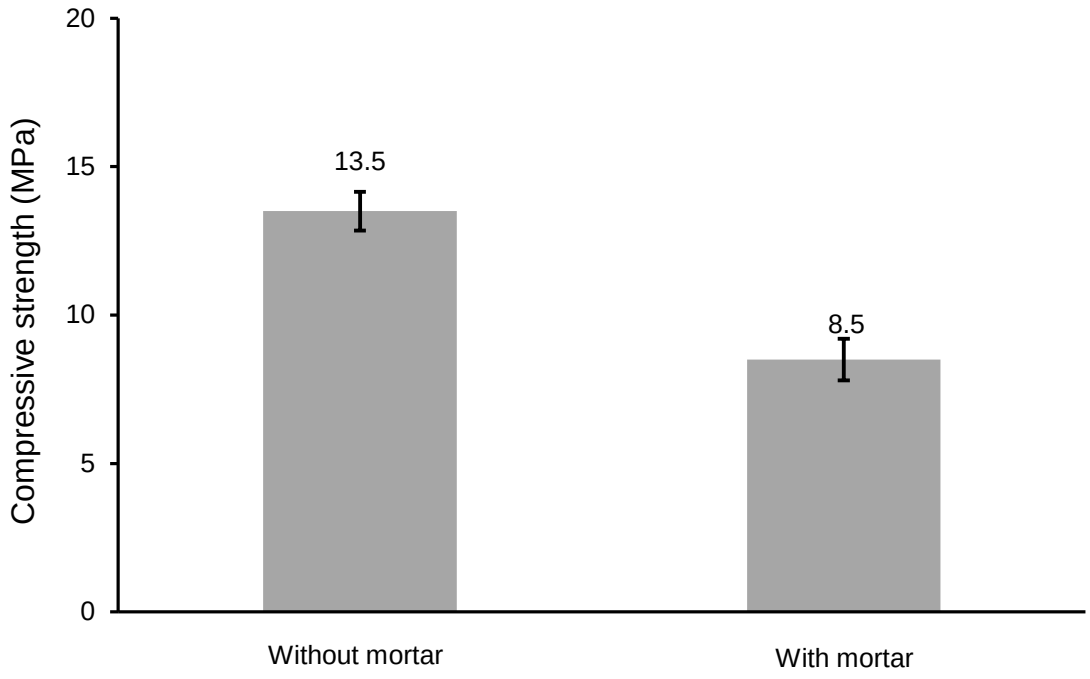

Figure 5.20. Compressive strength of superimposed half-bricks with or without cement mortar

5.4.4 Effect of anisotropy

The process of one-dimensional compaction generates anisotropy of material fabric in earthen bricks meaning that mechanical behaviour may be different depending on the direction of the applied load.

In order to investigate this aspect further, a number of earth bricks were dry-sawn by means of an electric circular saw in order to cut cubic specimens with dimension 50 x

50 x 50 mm^3. Three sets of six cubic specimens were obtained in this way from three identical bricks, respectively. The first set was loaded in direction 1, which is the direction perpendicular to the largest surface of the brick (i.e. parallel to the direction of compaction). The other two sets were loaded in directions 2 and 3, which are perpendicular to the intermediate and smallest surfaces of the brick, respectively (i.e. both directions are perpendicular to the direction of compaction). All specimens were loaded by using the Zwick/Roell Amsler HB250 press (Figure 3.3) without any Teflon capping.

Figure 5.21 shows the average compressive strength of each of the three sets of cubic specimens. Inspection of Figure 5.21 confirms that compaction-induced anisotropy influences the mechanical response of earthen material: specimens loaded in direction 1, i.e. the same direction of the compaction load, show a compressive strength that is on average 1.1 times higher than that measured along the other two perpendicular directions. Aubert et al. (2016) found that the anisotropy factor (ratio between the compressive strength measured along the direction perpendicular to the extrusion plane and that measured on the direction parallel to the extrusion plane) ranges between 1.2 and 1.5. Thus, it can be concluded that anisotropy influences compressed earth bricks slightly less than extruded bricks.

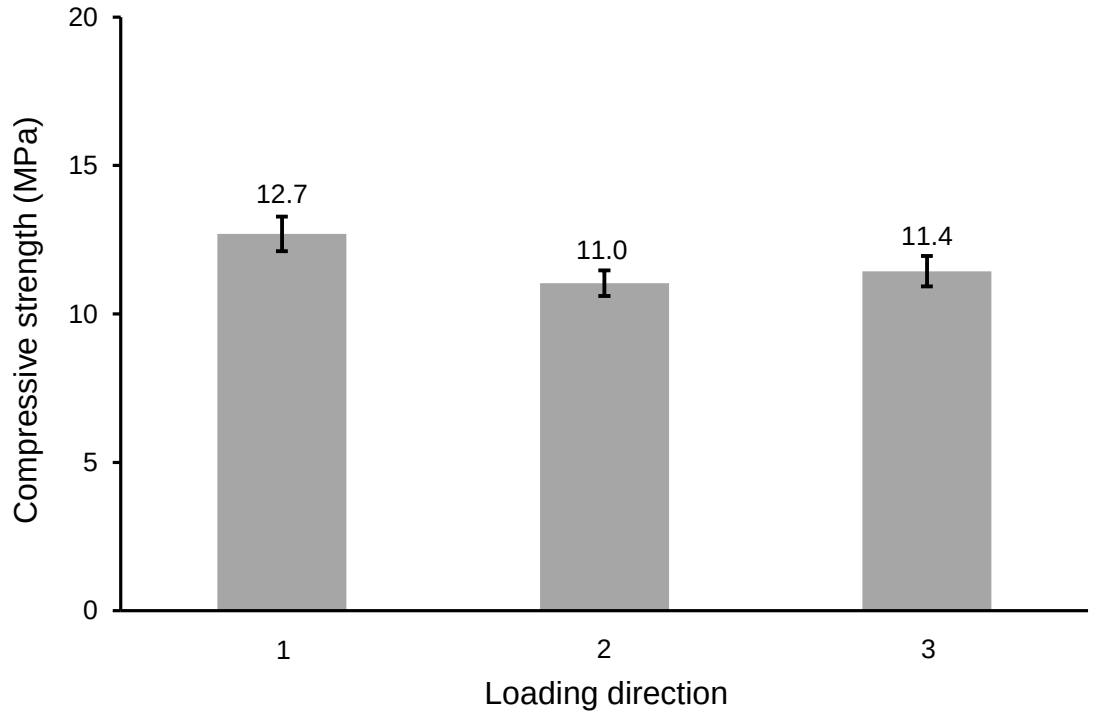

Figure 5.21. Compressive strength of cubic specimens: effect of anisotropy

5.5 Final remarks

This chapter has presented experimental results about the mechanical behaviour of stabilised and unstabilised earth samples. The main points are summarised as follows:

- Mechanical tests were performed on cylindrical samples compacted at the three pressure levels of 25, 50 and 100 MPa and at different water contents. Loading-unloading cycles were performed to measure Young modulus and Poisson ratio before the samples were loaded until failure to determine their unconfined compressive strength (see Section 5.1).
- During the loading-unloading cycles, the samples showed a hysteretic behaviour: elasto-plastic strains occurred during loading while the response was essentially elastic during unloading. The Young modulus and Poisson ratio were therefore determined from the unloading branches of the cycles (see Section 5.1.1).
- Samples compacted at a pressure of 100 MPa exhibited a very high Young modulus, about one order of magnitude greater than Proctor standard samples. Also, for all samples, the Young modulus tended to increase more than linearly with increasing dry density (see Section 5.1.1).
- Compressive strength also increased more than linearly with increasing dry density. This suggests that a small increase of dry density beyond the maximum value obtained in the present study could produce a significant augmentation of both strength and stiffness (see Section 5.1.4).
- Tests were performed on unstabilised and stabilised samples equalised at five different levels of ambient humidity (namely 25%, 44%, 62%, 77% and 95%) and at a constant temperature of 25 °C. Relative humidity and temperature were also used to calculate the equivalent total suction by means of Kelvin law. Results showed that the stiffness and strength of both stabilised and unstabilised samples increase with increasing suction. The increase was however more limited for stabilised samples compared to unstabilised samples (see Sections 5.2.1 and 5.2.2), which indicates that the mechanical properties of stabilised samples are less sensitive to the variation of ambient humidity. This is also consistent with the lower moisture buffering capacity of stabilised samples compared to unstabilised ones as it will be shown in Chapter 6.

- The proposed hypercompaction method assumes a relatively long consolidation, i.e. about 2.5 hours, which might be unviable for industrial applications. The possibility of reducing consolidation times was therefore investigated in this work. It was found that both stiffness and strength increase steeply during the first 20 minutes of consolidation but, after that, they tend to remain constant. This indicates that a less sever consolidation criterion than that adopted in the present work could be adopted without significant changes in mechanical performance. At the same time, the results indicate that a very short consolidation time of only few seconds (as it is often the case in current earth construction practice) cannot assure the attainment of the best mechanical properties (see Section 5.3).
- An extremely high compressive strength was measured when the load was applied on the largest brick surface (i.e. aspect ratio of 0.5). This is due to the strong confinement owed to the friction between the press plates and the brick. The compressive strength measured along the other two directions was much lower. When the load was applied on the intermediate surface (aspect ratio of 2), the measured strength was slightly less than that measured when the load was applied on the smallest surface (aspect ratio of 4). This slight difference is probably due to the distinct failure mechanisms observed in these two cases, i.e. shearing failure in the former case and compressive failure in the latter case (see Section 5.4.1).
- Some earth bricks were loaded on the smallest face with and without inclusion of Teflon plates between the press plates and the brick. Teflon capping reduced the friction between the brick and the press plates, which in turn decreased radial confinement. The average compressive strength measured on Teflon capped bricks was therefore lower than that measured on uncapped bricks by a factor of 0.88 (see Section 5.4.2).
- Reduction of friction and increase of sample slenderness minimise undesirable confinement of the samples during loading. The most realistic value of unconfined compressive strength is, therefore, the one measured on Teflon capped bricks loaded in the direction perpendicular to the smallest face (see Section 5.4.2).
- The presence of a cement mortar joint between bricks induced a significant reduction of compressive strength. This was probably due to the high water

content of the mortar, which damaged the surface of the bricks (see Section 5.4.3).

- Unconfined compression tests of entire bricks provide the most realistic assessment of the compressive strength of the material. This is only true, however, if the load is not applied on the laying surface of the brick (see Section 5.4.3).
- Compressive strength tests were also performed on small cubic specimens, which were dry-sawn from an entire brick. The cubic specimens were loaded along different directions to assess the effect of compaction-induced anisotropy. The compressive strength measured along the direction of compaction was higher than that measured along the other two perpendicular directions. The effect of anisotropy on compressive strength is however rather limited compared to that observed by Aubert et al. (2016) on extruded bricks (see Section 5.4.4).
- The hypercompaction method improved significantly the material strength compared to current manufacturing procedures for compressed earth bricks. The compressive strength of hypercompacted bricks is comparable with that of more traditional building materials such as stabilised earth and standard masonry bricks (see Section 5.4.2).

6

Hygroscopic behaviour

This chapter presents the results from laboratory tests carried out to investigate the hygroscopic behaviour of unstabilised and stabilised compacted earth. The capacity of the material to adsorb and release water vapour was experimentally assessed by measuring the practical Moisture Buffering Value (MBV) of hypercompacted cylindrical samples. According to Rode et al. (2005), the MBV "*indicates the amount of water that is transported in or out of a material per open surface area, during a certain period of time, when it is subjected to variations in relative humidity of the surrounding air".* A comparison between the above cylindrical samples and hypercompacted earth bricks was also performed to evaluate the influence of sample scale on the measured MBV.

6.1 Testing procedure

The MBV was determined by subjecting earth samples to cyclic variations of relative humidity at constant temperature inside the climatic chamber CLIMATS Type EX2221-HA (Figure 6.1). Cycles were carried out between two levels of relative humidity equal to 75% and 53%, respectively, with each level maintained for a period of 12 hours. This is consistent with the norm "Hygrothermal performance of building materials and products" ISO 24353 (2008), which aims to simulate the typical daily variations of relative humidity inside dwellings over a period of 24 hours. Temperature was fixed at 25 °C, which is consistent with the equalisation temperature adopted during all previous tests but slightly different from the norm ISO 24353 (2008) that prescribes a temperature of 23 °C. This small difference in temperature should, however, not have any major effect on the measured MBV.

Figure 6.1. Climatic chamber CLIMATS Type EX2221-HA

Prior to performing the cycles of relative humidity, the cylindrical samples were equalised at a temperature of 25 °C and at a relative humidity of 53% for a period of two weeks. Five cycles of relative humidity were then performed, which was generally sufficient to attain steady state conditions. Steady state was defined as the attainment of at least three cycles where moisture uptake at a humidity of 75% was equal to moisture release at a humidity of 53%. These steady state cycles are referred to as "stable cycles".

During testing in the climatic chamber, the cylindrical samples were placed upright inside individual aluminium disposable foil pans. Therefore only the top and lateral surfaces of the samples were directly exposed to the ambient humidity of the climatic

chamber. The total area of the exposed surfaces was about 0.018 m^2 which is higher than the minimum value of 0.010 m^2 required by the norm ISO 24353 (2008). Samples masses were recorded every two hours by means of a scale with a resolution of 0.01 grams. As already discussed in Section 2.3, the MBV was determined using the following equation:

$$MBV = \frac{\Delta m}{S\ \Delta\%RH} \tag{6.1}$$

where Δm is the variation of sample mass induced by the change in relative humidity, S is the exposed surface and $\Delta\%RH$ is the difference between the high and low levels of relative humidity.

6.2 Moisture buffering capacity of unstabilised samples

Tests were performed on cylindrical samples compacted at the three pressure levels of 25, 50 and 100 MPa and their corresponding optimum water contents. The samples were manufactured following the hypercompaction method described in Section 3.2. Given that all samples were compacted at their respective optimum water contents, drainage of pore liquid was considered negligible and no perforated disks to aid seepage was included in the compaction set-up. Three samples were tested for each compaction pressure according to the norm ISO 24353 (2008). The main properties of the unstabilised samples equalised at different relative humidities have already been given in Table 5.1.

Results from relative humidity cycles are typically presented in terms of moisture adsorption curves. Moisture adsorption is defined as the ratio between the variation of sample mass (i.e. the difference between the current and initial mass) and the area of the exposed surface. In turn, the exposed surface is calculated for each sample from the average of three height measurements and three diameter measurements taken both at the beginning of the test (i.e. at T = 25 °C and RH = 53%) and at the end of the first humidity step (i.e. at T = 25°C and RH = 75%). This assures that the small variations of sample dimensions, owed to swelling upon wetting at high humidity, are taken into account.

Figure 6.2 shows the moisture adsorption variation during five cycles of relative humidity imposed to samples compacted at different pressure levels. Each curve,

corresponding to a different compaction pressure, was obtained as the average of the measurements from three distinct samples of similar characteristics. The dashed line in Figure 6.2 represents the change of relative humidity, whose value can be read on the secondary vertical axis. Inspection of Figure 6.2 indicates that all samples, regardless of compaction level, show identical hygroscopic responses. This was expected considering that, under the imposed conditions of temperature and humidity, exchanges of water vapour take place within nanopores from 3 to 7 nm (as determined by means of Kelvin equation and Washburn equation), which are not affected by mechanical compression between 25 and 100 MPa (see Sections 4.2.1 and 4.3.2).

Figure 6.2 shows that all samples exhibit a hysteretic behaviour during the first two cycles of relative humidity with larger moisture uptakes at high ambient humidity than moisture releases at low ambient humidity. However, starting from the third cycle, the hygroscopic behaviour becomes virtually reversible with the moisture uptake becoming equal to the release. This means that the last three cycles can be considered as stable cycles.

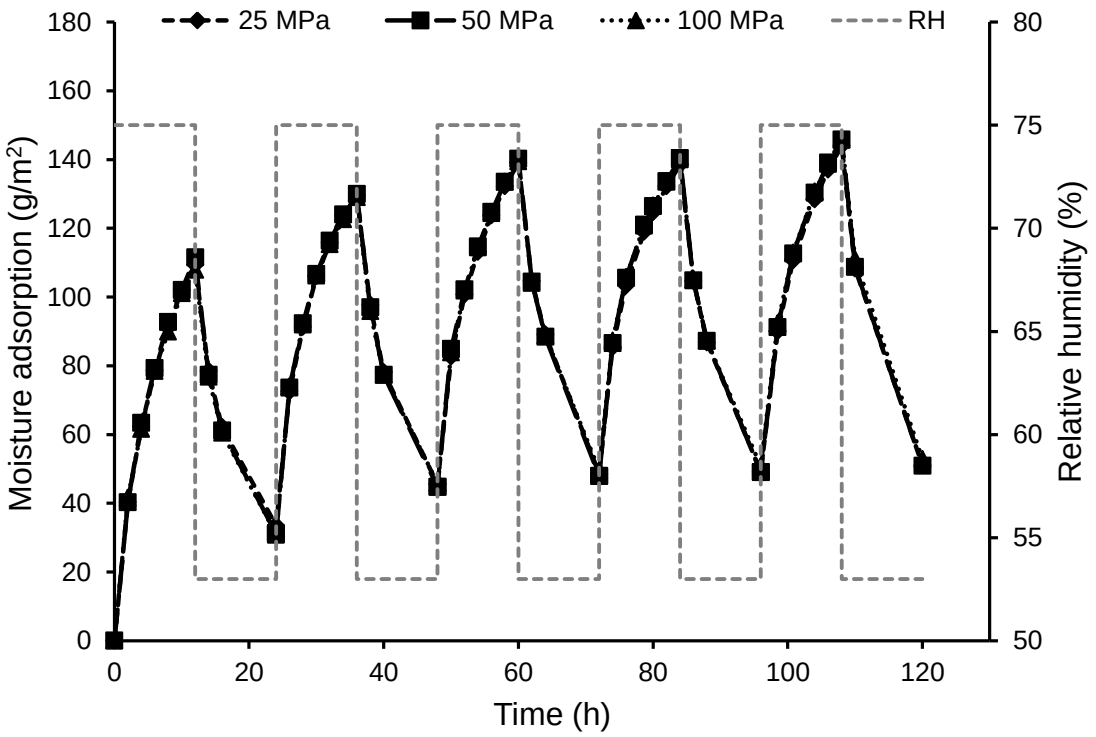

Figure 6.2. Moisture adsorption of unstabilised samples compacted at 25, 50 and 100 MPa

The MBVs were calculated by using Equation 6.1 during both the uptake and release of moisture in each cycle. In particular, the sample mass variation Δm was obtained as the difference between the values at the beginning and at the end of each humidity step. A value of Δm measured during an increase of relative humidity provides the "MBV uptake" while a value of Δm measured during a decrease of relative humidity provides the "MBV release".

Figure 6.3 shows the average MBVs measured during uptake and release of moisture in the samples compacted at different pressure levels. Inspection of Figure 6.3 confirms that the MBVs differ during moisture uptake and release for the first two cycles (owed to the hysteretic behaviour of the soil) but then become virtually identical during the last three stable cycles.

The characteristic MBV of the material is conventionally measured under steady state conditions. In the present work, it was therefore calculated as the average MBV from both the uptake and release stages of the last three cycles. This procedure yielded a MBV of 4.2 for unstabilised compressed earth.

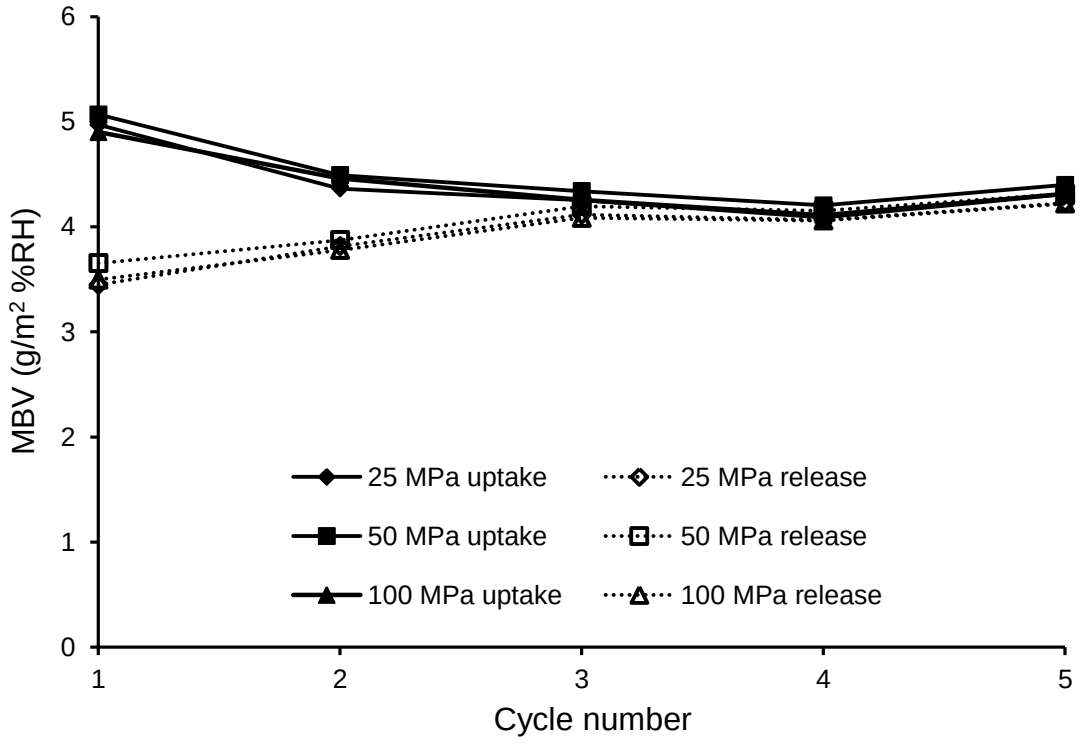

Figure 6.3. MBV uptake and MBV release of samples compacted at 25, 50 and 100 MPa

Figure 6.4 compares the MBV measured in the present work on cylindrical samples of unstabilised compressed earth (remember that this value is the same regardless of compaction pressure) with the MBV measured on traditional building materials by Rode et al. (2005) in the framework of the NORDTEST project. To aid interpretation, Figure 6.4 also shows the MBV classification defined by Rode et al. (2005) as discussed in Section 2.3. It is necessary to recall however that Rode et al. (2005) proposed the above classification by adopting a different testing procedure where relative humidity ranged between 33% and 75% with asymmetric step durations of 16h and 8h, respectively.

Figure 6.4 clearly shows that unstabilised earth samples exhibit an excellent capacity to buffer moisture during changes of ambient humidity with a MBV which is about ten times higher than that of traditional building materials such as concrete or fired bricks.

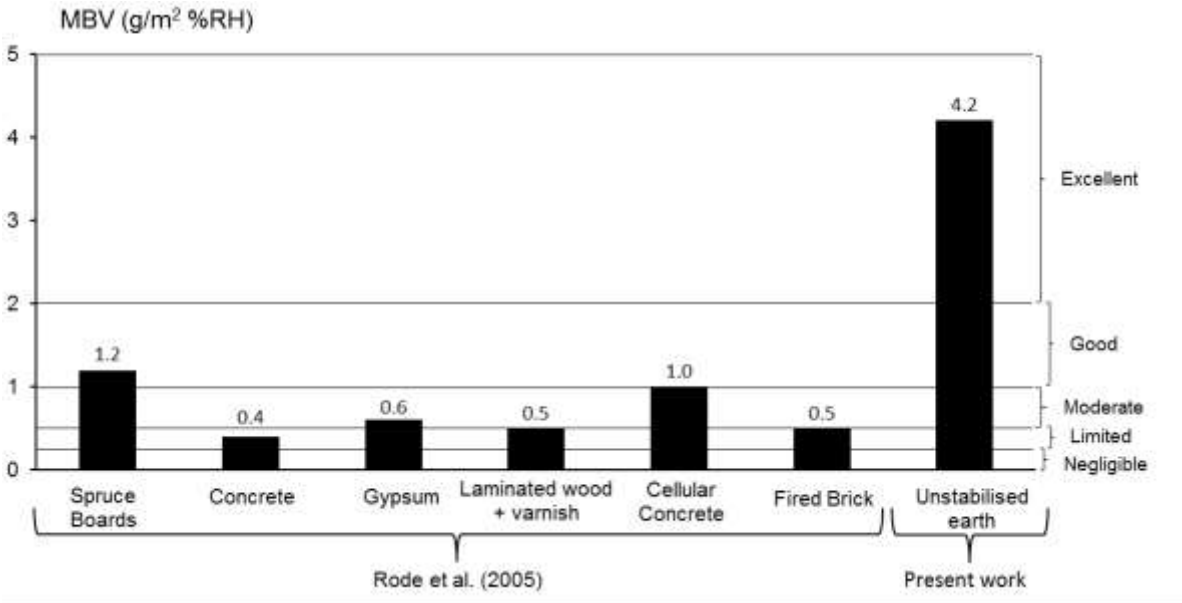

Figure 6.4. MBV of unstabilised compressed earth measured in the present work compared to results of Rode et al. (2005)

Figure 6.5 compares the MBV measured in the present work on unstabilised compressed earth with the MBVs measured by McGregor et al. (2014) on both unstabilised and stabilised earthen samples. The testing procedure adopted by McGregor et al. (2014) (i.e. the levels and durations of the relative humidity steps) is

identical to that adopted in the present work. To aid interpretation, Figure 6.5 also presents the MBV classification proposed by Rode et al. (2005).

Inspection of Figure 6.5 indicates that the material tested in the present study exhibits a moisture buffering capacity that is considerably higher than that of the unstabilised material tested by McGregor et al. (2014). The higher moisture buffering capacity of the material tested in the present study may be due to the larger fine fraction compared to the soil tested by McGregor et al. (2014). A finer soil is capable of retaining more water than a coarser soil when submitted to the same hygrothermal conditions, as observed by Jaquin et al. (2008) and by Beckett and Augarde (2012). Also, the MBV of the unstabilised compressed earth samples measured in the present work is about two times higher than that measured on stabilised samples by McGregor et al. (2014).

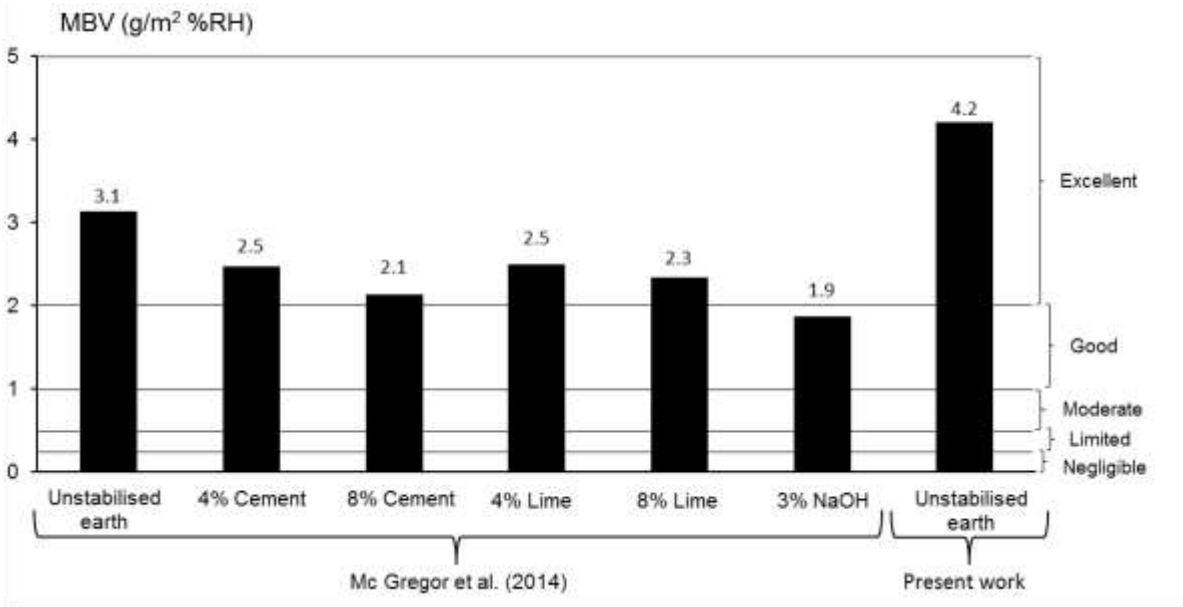

Figure 6.5. MBV of unstabilised compressed earth measured in the present work compared to results of McGregor et al. (2014)

6.3 Moisture buffering capacity of stabilised samples

Hypercompacted unstabilised earth shows good mechanical and moisture buffering characteristics but poor durability when exposed to liquid water as discussed in Section 3.4. Stabilisation appears therefore as an inevitable requirement for the manufacture of earthen materials fulfilling minimum durability criteria in wet environments. At the same time, stabilisation must not compromise the ability of earthen materials to buffer

moisture and hence to smooth variations of ambient humidity inside dwellings. Previous works have suggested that the addition of alkaline solutions or silane-siloxane emulsions to the base soil might provide a viable solution for meeting both the above requirements, i.e. to improve durability while preserving moisture affinity (Kebao and Kagi, 2012; Mc Gregor et al., 2014; Elert et al. 2015). To further explore the above issues, the moisture buffering capacity of stabilised cylindrical samples was measured and compared to that of unstabilised samples from the previous section. Three different stabilising liquid additives were mixed to the base soil as discussed in Section 3.4. These additives, which were chosen after a series of preliminary immersion tests, are:

- 5.2% silane-siloxane emulsion
- 5.2% NaOH solution at 2 mol/L concentration
- 1.08% silane-siloxane emulsion + 4.12% NaOH solution at 2 mol/L concentration

All stabilised samples were compacted at a pressure of 100 MPa and at a liquid content of 5.2 %, similar to the optimum water content of the unstabilised samples. For each type of liquid additive, three samples were tested to determine the MBV in agreement with the norm ISO 24353 (2008). The main properties of the unstabilised samples equalised at different relative humidities have already been given in Table 5.2.

Similar to unstabilised samples, five cycles of relative humidity at a constant temperature of 25 °C were performed, which was enough to obtain three final stable cycles. The moisture adsorption curves, as well as the resulting MBVs, were calculated as the average of three samples tested for each stabilising additive. Figure 6.6 shows the final stable cycle of the moisture adsorption curve for both unstabilised and stabilised earth samples. Inspection of Figure 6.6 indicates that stabilisation significantly reduces the moisture buffering capacity of the material and that the magnitude of this reduction is dependent on the type of stabiliser. NaOH stabilised samples show a higher moisture buffering capacity than samples stabilised with the silane-siloxane emulsion. Samples stabilised with a mix of both NaOH solution and silane-siloxane emulsion exhibit an intermediate behaviour between the above two. These results are in agreement with those of McGregor et al. (2014), who found that stabilised materials tend to perform more poorly than unstabilised ones in terms of their capacity to buffer moisture, even when a small percentage of stabiliser is added.

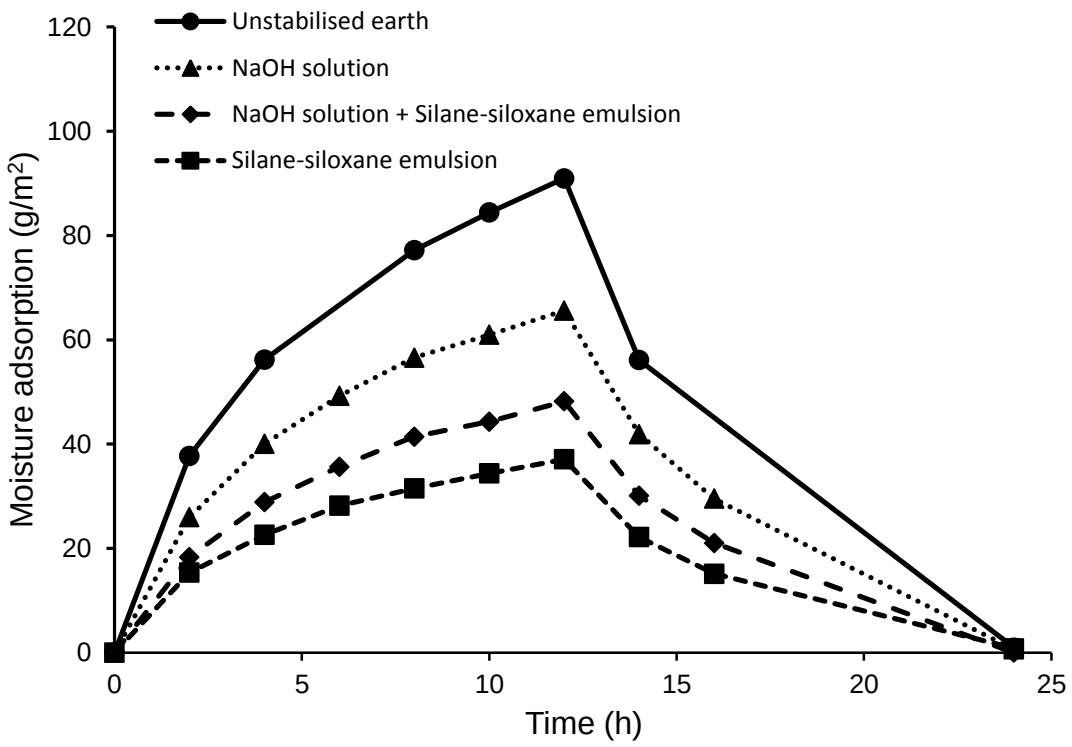

Figure 6.6. Last stable cycle of unstabilised and stabilised samples

Figure 6.7 shows the MBVs measured during uptake and release of moisture on the differently stabilised samples over the five cycles of relative humidity. Similar to unstabilised samples, the MBV of the stabilised materials was calculated as the average of the MBVs measured during uptake and release of moisture over the last three cycles. These average MBVs are plotted in Figure 6.8 together with the MBV of the unstabilised earth samples determined in Section 6.2. Inspection of Figure 6.8 confirms once again that stabilisation significantly reduces the moisture buffering capacity of earthen materials. Nevertheless, the hygroscopic performance of the stabilised materials investigated in this work is still very good according to the classification proposed by Rode et al. (2005). It ranges between excellent (for the material stabilised with the NaOH solution) and good (for the material stabilised with a mix of NaOH solution and silane-siloxane emulsion or for the material stabilised with the silane-siloxane emulsion).

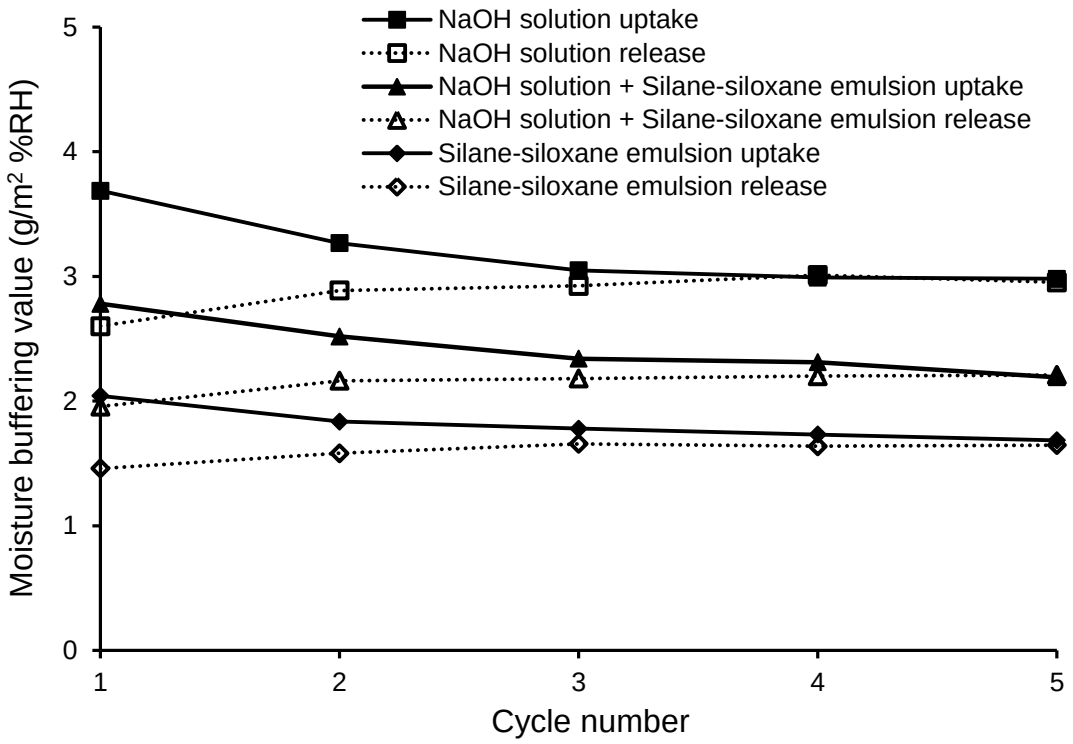

Figure 6.7. MBV uptake and MBV release of stabilised samples

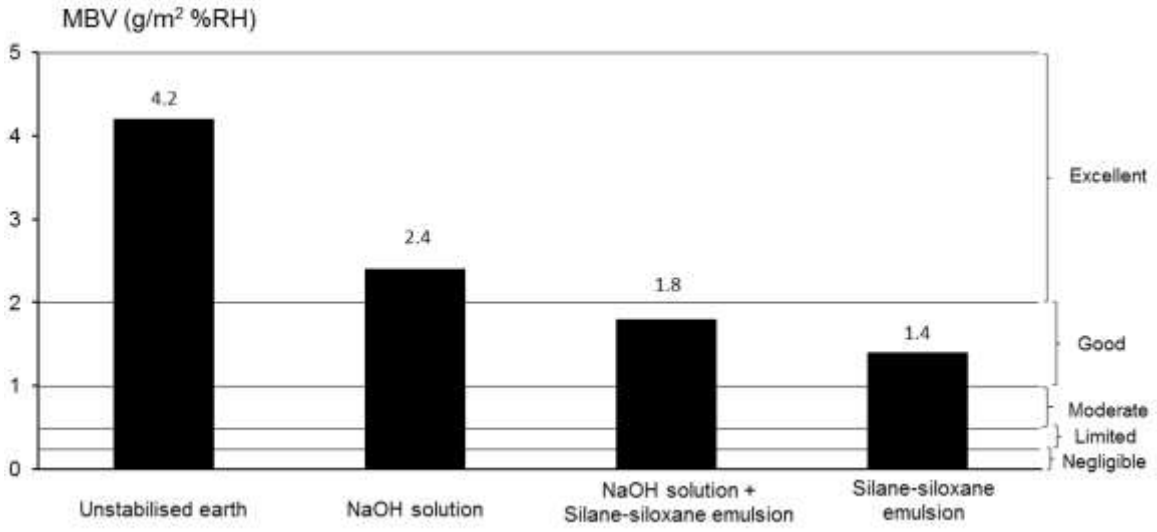

Figure 6.8. MBV of unstabilised and stabilised samples

These results highlight how the need of improving durability by means of stabilisation often contrasts with the equally important need of maintaining a high moisture buffering capacity. The choice of stabilisation technique must be carefully made to balance these opposing requirements. At the same time, stabilisation has an important effect on the stiffness and strength of the material, which must also be taken into account (see Section 5.2.2).

6.4 Comparison between bricks and cylindrical samples

The norm ISO 24353 (2008) requires that cyclic variations of relative humidity must be performed on samples sealed on all but one face with an exposed area higher than 0.01 m^2. In these conditions, exchanges of water vapour can only take place in the direction perpendicular to the exposed face.

Laboratory tests presented in Sections 6.2 and 6.3 were performed on small cylindrical earthen samples. Both the top and lateral surfaces of these samples was left exposed to the environment of the climatic chamber in order to achieve a total exposed area higher than the minimum required by the norm ISO 24353 (2008). In these conditions, the humidity load does not produce an unidirectional vapour flow through the sample but rather a multidirectional flow with components along both axial and radial directions. To further explore the effect of the direction of vapour flow on the measured MBV, additional tests were carried out in this work at the scale of larger bricks.

Unstabilised earth bricks of dimensions 200 x 100 x 50 mm^3 were compacted at a pressure of 100 MPa and at the optimum water content of 5.2%. The details about the compaction procedure and the properties of bricks have already been presented in Section 3.3. All brick faces were sealed with aluminium tape except one of the two largest faces (200 x 100 mm^2), which was left exposed to the humidity of the climatic chamber (Figure 6.9), thus resulting in unidirectional vapour flow across the brick as required by the norm ISO 24353 (2008). Three tests were performed on three different compressed earth bricks prepared in this way. The objective was to determine the effect of the different humidity load and vapour flow direction on the measured MBV (i.e. unidirectional flow in the compressed earth bricks versus multidirectional flow in the cylindrical samples).

After sealing, bricks were equalised at a temperature of 25 °C and at a relative humidity of 53% for a period of two weeks before testing.

Figure 6.9. View of the three earth bricks before testing: unsealed surface (200x100 mm^2) and two of the five sealed surfaces (200x50 mm^2 and 200x100 mm^2)

Similar to cylindrical samples, the earth bricks were submitted to five cycles of relative humidity between 53% and 75% at a constant temperature of 25 °C with mass being recorded every two hours.

Figure 6.10 shows the last stable cycle of the moisture adsorption by both earth bricks and cylindrical samples. In each case, the curve represents the average measurement of three different samples. Note that the results indicated as "Cylindrical samples" in Figure 6.10 coincide with the results indicated as "Unstabilised earth" in Figure 6.6.

Inspection of Figure 6.10 shows that, in the case of compressed earth bricks, the moisture uptake is slightly higher than the moisture release while, in the case of the cylindrical samples, the response appears perfectly reversible. Nevertheless, the observed behaviour is very similar in both cases and the measured MBV can be considered identical for both earth bricks and cylindrical samples. It can therefore be concluded that the MBV is independent of how the humidity load is applied, which also means that the results obtained on cylindrical samples are valid, despite the direction of flow was not unidirectional in this case.

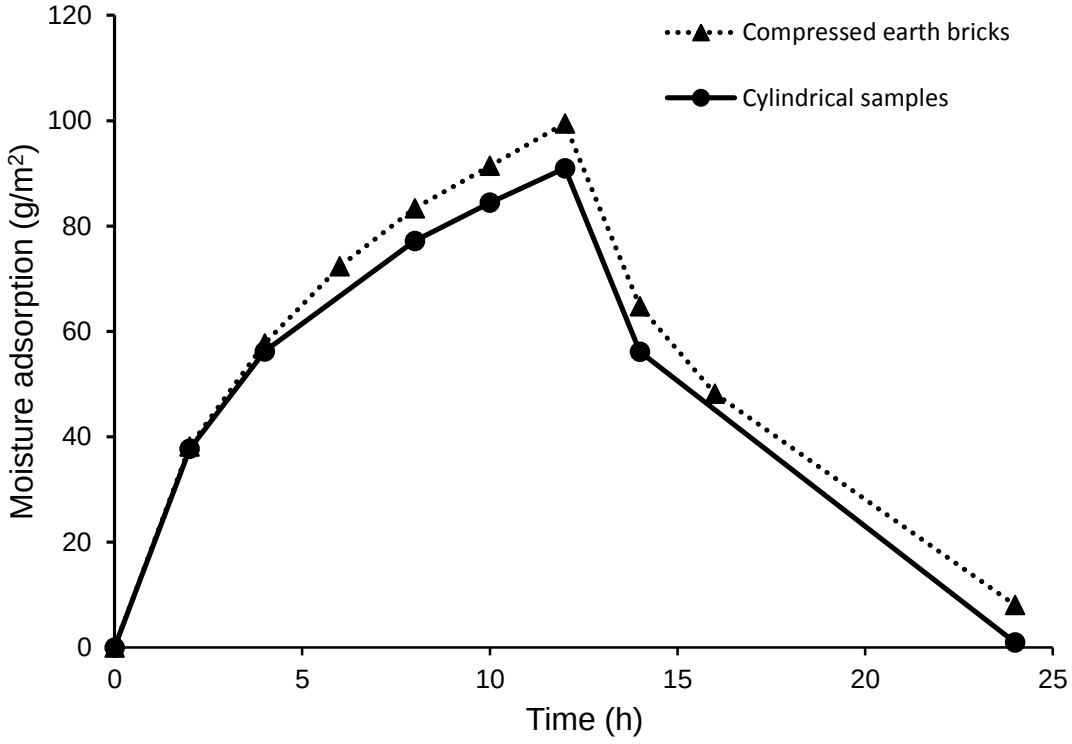

Figure 6.10. Last stable cycle of compressed earth bricks and cylindrical samples

6.5 Final remarks

This chapter has presented results from a series of tests aimed at measuring the moisture buffering capacity of unstabilised and stabilised compressed earth. The main points can be summarised as:

- Cyclic variations of relative humidity were performed on unstabilised cylindrical earth samples compacted at the three pressure levels of 25, 50 and 100 MPa and at the respective optimum water contents. These tests aimed to determine the effect of compaction pressure on hygroscopic behaviour and, in particular, on the measured MBV. All unstabilised samples showed identical hygroscopic behaviour, regardless of the compaction level. This was expected considering that, under the imposed conditions of temperature and relative humidity, exchanges of water vapour take place prevalently within pores with diameters from 3 to 7 nm (according to Kelvin equation and Washburn equation) which were not affected by mechanical compaction (see Section 6.3).

- The moisture buffering capacity of the unstabilised samples is about ten times higher than that of traditional building materials such as fired bricks or concrete (see Section 6.3).
- Laboratory tests were also performed on stabilised samples to investigate the effect of stabilisation on the measured MBV. Results showed that stabilisation reduces the moisture buffering capacity of the material and this reduction is dependent on the chosen type of stabiliser. The samples stabilised with a NaOH solution maintained an excellent capacity to buffer ambient humidity according to the classification of Rode et al. (2005). The samples stabilised with silane-siloxane emulsion and with a mix of silane-siloxane emulsion and NaOH solution showed instead a good moisture buffering capacity according to the classification of Rode et al. (2005) (see Section 6.4).
- Cyclic variations of relative humidity were also performed on compressed earth bricks compacted at a pressure of 100 MPa and at the optimum water content of 5.2%. The bricks were sealed on all but one of the two largest surfaces, which was left exposed to the testing environment. These tests aimed to investigate the effect of the humidity load and consequent vapour flow direction on the measured MBV (i.e. multidirectional flow for cylindrical samples versus unidirectional flow for bricks). Bricks and cylindrical samples compacted in the same way showed very similar hygroscopic responses, thus confirming that the measured MBV is independent of how the humidity load is applied and of the direction of vapour flow.

7

Durability properties

This chapter presents the results from different types of durability tests conducted to investigate the resistance to water erosion of unstabilised and stabilised earth bricks. Durability tests were performed according to the German norm "Earth blocks - Terms and definitions, requirements, test methods" DIN 18945 (2013) which includes suction tests and contact tests.

Raw earth is relatively hydrophilic, which is an advantageous characteristic for building applications as it enhances the ability of the material to buffer moisture as already discussed in Chapter 6. The hydrophilic nature of earthen materials may however pose some durability problems as it makes these materials particularly prone to water erosion. As already presented in Section 3.4, unstabilised earth samples exhibit low durability when submerged in water and can experience mass losses higher than 70% after only 10 minutes of immersion. Because of this, addition of stabilising additives to the base soil is often necessary to manufacture a material that fulfils the minimum durability criteria of building regulations especially in wet climates.

Unfortunately the addition of stabilisers reduces the capacity of earthen materials to absorb/release water vapour and hence partly compromises the ability of smoothing variations of ambient humidity inside dwellings (see Section 6.3). The results from preliminary immersion tests on cylindrical samples presented in Section 3.4 have however shown that some additives, such as alkaline solutions or silane-siloxane emulsions, can balance between these two contrasting needs, i.e. they can increase durability without significantly deteriorating moisture buffering capacity.

To further investigate these aspects, additional durability tests were performed on stabilised and unstabilised compressed earth bricks. The objective was to investigate the effect of different stabilisation methods on the resistance of the bricks against water erosion. Both unstabilised and stabilised earth bricks were compacted at a pressure of 100 MPa as described in Section 3.3. The unstabilised samples were prepared at a water

content of 5.2%, which corresponds to the optimum water content for a static compaction pressure of 100 MPa (see Section 3.2). The stabilised samples were instead manufactured by mixing the dry soil with one of the following three liquid additives instead of water (see Section 3.4):

- 5.2% silane-siloxane emulsion
- 5.2% NaOH solution at 2 mol/L concentration
- 1.08% silane-siloxane emulsion + 4.12% NaOH solution at 2 mol/L concentration

The above additives were selected after some preliminary immersion tests performed on cylindrical samples compacted at 100 MPa (see Section 3.4). Note that the liquid additive content is always equal to 5.2% of dry mass, which is the same value as the optimum water content of the unstabilised samples. Specific analyses (e.g. a life cycle assessment) must also be carried out to quantitatively assess the environmental impact of the different stabilisers employed in the present study. These analyses are outside the objectives of the present doctoral thesis but they may represent a valuable development for future investigation.

The results obtained from suction and contact tests on unstabilised and stabilised compressed earth bricks are presented in this chapter together with the corresponding durability classification in compliance with the norm DIN 18945 (2013).

7.1 Suction test

Suction tests investigate the durability of compressed earth bricks when exposed to a temporary excess of water. This condition might occur, for example, in exterior timber-frame walls during driving rains, with water collecting between the wooden frame and the earthen infill. Also, suction tests might reproduce the effect of a capillary water rise from the foundation of a building up into its walls.

For each stabilisation method (including the case of no stabilisation at all), three bricks were manufactured as previously described. These bricks were then equalised under constant hygrothermal conditions (T = 23 °C and RH = 50%) for two weeks, which was long enough to attain a constant mass.

A support made of a conventional fired brick with an absorbent cloth on top was placed inside a pan (Figure 7.1). The pan was then filled with water up to 1-5 mm below the

upper edge of the fired brick. After this, the compressed earth brick was placed over the absorbent cloth, which marks the start of the suction test. During the test, water was progressively absorbed by the earth brick through the cloth and the support underneath. As adsorption progressed, the water level inside the pan fell and was therefore topped up to keep it constant. According to the norm DIN 18945 (2013), samples were visually assessed at times of 30min, 3h and 24h from the beginning of the test in order to detect cracks and permanent deformations owed to swelling.

Figure 7.2 shows the results of suction tests performed on one brick for each stabilisation method. Very similar results were obtained for the other two bricks tested for each stabilisation method and not included in Figure 7.2. Inspection of Figure 7.2 indicates that, as expected, the unstabilised bricks exhibited the weakest response to water adsorption with cracks and irreversible deformations already visible after 30 minutes from the beginning of the test. This means that, according to the norm DIN 18945 (2013), the unstabilised earth bricks manufactured in the present work are only suitable for dry applications and cannot be exposed to running water. Instead, the earth bricks stabilised with a mix of silane-siloxane emulsion and NaOH solution exhibited greater durability as confirmed by the fact that cracks only appeared after 3 hours from the beginning of the test. The best results were, however, obtained from the tests performed on the compressed earth bricks stabilised with the NaOH solution or with the silane-siloxane emulsion. These bricks only started to show some cracking at the last visual examination after 24 hours from the beginning of the test. Therefore, according to the norm DIN 18945 (2013), the earth bricks stabilised with either the NaOH solution or the silane-siloxane emulsion are suitable for coated externals wall exposed to natural weathering (see Section 2.4).

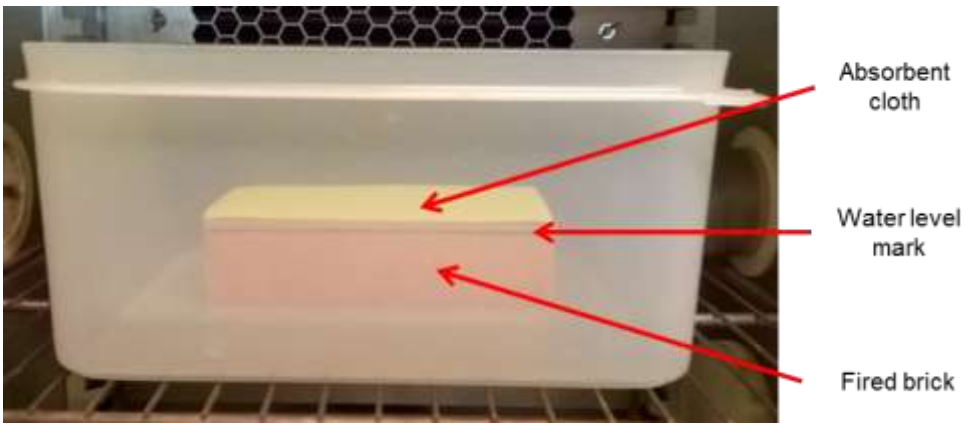

Figure 7.1. Set-up of suction test

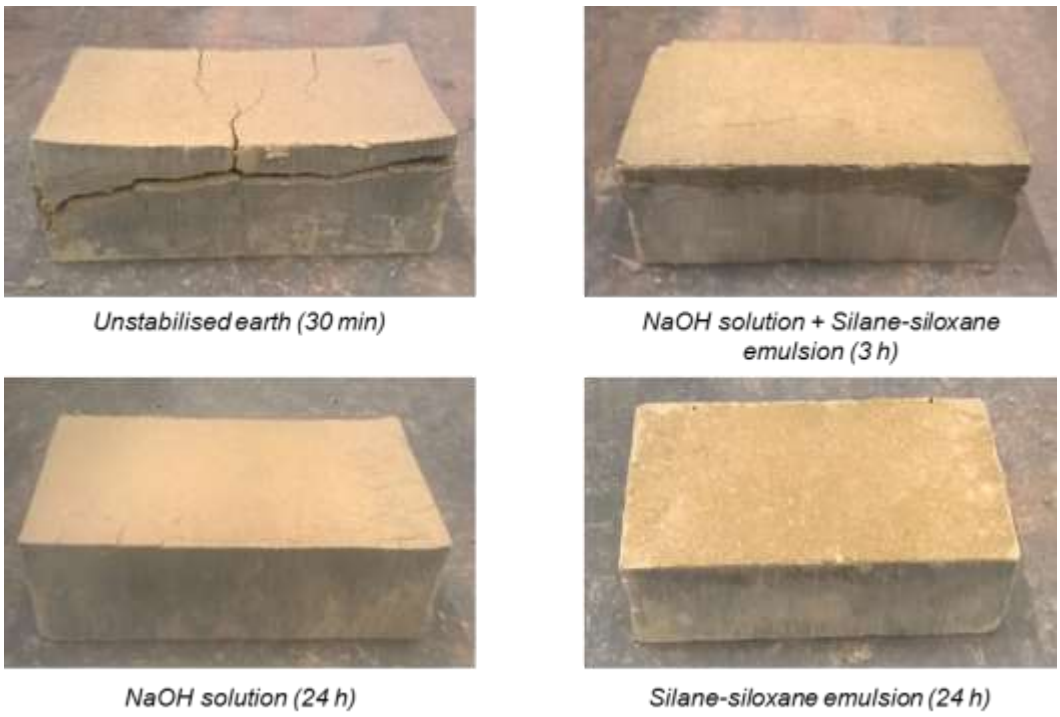

Figure 7.2. Results from suction tests on unstabilised and stabilised compressed earth bricks

7.2 Contact test

The objective of the contact test is to simulate the application of a mortar joint or coating onto the bricks and to assess the response of the material to the adsorption of moisture from the mortar joint or coating (DIN 18945, 2013). The experimental procedure consisted in applying on the intermediate face of the brick a wet cellulose cloth, which simulates the mortar joint or coating (Figure 7.3). The amount of water applied by the cellulose cloth to the brick surface must be equal to 0.5 g/cm^2. This reproduces the average amount of water contained in a 15 mm thick mortar layer (Schroeder, 2015). The earth bricks, together with their wet cellulose cloths, were then placed on two supports consisting of metallic nuts and stored in a sealed container for 24 hours. Before sealing some water was also introduced at the bottom of the container with the free surface about 0.5 cm below the top of the support nuts. Subsequently, the cellulose clothes were removed and the bricks were exposed to the atmosphere for a minimum time of two days. Finally, the bricks were visually examined to assess the presence of cracks and the occurrence of permanent deformations owed to water infiltration.

Unlike the suction test, in this case only one brick was tested for each stabilisation method (including the case of no stabilisation). The results are reported in Figure 7.4

where it can be observed that the bricks stabilised with the silane-siloxane emulsion exhibit less damages compared to other bricks. Nevertheless, all types of bricks showed some degree of cracking and permanent deformations which means that all bricks manufactured in this work are only suitable for dry applications according to the norm DIN 18945 (2013). In conclusion, the above stabilisation methods considerably improve the durability of earth bricks in the presence of water. However, they did not manage to fulfil all requirements for construction in wet environments according to the norm DIN 18945 (2013). Further investigation is therefore necessary to extend the range of applications of compressed earth bricks especially when exposed to natural weathering.

Figure 7.3. Set- up of contact test

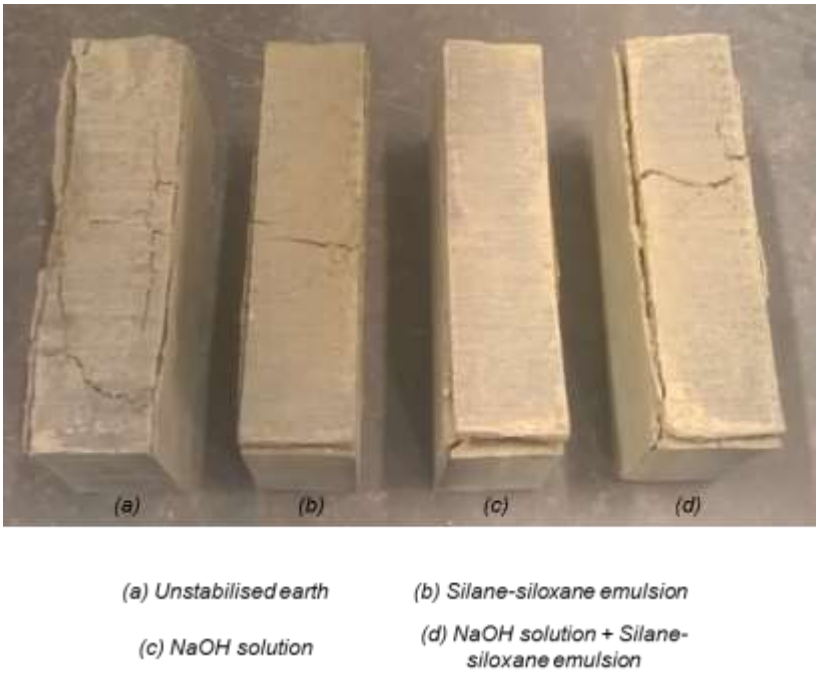

Figure 7.4. Results from contact tests on unstabilised and stabilised compressed earth bricks

7.3 Bricks classification

The norm DIN 18945 (2013) proposes a classification of compressed earth bricks based on their resistance to natural weathering and their suitability for different applications (see Table 7.1).

Table 7.1. Classes of compressed earth bricks (DIN 18945, 2013)

Application	Class
External wall exposed to natural weathering	Ia
Coated external wall exposed to natural weathering	Ib
External wall not exposed to natural weathering – Internal wall	II
Dry applications	III

The above classification was applied in the present work to both unstabilised and stabilised compressed earth bricks as described earlier. The result of this classification, which is based on results from immersion tests (presented in Section 3.4), suction and contact tests according to the norm DIN 18945 (2013), is summarised in Table 7.2. Note that, in Table 7.2, it is assumed that the results from the immersion tests on cylindrical samples (see Section 3.4) are also representative of the material behaviour at the brick scale.

Table 7.2 indicates that earth bricks stabilised with the silane-siloxane emulsion exhibit in general the best durability performance with a small mass loss of 1.36% after immersion in water (see Section 3.4) and some degree of cracking after both the suction and contact tests. In addition, it must be emphasised that the stabilisation by means of the silane-siloxane emulsion produces a larger reduction of mechanical characteristics (see Section 5.2.2) and moisture buffering capacity (see Section 6.4) compared to the other two stabilisation techniques. Therefore, what is gained in terms of improved durability appears to be lost in terms of mechanical characteristics and moisture buffering capacity.

Inspection of Table 7.2 also shows that the three durability tests prescribed by the norm DIN 18945 (2013) provide results that are not in complete agreement between them. The worst durability performance is observed during the contact test, which concludes that all bricks fall into the third class and are therefore only suitable for dry applications. A similar result was obtained by the laboratory LMDC (TERCRUSO, 2013) which found that the contact test provides the most severe assessment of material durability. In

the work performed at the LMDC, a better durability was recorded during the immersion and suction tests than during the contact test, with only one of the six bricks tested in that work showing no sign of cracking and therefore suitable for use within class I or II (TERCRUSO, 2013).

The above results represent an important development of the present study. They demonstrate the urgency of further investigation about the development of sustainable stabilisation methods that can improve material durability without negatively impacting on mechanical and moisture buffering performance.

Table 7.2. Classification of earth bricks depending on type of stabilisation

Type of stabilisation	Immersion test	Suction test	Contact test
Unstabilised	III	III	III
Silane-siloxane emulsion	I	Ib	III
NaOH solution	II	Ib	III
NaOH solution + Silane-siloxane emulsion	I	II	III

7.4 Final remarks

In this chapter, the durability of unstabilised and stabilised earth bricks was assessed by performing different types of tests as prescribed by the norm DIN 18945 (2013). The main outcomes of this part of the work can be summarised as follows:

- After preliminary immersion tests on cylindrical samples, three different stabilisers were selected for further investigation during suction tests and contact tests at the brick scale. These stabilisers are a silane-siloxane emulsion, a NaOH solution and a mix of silane-siloxane emulsion and NaOH solution (see Section 3.4).
- Immersion tests, suction tests and contact tests lead to different conclusions about the durability of unstabilised and stabilised earth bricks exposed to natural weathering. The contact test provides the most severe assessment of material durability among all tests prescribed by the norm DIN 18945 (2013). In fact, all stabilised bricks were classified as I or II class according to immersion and suction tests but not according to the contact test.

- The best durability performance was observed for the samples stabilised with the silane-siloxane emulsion. However, even these samples showed some mass loss during immersion (see Section 3.4) and some cracks after both suction and contact tests. Moreover, silane-siloxane stabilisation resulted in a considerable deterioration of the mechanical and moisture buffering properties of the material. Further investigation is therefore needed to identify a suitable stabilisation method that can carefully balance the different needs of sustainability, durability, moisture buffering and mechanical performance.

8

Conclusions

The present work investigated the hygro-mechanical behaviour of raw earth as a construction material. An innovative manufacturing method based on the application of very high compaction pressures (hypercompaction) was proposed. The mechanical and moisture buffering properties of the resulting material were investigated at the scale of small cylindrical samples and large bricks. Different methods to improve durability against water erosion were also proposed. The present chapter summarises the main outcomes of this research together with some recommendations for future work.

8.1 Material and methods

The grain size distribution and plasticity characteristics of the base soil were first determined. The fine fraction was classified as normally active. This is consistent with the mineralogy of the clay component which consists of illite and a small quantity of montmorillonite. These results confirmed that the soil used in this work is compliant with current recommendations for the manufacture of compressed earth bricks (see Sections 3.1.1 and 3.1.2).

Small scale cylindrical samples (50 mm diameter and 100 mm high) were initially manufactured by means of the proposed hypercompaction method. This method is based on the application of a very high compaction stress to increase material density. A double compaction procedure was adopted to increase stress uniformity across the height of the sample. A specific mould was designed and manufactured to withstand the high compaction load and to allow pore water drainage during consolidation. Consolidation was considered complete when the displacement rate became less than 0.01 μm/s over a period of at least one hour. This assured that the samples experienced the whole primary consolidation and a large share of the secondary consolidation (see Section 3.2.1). The formulation of the hypercompaction method and the design of the compaction mould are among the original contributions of the present project (see Section 3.2.1).

Cylindrical samples were manufactured at three pressure levels of 25, 50 and 100 MPa and different water contents. This allowed the determination of the compaction curve in the water content versus dry density plane for each pressure level. As compaction energy increased, the optimum water content decreased while the corresponding dry density increased, which means that the compaction curve shifted towards the theoretical "no porosity" point (see Figure 3.7 in Section 3.2.3). The optimum dry density increased less than linearly with compaction pressure, which means that an unfeasibly high pressure would be required to attain the theoretical "no porosity" point.

No water drainage was observed during compaction of samples at the optimum water content or drier. For these samples, the water drainage system of the compaction mould resulted unnecessary (see Section 3.2.3).

After compaction, all samples were stored inside a climatic chamber at a temperature of 25 °C and a relative humidity of 62% until a constant mass was measured. During this time, the material experienced desaturation and shrinkage as the water content reduced to about 3.5% (for all samples) and dry density increased (mainly for the wettest samples). At the end of equalisation, the samples compacted at the highest pressure of 100 MPa exhibited also similar values of dry density regardless of the compaction water content. This suggests that the application of a high compaction pressure can reduce the variability of dry density associated to small changes of compaction water content, which helps to standardise material properties. This is an important result for industrial application.

In the second part of the experimental campaign, the hypercompaction method was extended to manufacture compressed earth bricks of dimensions 200 x 100 x 50 mm^3. For this purpose, a specific mould for the compaction of bricks was designed and manufactured. Forty earth bricks were compacted at a pressure of 100 MPa and at the optimum water content as determined on cylindrical samples.

These bricks exhibited an average dry density of 2325 kg/m^3 which is slightly higher than that of the cylindrical samples compacted at the same pressure. This is due to the fact that bricks have a ratio of volume to lateral surface higher than cylindrical samples and the effect of lateral friction during compaction is therefore considerably reduced (see Section 3.3).

Unstabilised samples showed poor durability and therefore stabilisation was considered indispensable. In order to reduce the carbon footprint, stabilisers other than cement or lime were initially explored by means of simple immersion tests. Based on these preliminary results, the following additives were selected for further testing:

- silane-siloxane emulsion (5.2% by dry mass of soil)
- NaOH solution at 2 mol/L concentration (5.2% by dry mass of soil)
- silane-siloxane emulsion (1.08% by dry mass of soil) + NaOH solution at 2 mol/L concentration (4.12% by dry mass of soil)

8.2 Microstructural analysis

Mercury intrusion porosimetry MIP and nitrogen adsorption tests were performed to better understand the effect of hypercompaction on material fabric. Samples were equalised inside a climatic chamber under constant hygrothermal conditions (T= 25 °C and RH = 62%) and then subjected to freeze-drying to remove all pore water while preserving the original material fabric.

Results from both MIP and nitrogen adsorption tests confirmed that compaction affects only the inter-aggregate porosity, i.e. pore diameters larger than 50 nm, while the effect on intra-aggregate pores, i.e. pore diameter smaller than 50 nm, is negligible for all three compression levels investigated in this work (see Section 4.2.1 and 4.3.2).

MIP tests were performed on small specimens taken at different heights of the cylindrical samples to investigate material homogeneity. It was observed that porosity changes very little along the sample height and that the top and bottom extremities were only slightly more compacted than the middle. The double compaction process was considered essential to attain such uniform density despite the considerable lateral friction between the sample and the mould during compaction (see Section 4.2.2). A larger inhomogeneity would be expected if compaction was performed from only one side of the sample.

The effect of compaction water content on material fabric was also investigated. For this purpose, MIP tests were performed on two samples compacted to the same density but different water contents corresponding to the dry and wet side of optimum, respectively. Two samples were compacted to Proctor standard and two samples were compacted to 100 MPa. Results confirmed that the application of a higher pressure of 100 MPa considerably reduced the dependency of density on compaction water content. This has

important repercussions on the standardisation of material properties during manufacturing of raw earth (see Section 4.2.3).

8.3 Mechanical behaviour

An extensive experimental campaign of mechanical tests was conducted to determine the stiffness and strength of both unstabilised and stabilised raw earth at the scale of both small cylindrical samples and large bricks.

In the first part of this campaign, mechanical tests were performed on cylindrical samples compacted at the three pressure levels of 25, 50 and 100 MPa and at different water contents resulting in different dry densities. All samples were subjected to five loading-unloading cycles to measure the Young modulus and Poisson ratio and then loaded until failure to determine the unconfined compressive strength. During the loading-unloading cycles, earthen samples exhibited a hysteretic mechanical response as material behaviour was elasto-plastic during loading but essentially elastic during unloading. The Young modulus and Poisson ratio were therefore determined from the unloading branches of the cycles. Material stiffness tended to increase more than linearly with increasing dry density. In particular, the samples compacted at a pressure of 100 MPa exhibited a Young modulus about one order of magnitude greater than the samples compacted to Proctor standard (see Section 5.1.1).

Similar to the Young modulus, the compressive strength increased more than linearly with increasing dry density. Therefore, any small augmentation of dry density beyond the maximum value obtained in the present work could induce a significant improvement of mechanical performance (see Section 5.1.4).

The effect of ambient humidity on mechanical properties was also investigated. Additional tests were conducted on both unstabilised and stabilised cylindrical samples equalised at five different levels of ambient humidity (i.e. 25%, 44%, 62%, 77% and 95%) and at a constant temperature of 25 °C. The values of temperature and relative humidity imposed during equalisation were converted into corresponding values of total suction by means of Kelvin law (see Section 5.2). Results showed that the stiffness and strength of both unstabilised and stabilised samples increased as suction increased from 7 MPa to 112 MPa but then tend to level off as suction increased further. Stabilised samples showed a more limited increase of stiffness and strength with increasing suction compared to unstabilised samples, which suggests that their mechanical

behaviour is less sensitive to relative humidity (see Sections 5.2.1 and 5.2.2). This is also consistent with the lower moisture buffering capacity of stabilised samples compared to unstabilised samples (see Chapter 6). Interestingly, all three stabilisation techniques adopted in this work resulted in a reduction of stiffness and strength, as well as of their dependency on suction, compared to unstabilised samples. This is probably because the addition of binders attenuates the influence of water capillarity on inter-particle bonding which, in turns, limits the improvement of mechanical properties with increasing suction (see Section 5.2.2).

The proposed hypercompaction method requires the application of a constant load for more than two hours, which might be too long for industrial applications. Another set of tests was therefore performed to investigate the potential effect of a reduction of this consolidation time on mechanical properties. These tests were performed on unstabilised cylindrical samples all compacted to 100 MPa and at the optimum water content but consolidated for different times of 0.5, 1, 2, 5, 10, 20, 40, 80 and 160 minutes. The results showed that both stiffness and strength grew steeply up to a consolidation time of 20 minutes but remained constant after this point. A less severe consolidation criterion than that employed in the present work could therefore be adopted without significant loss of mechanical performance. At the same time, a very short consolidation time of the order of seconds, as it is often the case in common construction practice, cannot assure the best mechanical properties (see Section 5.3).

Compression tests were also performed at the brick scale to demonstrate that the proposed hypercompaction method can largely improve strength compared to traditional manufacturing procedures for compressed earth bricks. In particular, it was observed that the compressive strength of the hypercompacted bricks is comparable with that of more traditional building materials such as stabilised compacted earth and standard masonry bricks (see Section 5.4.2).

The effect of different testing procedures on the measured strength of compressed earth bricks was explored.

The effect of the testing aspect ratio was investigated by varying brick orientation. An extremely high compressive strength was measured when the load was applied on the largest brick face (i.e. aspect ratio of 0.5). This is due to the large confinement exerted by the friction between the press plates and the brick faces which increases the measured strength. Lower but more realistic values of strength were measured when the

load was applied on the intermediate faces (aspect ratio of 2) and smallest faces (aspect ratio of 4) of the brick, with a slightly lower value in the former case compared to the latter one. This is probably due to the distinct failure mechanisms observed in these two cases, with a shearing mechanism occurring in the former case and a compressive mechanism in the latter case (see Section 5.4.1).

The confining effect of friction between press plates and brick faces was explored by testing two sets of six bricks loaded on their smallest faces (aspect ratio of 4). The first set of bricks was capped with Teflon plates to reduce friction while the second one was left uncapped. Teflon capped bricks exhibited a slightly lower compressive strength than uncapped bricks due to the reduced friction which in turn lowered confinement.

Since the effect of friction is reduced by both a high aspect ratio and Teflon capping, the compressive strength measured on capped bricks loaded on their smallest faces is considered to be the most representative value.

The effect of a cement mortar joint on the strength of unstabilised earth bricks was also investigated. Compression tests were performed on two sets of six samples made of superimposed dry-sawn brick halves. In the first set, the two halves were simply superposed without any mortar joint while, in the second set, the two halves were bonded by a cement mortar joint. Results showed that the presence of the mortar joint induced a significant reduction of compressive strength. This is due to the high water content of the mortar joint that wets the surface of the bricks thus damaging the material (see Section 5.4.3). It was also observed that the compressive strength of the samples without mortar joints was lower than the strength of the entire bricks measured along all loading directions. This is probably due to dry-sawing the brick into two halves, which weakens the material by creating micro-cracks (see Section 5.4.3)

The effect of compaction-induced anisotropy on strength was assessed by testing small cubic specimens dry-sawn from an entire brick. The small cubic specimens were loaded along the three perpendicular directions. Results showed that the compressive strength measured along the direction of compaction was higher than that measured along the other two perpendicular directions. The influence of anisotropy on material strength is lower for the compacted bricks tested in this study than for the extruded bricks tested by Aubert et al. (2016) (see Section 5.4.4).

8.4 Hygroscopic behaviour

Laboratory tests were conducted to analyse the hygroscopic behaviour of unstabilised and stabilised compacted earth samples. The capacity of the material to absorb/release vapour was assessed by subjecting samples to cyclic variations of relative humidity at constant temperature according to the norm ISO 24353 (2008). These tests allowed the measurement of the moisture buffering value (MBV) of the material.

The effect of compaction pressure on the measured MBV was assessed by testing unstabilised cylindrical samples compacted at the three pressures of 25, 50 and 100 MPa and their respective optimum water contents. Results from these tests confirmed that unstabilised earth has an excellent capacity of buffering ambient humidity, which is about ten times higher than that of traditional building materials such as fired bricks or concrete (see Figure 6.4 in Section 6.2). This hygroscopic behaviour was also identical for all samples, regardless of compaction pressure. This is because exchanges of water vapour take place within nanopores which are not affected by mechanical compaction (see Section 6.2).

The effect of stabilisation on moisture buffering was also investigated. It was found that stabilisation induced a significant reduction of the moisture buffering capacity of the material which also depended on the type of stabiliser employed. Samples stabilised with a NaOH solution maintained an excellent moisture buffering capacity according to the classification of Rode et al. (2005), similar to unstabilised earth. Samples stabilised with a silane-siloxane emulsion or a mix of the silane-siloxane emulsion and the NaOH solution fell instead into the category of good buffers according to the same classification (see Section 6.3).

Finally, cycles of relative humidity were performed on compressed earth bricks sealed on all but one of the two largest surfaces. These experiments aimed to analyse the effect of the different testing conditions for the small cylindrical samples and the larger bricks. The vapour flow path can be considered multidirectional in the case of cylindrical samples and unidirectional in the case of bricks. The measured MBV was very similar in both cases, which indicates that the hygroscopic behaviour is only marginally affected by how the humidity load is applied.

8.5 Durability properties

The durability against water erosion of both unstabilised and stabilised bricks was assessed by performing different tests as prescribed by the norm DIN 18945 (2013).

It was found that samples stabilised with the NaOH solution or with a mix of the silane-siloxane emulsion and the NaOH solution showed higher resistance against water erosion than unstabilised samples. Still, these materials cannot be employed for applications which entail exposure to natural weathering according to the norm DIN 18945 (2013). The best durability performance was obtained for the samples stabilised with the silane-siloxane emulsion, which exhibited a mass loss of only 1.36% during immersion tests (see Section 3.4). Nevertheless, also these samples exhibited some cracks during both suction and contact tests (see Section 7.1 and 7.2). Stabilisation with silane-siloxane emulsion also induced the largest reduction of mechanical performance and moisture buffering capacity.

Immersion, suction and contact tests resulted in different assessments of the durability of compressed earth bricks (see Table 7.2 in Section 7.3). Among all tests, the contact tests were the most severe with all tested bricks falling into Class III, which is only suitable for dry applications according to the norm DIN 18945 (2013).

8.6 Recommendations for future work

Some potential developments of the present work are summarised as follows:

- Further work could be conducted to investigate the mechanical and hygroscopic behaviour at the scale of a small masonry assembly, i.e. at the scale of a small wall of compressed earth bricks. For this purpose, preliminary tests should be carried out on half-bricks joined with different types of mortar (see Section 5.4.3).

- Further work could be performed to characterise the thermal behaviour of raw earth (e.g. thermal conductivity, specific heat, etc.). Based on these results, laboratory tests could be developed to investigate the heat and moisture transport behaviour across a wall of compressed earth bricks

- Further investigation should be conducted to develop novel stabilisation methods that can protect earthen materials from water erosion while maintaining a high moisture buffering capacity, adequate mechanical performance and a low environmental impact.

- The influence of compressed earth bricks on the quality of indoor air has not been assessed in the present work. Further research in this direction could investigate the potential of earthen materials to improve living conditions inside dwellings.

- A full life cycle assessment of earth structures should be performed to quantify the environmental impact of this construction technique. This life cycle assessment could also inform the choice of stabilisation method.

REFERENCES

ADEME (2013). Consommation d'énergie dans les bâtiments – chiffres clés 2013. *http://reseaux-chaleur.cerema.fr/consommation-denergie-dans-les-batiments-chiffres-cles-2013* (last accessed: 22 August 2016).

AENOR (2008). Compressed earth blocks for walls and partitations. Definitions, specifications and test methods. UNE 41410. Madrid (Spain): Spanish Association for Standardisation and Certification.

AFNOR (1991). NF P 94-054; Soils: investigation and testing – Determination of particle density- Pycnometer method.

AFNOR (1992). NF P 94-057. Soils: investigation and testing – Granulometric analysis – Hydrometer method.

AFNOR (1993). NF P 94-051; Soils: Investigation and testing – Determination of Atterberg's limits – Liquid limit test using Casagrande apparatus – Plastic limit test on rolled thread.

AFNOR (1995). NF P 94-050. Soils: investigation and testing – Determination of the moisture content – Oven drying method.

AFNOR (1995). XP P 94-041. Soils: investigation and testing – Granulometric description – Wet sieving method.

AFNOR (1999). NF P 94-093. Soils : Investigation and testing — Determination of the compaction characteristics of a soil — Standard Proctor test — Modified Proctor test.

AFNOR (2006). NF EN 196-1. Methods of testing cement - Part 1 : determination of strength.

AFNOR (2001). XP P13-901; Compressed earth blocks for walls and partitions: definitions – Specifications – Test methods – Delivery acceptance conditions.

Allinson, D., & Hall, M. (2010). Hygrothermal analysis of a stabilised rammed earth test building in the UK. *Energy and Buildings*, *42*(6), 845-852.

ASTM D559-03 (2012). Standard Test Methods for Wetting and Drying Compacted Soil-Cement Mixtures. American Society for Testing and Materials International.

ASTM C270 (2014). Standard Specification for Mortar for Unit Masonry. American Society for Testing and Materials International.

Attom, M. F. (1997). The effect of compactive energy level on some soil properties. *Applied Clay Science*, *12*(1), 61-72.

Aubert, J. E., Fabbri, A., Morel, J. C., & Maillard, P. (2013). An earth block with a compressive strength higher than 45MPa!. *Construction and Building Materials*, *47*, 366-369.

Aubert, J. E., Maillard, P., Morel, J. C., & Al Rafii, M. (2016). Towards a simple compressive strength test for earth bricks?. *Materials and Structures*, *49*(5), 1641-1654.

Barrett, E. P., Joyner, L. G., & Halenda, P. P. (1951). The determination of pore volume and area distributions in porous substances. I. Computations from nitrogen isotherms. *Journal of the American Chemical society*, *73*(1), 373-380.

Beckett, C. T. S., & Augarde, C. E. (2012). The effect of humidity and temperature on the compressive strength of rammed earth. In *Proceedings of 2nd European Conference on Unsaturated Soils* (pp. 287-292).

Bossink, B. A. G., & Brouwers, H. J. H. (1996). Construction waste: quantification and source evaluation. *Journal of construction engineering and management*, *122*(1), 55-60.

Bossink, B. A. G., Brouwers, H. J. H., & Kessel, R. V. (1996, October). Financial consequences of construction waste. In *Proceedings of International Conference CIB W98*.

British Building Regulations (2010). Approved Document E: Resistance to the Passage of Sound, published by the National Building Specification (NBS) part of the Royal Institute of British Architects (RIBA) Enterprises Ltd

British Standard 3921 (1985). Specification for clay bricks.

British Standard 8233 (1999). Sound Insulation and Noise Reduction for Buildings: Code of Practice, British Standards Institute, London

Brunauer, S., Emmett, P. H., & Teller, E. (1938). Adsorption of gases in multimolecular layers. *Journal of the American chemical society*, *60*(2), 309-319.

Bui, Q. B., & Morel, J. C. (2009). Assessing the anisotropy of rammed earth. *Construction and building Materials*, *23*(9), 3005-3011.

Bui, Q. B., Morel, J. C., Hans, S., & Walker, P. (2014). Effect of moisture content on the mechanical characteristics of rammed earth. *Construction and Building materials*, *54*, 163-169.

Bui, Q. B., Morel, J. C., Reddy, B. V., & Ghayad, W. (2009). Durability of rammed earth walls exposed for 20 years to natural weathering. *Building and Environment*, *44*(5), 912-919.

Cheng, M. Y., & Saiyouri, N. (2015). Effect of long-term aggressive environments on the porosity and permeability of granular materials reinforced by nanosilica and sodium silicate. *Geotechnical Engineering*, 46(3), 62-72.

Chilkoti, A. (2012). Mud world. Financial Times, 19 October 2012. http://www.ft.com/cms/s/2/791620e6-13c2-11e2-9ac6-00144feabdc0.html#axzz2K8Pbgvq1 (last accessed: 19 August 2016).

Ciancio, D., & Gibbings, J. (2012). Experimental investigation on the compressive strength of cored and molded cement-stabilized rammed earth samples. *Construction and Building Materials*, *28*(1), 294-304.

Cointeraux, F. (1790-1791). École d'architecture rurale. Premier, deuxième, troisième et quatrième cahier. Published by Vezard & Le Normant.

CRATerre-EAG (1998). CDI, Compressed earth blocks: Standards – Technology series No.11. Brussels: CDI.

Crooks, R. W., Kilgour, C. L., & Winslow, D. N. (1986). Pore structure and durability of bricks. In *Proc. 4th Canadian Masonry Symposium (2nd edn.), 1Department of Civil Engineering, The University of New Brunswick, Fredericton NB, Canada (2–4 June 1986)* (pp. 314-323).

Crowley, M. (1997). Quality control for earth structures. *Australian Institute of Building Papers* 8:109-118.

Cuisinier, O., Auriol, J. C., Le Borgne, T., & Deneele, D. (2011). Microstructure and hydraulic conductivity of a compacted lime-treated soil. *Engineering geology*, *123*(3), 187-193.

Cuisinier, O., & Laloui, L. (2004). Fabric evolution during hydromechanical loading of a compacted silt. *International Journal for Numerical and Analytical Methods in Geomechanics*, *28*(6), 483-499.

Dahmen, A. J. (2015). Who's afraid of raw earth? Experimental wall in New England and the environmental cost of stabilization. *Rammed Earth Construction: Cutting-Edge Research on Traditional and Modern Rammed Earth*, 85.

Davidovits, J. (2011). Geopolymer chemistry and applications. *3rd ed. Institut Géopolymère*.

Deboucha, S., & Hashim, R. (2011). A review on bricks and stabilized compressed earth blocks. *Scientific Research and Essays*, *6*(3), 499-506.

Delage, P., & Pellerin, F. M. (1984). Influence de la lyophilisation sur la structure d'une argile sensible du Québec. *Clay Minerals*, *19*(2), 151-160.

de la Torre López, M. J., Sebastián, P. E., & Rodríguez, G. J. (1996). A study of the wall material in the Alhambra (Granada, Spain). *Cement and concrete Research*, *26*(6), 825-839.

Delgado, M. C. J., & Guerrero, I. C. (2007). The selection of soils for unstabilised earth building: A normative review. *Construction and building materials*, *21*(2), 237-251.

Diamond, S. (1970). Pore size distributions in clays. *Clays and clay minerals*,*18*(1), 7-23.

Dierks, K., & Ziegert, C. (2002). Neue Untersuchungen zum Materialverhaltenvon Stampflehm. *Steingass, P.: Moderner Lehmbau 2002*.

DIN 18945 (2013). Earth blocks - Terms and definitions, requirements, test methods.

DIN 52617 (1987). Determination of the water absorption coefficient of construction materials.

Eckermann, W. and Ziegert, C. (2006). Auswirkung von Lehmbaustoffen auf die Raumluftfeuchte. *http://www.claytec.de/fileadmin/user_upload/pdf_download/lehmputz raumklima.pdf* (last accessed: 20/08/2016).

EEA (2010). The European environment state and outlook 2010. Material resources and waste. European Environment Agency, Copenaghen.

Elert, K., Pardo, E. S., & Rodriguez-Navarro, C. (2015). Alkaline activation as an alternative method for the consolidation of earthen architecture. *Journal of Cultural Heritage*, *16*(4), 461-469.

Eurostat (2011). Online Statistics. http://www.epp.eurostat.ec.eduropa.eu

Fisher, R. A. (1926). On the capillary forces in an ideal soil; correction of formulae given by WB Haines. *The Journal of Agricultural Science*, *16*(03), 492-505.

Garcia-Bengochea, I., Altschaeffl, A. G., & Lovell, C. W. (1979). Pore distribution and permeability of silty clays. *Journal of the Geotechnical Engineering Division*, *105*(7), 839-856.

Giesche, H. (2006). Mercury porosimetry: a general (practical) overview.*Particle & particle systems characterization*, *23*(1), 9-19.

Guetlala, A., & Guenfoud, M. (1997). Béton de terre stabilisé: Propriétés physico-mécaniques et influence des types d'argiles. *La technique moderne*,*89*(1-2), 21-26.

Guettala, A., Abibsi, A., & Houari, H. (2006). Durability study of stabilized earth concrete under both laboratory and climatic conditions exposure. *Construction and Building Materials*, *20*(3), 119-127.

Hall, M., & Djerbib, Y. (2004). Moisture ingress in rammed earth: Part 1—the effect of soil particle-size distribution on the rate of capillary suction. *Construction and Building Materials*, *18*(4), 269-280.

Haynes, J. M., & Sneck, T. (1972). Pore properties in the evaluation of material. In *Performance concept in buildings. Proceedings of a joint symposium held in Philadelphia, May 2-5, 1972* (pp. 669-675). National bureau of standards.

Heathcote, K. A., & Jankulovski, E. (1992). Aspect ratio correction factors for soilcrete blocks. *Transactions of the Institution of Engineers, Australia. Civil engineering*, *34*(4), 309-312.

Hoffmann, C., Alonso, E. E., & Romero, E. (2007). Hydro-mechanical behaviour of bentonite pellet mixtures. *Physics and Chemistry of the Earth, Parts A/B/C*, *32*(8), 832-849.

Houben, H., & Guillaud, H. (1994). *Earth construction: a comprehensive guide*. Intermediate Technology Publications.

Houben, H. & Guillaud, H. 1996. Earth construction - A com-prehensive guide. Second Edition. *Intermediate Technology Publications*. London, UK.

Houben, H., & Guillaud, H. (2006). Traité de construction en terre. *Editions Parenthèses*.

ISO 24353 (2008). Hygrothermal performance of building materials and products determination of moisture adsorption/desorption properties in response to humidity variation. Geneva, Switzerland: International Organization for Standardization.

Jaquin, P. A., Augarde, C. E., Gallipoli, D., & Toll, D. G. (2009). The strength of unstabilised rammed earth materials. *Géotechnique.*, *59*(5), 487-490.

Jaquin, P. A., Augarde, C. E., & Legrand, L. (2008, June). Unsaturated characteristics of rammed earth. In *First European Conference on Unsaturated Soils, Durham, England* (pp. 417-422).

Jayasinghe, C., & Kamaladasa, N. (2007). Compressive strength characteristics of cement stabilized rammed earth walls. *Construction and Building Materials*, *21*(11), 1971-1976.

JIS A 1470-1 (2002). Test method of adsorption/desorption efficiency for building materials to regulate an indoor humidity-part 1: response method of humidity. Tokyo, Japan: Japanese Industrial Standards Committee.

Keable, J. (1996). *Rammed earth structures: a code of practice*. Intermediate Technology.

Kebao, R., Kagi, D., & building Protection, T. D. (2012). Integral admixtures and surface treatments for modern earth buildings. *Modern Earth Buildings: Materials, Engineering, Constructions and Applications*, 256.

Kouakou, C. H., & Morel, J. C. (2009). Strength and elasto-plastic properties of non-industrial building materials manufactured with clay as a natural binder.*Applied Clay Science*, *44*(1), 27-34.

Krefeld, W. J. (1938). Effect of shape of specimen on the apparent compressive strength of brick masonry. *Proceedings of the American Society of Materials, Philadelphia p*, 363-369.

Lawson, B., & Rudder, D. (1996). *Building materials energy and the environment: Towards ecologically sustainable development*. Royal Australian Institute of Architects.

Lucas, R. (1918). Ueber das Zeitgesetz des kapillaren Aufstiegs von Flüssigkeiten. *Colloid & Polymer Science*, *23*(1), 15-22.

Maage, M. (1984). Frost resistance and pore size distribution in bricks.*Matériaux et Construction*, *17*(5), 345-350.

Maniatidis, V., & Walker, P. (2003). A review of rammed earth construction. *Innovation Project "Developing Rammed Earth for UK Housing", Natural Building Technology Group, Department of Architecture & Civil Engineering, University of Bath*.

McGregor, F., Heath, A., Fodde, E., & Shea, A. (2014). Conditions affecting the moisture buffering measurement performed on compressed earth blocks.*Building and Environment*, *75*, 11-18.

McGregor, F., Heath, A., Maskell, D., Fabbri, A. and Morel, J.C. (2016). A review on the buffering capacity of earth building materials. *Proceedings of the Institution of Civil Engineers – Construction Materials*. DOI: 10.1680/jcoma.15.00035

McHenry, P. G. (1984). *Adobe and rammed earth buildings: design and construction*. University of Arizona Press.

Mesbah, A., Morel, J. C., & Olivier, M. (1999). Clayey soil behaviour under static compaction test. *Materials and structures*, *32*(223), 687-694.

MOPT (1992). Bases Para el Diseño y Construcción con Tapial. Madrid, Spain: Centro de Publicaciones, Secretaría General Técnica, Ministerio de Obras Públicas y Transportes.

Morel, J. C., Mesbah, A., Oggero, M., & Walker, P. (2001). Building houses with local materials: means to drastically reduce the environmental impact of construction. *Building and Environment*, *36*(10), 1119-1126

Morel, J. C., Pkla, A., & Walker, P. (2007). Compressive strength testing of compressed earth blocks. *Construction and Building Materials*, *21*(2), 303-309.

Moro, F., & Böhni, H. (2002). Ink-bottle effect in mercury intrusion porosimetry of cement-based materials. *Journal of Colloid and Interface Science*, *246*(1), 135-149.

Morton, T., & Little, B. (2001). Building with earth in Scotland: Innovative design and sustainability. *Central Research Unit, Scottish Executive, Edinburgh*.

Norton, J. 1997. Building with Earth. A handbook. Second Edi-tion. *Intermediate Technology Publications*, London, UK.

Nowamooz, H., & Masrouri, F. (2010). Relationships between soil fabric and suction cycles in compacted swelling soils. *Engineering geology*, *114*(3), 444-455.

NZS 4298 (1998). Materials and workmanship for earth buildings. Wellington: Standards New Zealand.

OECD (2003). Environmentally Sustainable Buildings: Challenges and Policies.

Olivier, M., & Mesbah, A. (1986). Le matériau terre: Essai de compactage statique pour la fabrication de briques de terre compressées. *Bull. Liaison Lab. Ponts et Chaussées*, *146*, 37-43.

Pacheco-Torgal, F., & Jalali, S. (2012). Earth construction: Lessons from the past for future eco-efficient construction. *Construction and building materials*,*29*, 512-519.

Radanovic, J. (1996). Design Criteria for Reinforced Stabilised Earth Structures. University of Western Australia, Crawley, Australia.

Rigassi, V. (1995). Compressed earth blocks: Manual of production. *Deutsches Zentrum fur Entwicklungstechnologien-GATE*.

RILEM Technical Committee 164 (1994). Recommendations for the Testing and Use of Constructions Materials

Robinson, G. C. (1984). The relationship between pore structure and durability of brick. *American Ceramic Society bulletin*, *63*(2), 295-300.

Rode, C., Peuhkuri, R. H., Mortensen, L. H., Hansen, K. K., Time, B., Gustavsen, A., ... & Harderup, L. E. (2005). *Moisture buffering of building materials*. Technical University of Denmark, Department of Civil Engineering.

Röhlen, U., & Ziegert, C. (2013). *Construire en terre crue: construction, rénovation, finitions*. Ed. Le Moniteur.

Romero, E., Gens, A., & Lloret, A. (1999). Water permeability, water retention and microstructure of unsaturated compacted Boom clay. *Engineering Geology*, *54*(1), 117-127.

Sasanian, S., & Newson, T. A. (2013). Use of mercury intrusion porosimetry for microstructural investigation of reconstituted clays at high water contents.*Engineering Geology*, *158*, 15-22.

SAZS 724 (2001). Zimbabwe Standard. Rammed Earth Struc-tures. Standards Association of Zimbabwe, Harare, Zimbabwe.

Schrader, C. A. (1981). Rammed earth construction: a re-emerging technology. *Proc. Annu. Meet.-Am. Sect. Int. Sol. Energy Soc.;(United States)*, *6*(CONF-810925-).

Schroeder, H. (2016). *Sustainable Building with Earth*. Springer.

Simms, P. H., & Yanful, E. K. (2004). A discussion of the application of mercury intrusion porosimetry for the investigation of soils, including an evaluation of its use to estimate volume change in compacted clayey soils.*Geotechnique*, *54*(6), 421-426.

Skempton, A. W. (1953). The colloidal activity of clays. *Selected Papers on Soil Mechanics*, 106-118.

Slaty, F., Khoury, H., Rahier, H., & Wastiels, J. (2015). Durability of alkali activated cement produced from kaolinitic clay. *Applied Clay Science*, *104*, 229-237.

Soudani, L., Fabbri, A., Morel, J. C., Woloszyn, M., Chabriac, P. A., Wong, H., & Grillet, A. C. (2016). Assessment of the validity of some common assumptions in hygrothermal modeling of earth based materials. *Energy and Buildings*, *116*, 498-511.

Szalay, A. Z. Z. (2007). What is missing from the concept of the new European Building Directive?. *Building and Environment*, *42*(4), 1761-1769.

Tarantino, A., & De Col, E. (2008). Compaction behaviour of clay.*Géotechnique*, *58*(3), 199-213.

Taylor, D. W., & Merchant, W. (1940). A theory of clay consolidation accounting for secondary compression. *Journal of Mathematics and Physics*, *19*(1), 167-185.

TERCRUSO (2013). Caractérisation des briques de terre crue de Midi-Pyrénées. *http://www.cercad.fr/IMG/pdf/tercruso_rapport_final_lmdc-2013-04-r120.pdf* (last accessed: 25/07/2016).

ASTM D2487-11 (2011). Standard Practice for Classification of Soils for Engineering Purposes. Unified Soil Classification System, USCS.

Venkatarama-Reddy, B. V., & Jagadish, K. S. (1993). The static compaction of soils. *Geotechnique*, *43*(2).

Walker, P. (2000). Strength and durability testing of earth blocks. In *Proceedings of the 6th international seminar on Structural Masonry for developing countries* (pp. 110-118). University of Bath.

Washburn, E. W. (1921). The dynamics of capillary flow. *Physical review*,*17*(3), 273.

WCED - World Commission on Environment and Development (1987). Our Common Future. Oxford: Oxford University Press.

Winslow, D. (1991). Predicting the durability of paving bricks. *Journal of testing and evaluation*, *19*(1), 29-33.

Winslow, D. N., Kilgour, C. L., & Crooks, R. W. (1988). Predicting the durability of bricks. *Journal of Testing and Evaluation*, *16*(6), 527-531.

Wu, F., Li, G., Li, H. N., & Jia, J. Q. (2013). Strength and stress–strain characteristics of traditional adobe block and masonry. *Materials and structures*, *46*(9), 1449-1457.

Annexe

List of publications

International journal publications

J1) D. Gallipoli, A.W. Bruno, F. D'Onza, C. Mancuso (2015). A bounding surface hysteretic water retention model for deformable soils. Géotechnique, 65(10): 793–804. DOI: http://dx.doi.org/10.1680/jgeot.14.P.118

Conference publications

C1) A.W. Bruno, D. Gallipoli, C. Perlot, J. Mendes (2016). Effects of compaction stress on the physical, hygroscopic and mechanical properties of an earthen construction material. 13èmes Journées d'Etude des Milieux Poreux. Côte Basque, France, 12-13-14 October 2016.

C2) A.W. Bruno, D. Gallipoli, C. Perlot, J. Mendes (2016). Effect of very high compaction pressures on the physical and mechanical properties of earthen materials. Proceedings 3rd European conference on unsaturated soils E-UNSAT 2016, Paris, France.

C3) D. Gallipoli, A.W. Bruno, C. Perlot, J. Mendes (2016). Terre crue compactée à haute pression et méthodes de stabilisation : propriétés mécaniques, hydriques et durabilité. Actes des Journées sur la Constructions en terre crue : avancées scientifiques. Chambéry, France, 17-18 Mars 2016

C4) A.W. Bruno, D. Gallipoli, C. Perlot, J. Mendes (2015). Développement d'une procédure de compactage pour améliorer les propriétés de briques de terre crue compressée. Proceedings 2nd International Conference on New Materials and Durability: Douai, France, 5-6 November 2015.

C5) A.W. Bruno, D. Gallipoli, C. Perlot, J. Mendes, N. Salmon (2015). Mechanical properties of unstabilized earth compressed at high pressures. Proceedings 1st International Conference on Bio-based Building Materials. Clermont-Ferrand, France, 21-24 June 2015, e-ISBN PRO99: 978-2-35158-154-4.

C6) A.W. Bruno, D. Gallipoli, C. Perlot, J. Mendes, N. Salmon (2015). Briques de terre crue : procédure de compactage haute pression et influence sur les propriétés mécaniques. Actes des 33èmes Rencontres universitaires de Génie Civil. Anglet, France, 27-29 May 2015 - https://hal.archives-ouvertes.fr/hal-01167676

C7) D. Gallipoli, A.W. Bruno, C. Perlot, N. Salmon (2014). Raw earth construction: is there a role for unsaturated soil mechanics ? Proceedings 6th International Conference on Unsaturated Soils (invited keynote): 55-62. Sydney, Australia, 2-4 July 2014, CRC Press, ISBN: 978-1-138-00150-3 - http://dx.doi.org/10.1201/b17034-8